

# **Coronavirus spike-receptor interactions**

**Huihui Mou**

**ISBN: 978-90-393-6390-4**

**Cover design:** Xueqing Wu, Huihui Mou

**Layout design:** Huihui Mou

**Printing:** Proefschrift-aio

**Copyright ©Huihui Mou 2015**

All rights reserved. No part of this publication may be reproduced or transmitted in any form or by any means without written permission of the author and the publisher holding the copyrights of the published articles.

To my beloved parents: your love and support pave my way to the achievement.

**致**我最爱的爸爸妈妈：你们对我无私的爱和无尽的支持成就了今天的我。



古人之观於天地、山川、草木、虫鱼、鸟兽，往往有得，以其求思之深，而无不在也。夫夷以近，则游者众；险以远，则至者少。而世之奇伟、瑰怪、非常之观，常在於险远，而人之所罕至焉，故非有志者不能至也。有志矣，不随以止也，然力不足者亦不能至也。有志与力，而又不随以怠，至於幽暗昏惑而无物以相之，亦不能至也。然力足以至焉而不至，於人为可讥，而在己为有悔；尽吾志也，而不能至者，可以无悔矣，其孰能讥之乎？此余之所得也！

---王安石 《游褒禅山记》节选



# **Coronavirus spike-receptor interactions**

Coronavirus spike-receptor interacties

(met een samenvatting in het Nederlands)

## **Proefschrift**

ter verkrijging van de graad van doctor aan de Universiteit Utrecht op gezag van de rector magnificus, prof.dr. G.J. van der Zwaan, ingevolge het besluit van het college voor promoties in het openbaar te verdedigen op

dinsdag 25 augustus 2015 des middags te 2.30 uur

door

**Huihui Mou**

geboren op 6 oktober 1985 te Yichang, Hubei (China)

**Promotor:** Prof. dr. P.J.M. Rottier

**Copromotor:** Dr. B.J. Bosch

The research described in this thesis was financially supported by Chinese Scholarship Council (CSC).



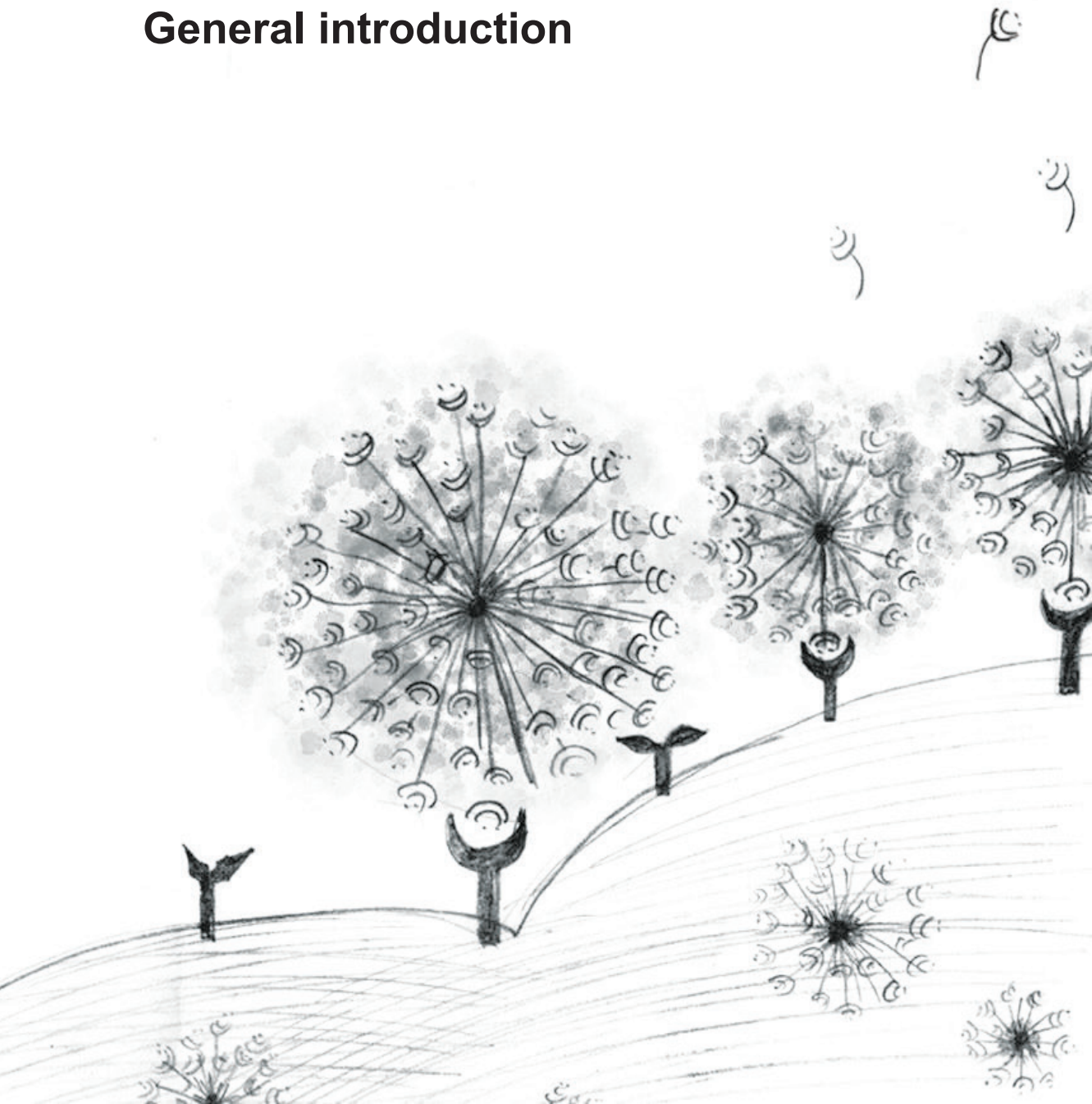
# Contents

Chapter 1	General Introduction	11
Chapter 2	Dipeptidyl peptidase 4 is a functional receptor for the emerging human coronavirus-EMC	39
Chapter 3	The receptor binding domain of the new MERS coronavirus maps to a 231-residue region in the spike protein that efficiently elicits neutralizing antibodies	65
Chapter 4	Specific serology for emerging human coronaviruses by protein microarray.	75
Chapter 5	An S protein mutation adapting feline enteric coronavirus to using DC-SIGN for cell entry does not confer macrophage tropism	89
Chapter 6	Summarizing discussion	113
Chapter 7	English and Dutch summaries	135
	Acknowledgements / 致谢	143
	Curriculum Vitae	149
	List of publications	151



# CHAPTER 1

## General introduction





The history of coronaviruses started in the 1930s when avian infectious bronchitis virus (IBV) was first described as the causative agent of infectious bronchitis in poultry flocks (1-2). In the mid-1960s, two human coronaviruses, 229E (HCoV-229E) and OC-43 (HCoV-OC43), were identified as pathogens for common-colds in humans (3-5). Early studies on human coronaviruses were primarily focused on the epidemiology of these viruses using serological techniques. Coronaviruses were demonstrated to contribute to as much as 35% of respiratory infections in humans during epidemics (6). In 1975, the Coronaviridae family with one genus, coronavirus, was officially established, referring to the crown-like appearance of spikes on the surface of these viruses (7).

Coronaviruses can cause a variety of diseases in mammals and birds mainly affecting the respiratory and gastrointestinal tract (8). They have gained increased attention after the outbreak of the severe acute respiratory syndrome (SARS) in 2002-2003, caused by the SARS-coronavirus (SARS-CoV) (9-10). During this worldwide epidemic, SARS-CoV infected more than 8000 humans with a mortality rate as high as 10% (9-11). After the identification of SARS-CoV, three other coronaviruses were identified to infect humans. In 2004, a new human coronavirus named human coronavirus NL63 (HCoV-NL63) was reported by two independent groups, which caused respiratory tract illness in infants and immunocompromised adults (12-13). In 2005, another novel human coronavirus HKU1 (HCoV-HKU1) was described associated with pneumonia (14). In September 2012, a novel coronavirus was identified from a patient with pneumonia in Saudi-Arabia. This coronavirus was provisionally named human coronavirus EMC and then designated Middle East respiratory syndrome coronavirus (MERS-CoV) (15). Until March 26<sup>th</sup> 2015, there were 1090 laboratory-confirmed MERS cases globally, including at least 412 related deaths officially reported to WHO (<http://www.who.int/csr/don/26-march-2015-mers-saudi-arabia/en/>).

Emerging coronaviruses, especially zoonotic coronavirus species, pose a challenge to both science and health care since they may emerge from unrecognized animal sources and induce highly pathogenic diseases. Zoonotic transmission occurs via a virus spillover event from an animal reservoir to humans sometimes through an intermediate host. Just after its identification, SARS-CoV was hypothesized to originate from an animal host. Epidemiological evidence connected SARS-CoV with masked palm civets that were traded on game-food animal markets (16). Later on, SARS-like coronaviruses were identified in horseshoe bats, the latter being the reservoirs for SARS-CoV (17). Although SARS-like viruses isolated from these horseshoe bats were able to infect human cells in vitro, infection of an intermediate host - such as the Himalayan palm civets or the raccoon dogs - likely has facilitated the cross-species transmission of SARS-CoV during the global epidemic early 2002 to 2003 (18).

## Coronavirus spike-receptor interactions

Apart from switching between hosts, coronaviruses can also change their cell tropism within an infected animal, as exemplified by feline coronaviruses (FCoV). FCoV are divided into two pathotypes: feline enteric coronavirus (FECV) and feline infectious peritonitis virus (FIPV) (19). FECV mainly replicates in enteric epithelium causing mild or clinically unapparent enteritis in cats. Occasionally it converts to a highly virulent form, FIPV, by changing its cell tropism from enterocytes to macrophages mostly leading to a systemic and often lethal infection (20-25).

# 1. Biology of coronavirus

## 1.1 Classification of coronaviruses

Based on genetic relationships, coronaviruses, belonging to the subfamily of Coronavirinae within the Coronaviridae family and the order of Nidovirales, are divided into four genera, the alpha-, beta-, gamma- and deltacoronavirus (Figure 1.1, reviewed in (26)). Generally, alpha- and betacoronaviruses infect mammalian hosts whereas gamma- and deltacoronaviruses are found in avian hosts (27).

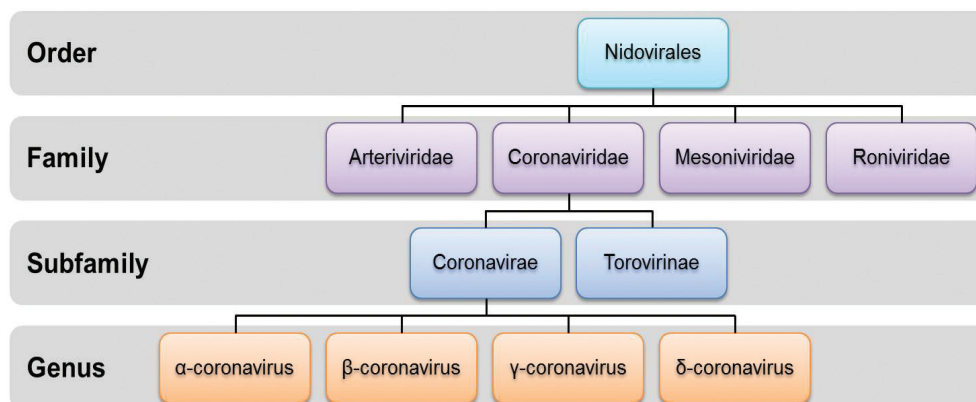


**Figure 1.1 Taxonomic classification of coronaviruses** (classification according to 'Virus Taxonomy: 2014 Release' of the ICTV, <http://www.ictvonline.org/virusTaxonomy.asp>).

## 1.2 Structure and genome organization of coronavirus

Coronaviruses are enveloped virus particles which measure 80 to 120nm in diameter (8). Surrounding the nucleocapsid, the envelope of coronaviruses comprises a host-derived lipid bilayer containing at least three viral membrane proteins: the spike protein (S), the membrane protein (M), and the envelope protein (E) (Figure 1.2b) (28). The **S** protein (formerly called E2) is a large, highly glycosylated membrane protein measuring 180 to 200 kDa in size. Trimers of the S protein create the large, bulbous projections on the surface of viral particles and generate the corona-

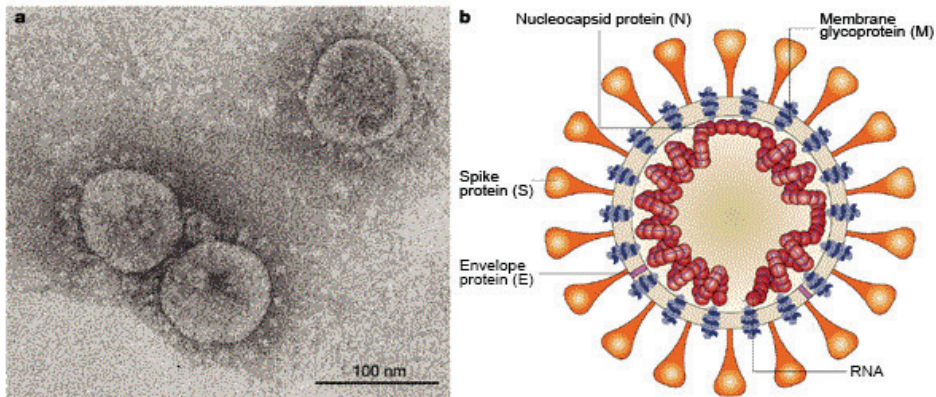


**Figure 1.2 Morphology of coronavirus.** (a) SARS-CoV particles visualized by negative stain electron microscopy. (b) Schematic representation of a coronavirus. This figure is taken from (38).

like virus particle morphology as seen by negatively stained electron microscopy (Figure 1.2a) (29). The S protein mediates cell entry and is a major determinant for the host range and pathogenesis of coronaviruses (30-33). The **M** protein (formerly called E1) is a triple-spanning membrane protein with a molecular weight of 25 to 30 kDa. M proteins are considered as the building blocks of the virion and interact with each other as well as with all other virion components. The **E** protein (formerly called Es) is a small type III membrane protein of ~8.4 to 12 kDa. It comprises a short hydrophilic amino terminus, followed by a large hydrophobic region and a hydrophilic carboxy-terminal tail. The M and E proteins are indispensable for virus assembly, budding and maturation. The **HE** protein (formerly called E3) is the fourth membrane protein found in a subset of betacoronaviruses and possesses hemagglutinating and acetyltransferase activity (34-37).

The nucleocapsid of coronaviruses contains a linear, positive-sense RNA genome encapsidated by the fourth structural protein, the nucleocapsid protein (N), for stabilization and protection. Coronaviruses contain the largest RNA genomes ranging from 27.3 (HCoV-229E) to 31.3 kilobases (murine hepatitis virus, MHV) in length with a 5'-cap and a 3'-poly(A) tail. The first two-thirds of the genome codes for a large polymerase precursor protein, which is post-translationally cleaved by viral proteases *in cis* or *in trans*, generating approximately 16 non-structural proteins. These non-structural proteins are primarily involved in the synthesis of genomic and sub-genomic RNA. The 3'-terminal one third of the genome encodes the structural proteins, as well as a group of accessory proteins (Fig. 1.3). The structural proteins S, M, E and N are found in all coronaviruses and are essential for virus replication. Apart from their contributions to virulence and pathogenicity *in vivo*, the accessory proteins are rather genus-specific and are non-essential for virus replication *in vitro*, yet might function in interfering with host innate immunity.

## Coronavirus spike-receptor interactions

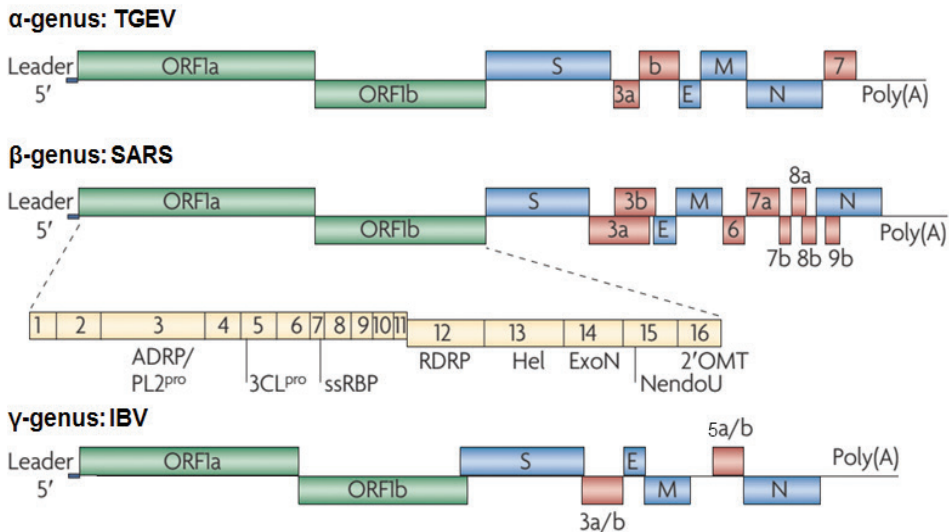


**Figure 1.3** Genome organizations of coronaviruses of different genera. This figure is reproduced according to (39).

### 1.3 Replication cycle

The life cycle of coronaviruses starts with the binding of the S proteins on virions to receptors on the cell surface (Figure 1.4). After fusion of the viral membrane with the host cell membrane mediated by the S protein, the viral genome is released into the cytoplasm where viral RNA translation takes place. The overlapping open reading frames (ORF) 1a and ORF1b are directly translated by the host translation machinery through a ribosomal frame-shifting mechanism to produce two polyprotein precursors: pol1a from ORF1a and pol1ab from the read-through of ORF1a and 1b. The translated precursor proteins are further proteolytically cleaved by viral proteases to create the components that make up the viral replication complex. The incoming viral genome serves as a template for the synthesis of complementary negative-stranded, full-length RNA and a nested set of sub-genomic RNAs with a common 3' end. These negative-stranded RNAs are subsequently used for the transcription of positive-sense, RNA genomes and sub-genomic messenger RNAs. The sub-genomic mRNAs encode structural and accessory proteins. Progeny genomic RNA and newly synthesized N proteins co-assemble in the cytoplasm to form the helical nucleocapsid. The M, E and S proteins are translated at the rough ER and then transported to the budding compartment where the progeny viral particles are assembled. The virus acquires its envelope after budding of the nucleocapsid through intracellular membranes of the endoplasmic reticulum (ER) and the Golgi intermediate compartment (ERGIC). Finally, the virus is released from the host cell by exocytosis (40).



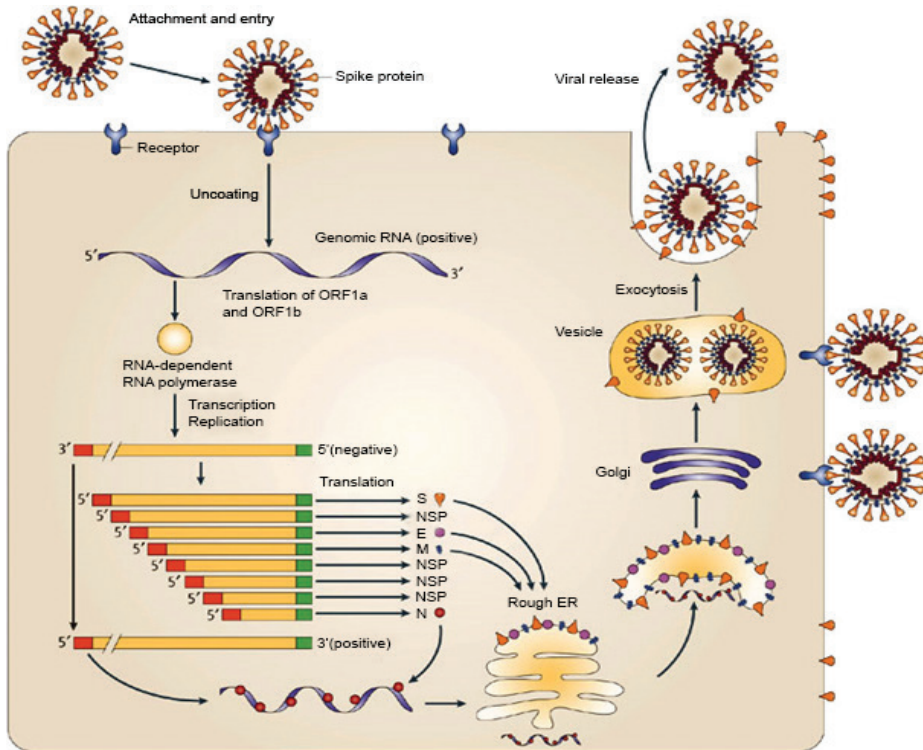


Figure 1.4 The coronavirus life cycle. This figure is taken from (40).

## 2. Spike-receptor interaction and virus entry

In order to have access to host components needed for replication, coronaviruses need to pass the host cell membrane and release their genome into the cell cytoplasm. The entry of coronaviruses into host cells is mediated by the viral spikes on the virion surface.

### 2.1 The S protein

The spikes of coronaviruses are composed of three S proteins that are highly glycosylated type I membrane proteins (Figure 1.5) (26, 30, 41-43). The S protein contains a signal peptide at the N terminus that is cleaved upon ER translocation, an extracellular domain, a transmembrane domain and a cytoplasmic tail (26). The S protein can be divided into two functionally distinct subunits, the N-terminal, soluble S1 subunit and the C-terminal, membrane-anchored S2 subunit (26).

## Coronavirus spike-receptor interactions

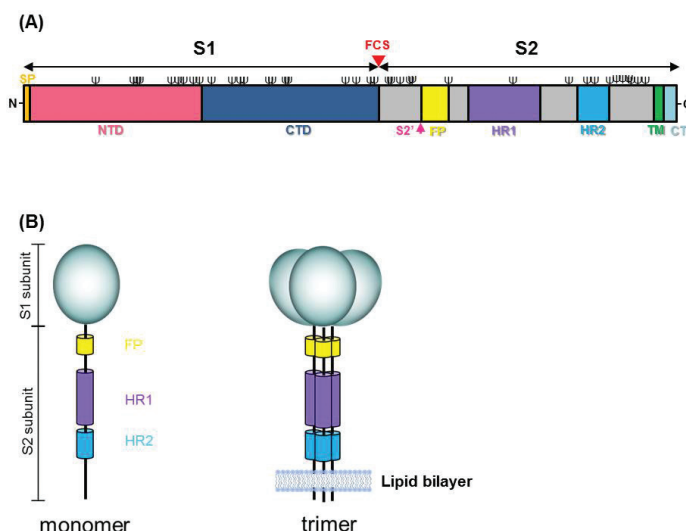


**Figure 1.5 The coronavirus S protein.** (A) Schematic presentation using the S protein of a feline coronavirus as an example (FCoV strain UCD). N-glycosylation sites are indicated with  $\psi$ . The furin cleavage site (FCS) between the S1 and S2 subunits is represented by a red triangle. The N- and C-terminal domain (NTD and CTD, respectively) in the S1 subunit, and the fusion peptide (FP), heptad repeat (HR) regions, transmembrane domain (TM) and cytoplasmic tail (CT) are indicated. (B) Schematic presentation of the S protein represented as a monomer and trimer.

The S1 subunit is responsible for binding to the cellular receptor. The interaction of S1 with the receptor is considered the main determinant of the cell and host tropism of coronaviruses (31-33). Within the S1 subunit, the receptor binding domain (RBD), situated in the N-terminal domain (NTD) or C-terminal domain (CTD) of S1, mediates the actual receptor binding. The RBD also contains the majority of neutralizing epitopes (44-47).

The S2 subunit is responsible for membrane fusion. It has a class I viral fusion protein architecture with a putative fusion peptide (FP), two heptad repeat (HR) domains (HR1 and HR2) and a C-terminal transmembrane domain (26,48). Conformational changes within the S2 fusion domain, triggered by S1-receptor interaction, leads to the insertion of the putative FP into the target cell membrane and subsequent association of HR1 and HR2 domains to form a six-helix bundle fusion core. The collaboration among different domains within the S2 subunit draws the viral envelope and target cell membrane into close proximity enabling membrane fusion, which leads to the release of the viral genome into the cytoplasm.

As for most class I fusion proteins, the coronavirus S proteins are functionally regulated by cellular proteases. Two cleavage sites in the S protein have been reported (30). Proteolytic cleavage between the S1 and S2 subunits occurs for S proteins of some representatives of the alpha-, beta- and gammacoronaviruses. This

cleavage is mediated by cellular Golgi-resident furin or furin-like serine proteases acting at furin cleavage sites R-X-(R/K)-R (R-arginine, K=lysine and X=any amino acid) during exocytic transport (49-50). Cleavage at the S1/S2 junction in the host cell is sometimes proposed to be related to cell-cell fusion (49, 51-53). Apart from cleavage at the S1/S2 junction, a more crucial and common cleavage site was reported just upstream of the conserved FP of coronavirus S2 subunits, at the so-called S2' position (24, 54-55). The cleavage at the S2' site occurs during cell entry by plasma membrane or endosomal proteases and is considered to be critical for activation of the fusion potential of S proteins (55-56).

## 2.2 Receptor

Coronaviruses are able to exploit different cell surface molecules, either proteins or carbohydrates, as receptors. As summarized in Table 1.1, receptor usage among coronaviruses of different genera does not show an obvious preference for one specific molecule. The aminopeptidase N (APN) protein especially from feline origin was proposed as a widely used receptor for alphacoronaviruses (57), but HCoV-NL63 was later found to recruit angiotensin-converting enzyme 2 (ACE2) for entry, similarly to the betacoronavirus SARS-CoV. Coronavirus species in different genera are able to use carbohydrates (i.e. sialic acids) on the cell-surface for entry. Moreover, calcium-dependent lectins such as dendritic cell-specific intercellular adhesion molecule-3-grabbing nonintegrin (DC-SIGN) can also be recruited by coronaviruses as receptors. The differential receptor usage reflects the long and complex evolution path of coronaviruses.

## 2.3 Determinants of cell tropism, host tropism and pathogenesis at the level of virus entry

Cell entry of coronaviruses involves two steps, receptor binding and membrane fusion. Virus-receptor interaction and host proteases that are critical for activating fusion are important determinants of cell tropism, host tropism and pathogenesis.

Entry is initiated by receptor binding which is the first strategy used by coronaviruses to control tropism specificity. Spike-receptor interaction is highly specific, and even subtle amino acid changes at the binding interface either in the RBD or the receptor may disrupt the interaction. A good example is the S protein of SARS-CoV of which the functional recruitment of the human ACE2 receptor was almost abolished after introduction of two amino acid substitutions - K479N and S487T - in the RBD by those found in a SARS-CoV virus isolated from the palm civet (89). Likewise, mutations introduced in the receptor are also able to interrupt RBD-receptor interaction. Civet and human SARS-CoV strains cannot replicate efficiently in bat cells which is associated with residue differences in ACE2 - K31N, E35K and Y41H - that weaken salt bridge interactions between SARS-RBD and bat ACE2 (90-92).

# Coronavirus spike-receptor interactions

**Table 1.1 Summary of receptor usage and tissue and host tropism of coronaviruses**

Genus	Species	Receptor	Target tissue	Host	References
<b>α-Coronavirus</b>					
	Alphacoronavirus 1				
	Canine coronavirus	cAPN and fAPN**	Enteric	Dog	(57)
	Feline coronavirus	Neu5Ac*, fAPN, DC-SIGN***	Enteric and systemic	Cat	(58) (59)(60) (61) (62) (63)
	Porcine respiratory coronavirus	pAPN	Respiratory	Pig	(64)
	Transmissible gastroenteritis virus	Neu5Gc, Neu5Ac, pAPN and fAPN	Enteric	Pig	(65) (66) (57)
	Porcine epidemic diarrhea virus	pAPN	Enteric	Pig	(67) (68)
	Human coronavirus 229E	hAPN and fAPN, L-SIGN	Respiratory	Human	(69) (57) (60) (70)
	Human coronavirus NL63	ACE2, DC-SIGN	Respiratory	Human	(71) (72)
<b>β-Coronavirus</b>					
	Bovine coronavirus	α2,3-linked Neu5,9Ac2	Respiratory	Cow	(37) (73) (74)
	Human coronavirus OC43	α2,6-linked Neu5,9Ac2	Respiratory	Human	(37) (74)
	Murine hepatitis virus MHV	CEACAM1a, Neu5,9Ac2, Neu4,5Ac2	Polytropic; enteric, hepatic, central nervous system	Mouse	(75-77) (78) (63)
	SARS and bat related coronaviruses	ACE2, DC-SIGN, L-SIGN	Respiratory and systemic	Human, bat	(79) (80-82)
	Middle East respiratory syndrome coronavirus	DPP4	Respiratory	Human, bat	(83)
	Tylosyncytis bat coronavirus HKU4	DPP4	?	Bat	(84) (85)
<b>γ-Coronavirus</b>					
	Infectious bronchitis virus	α2,3-linked Neu5Ac, DC-SIGN, L-SIGN	Respiratory	Chicken	(86) (87) (88)

\*Red font: receptor binding domain located in the N-terminal domain of S1 subunit. \*\*Blue font: receptor binding domain located in the C-terminal domain of S1 subunit. \*\*\* Grey font: location of the receptor binding domain is unknown.

Presence of proteases that can activate membrane fusion may also contribute to virus tropism as well as pathogenesis. PEDV shows a preference for replication in the epithelia of the porcine intestine, an environment full of proteases. Virus propagation *in vitro* is strictly dependent on the supplementation of trypsin to the cell culture medium (93). The requirement for trypsin may hence confine the virus' tropism to the enteric tract. In addition, expression of the transmembrane protease serine 2 (TMPRSS2) in Vero cells enhanced virus entry by activating the S fusion protein. *In vivo*, the TMPRSS2 expression pattern in cells correlated with infection of SARS-CoV in the upper lobe of the lung. This indicates that proteases such as trypsin and TMPRSS2 may act as a determinant of viral tropism and pathogenesis of coronaviruses (94).

### 3. Identified receptors for coronaviruses

Functional receptors of a number of coronavirus species have been identified (Table 1.1). Based on the interaction mode of coronavirus spikes with their receptors, the receptors for coronaviruses can be classified into three categories: protein receptors involved in protein-protein interactions, carbohydrate receptors in viral protein-host carbohydrate interactions and lectin receptors in viral carbohydrate-host lectin interactions.

#### 3.1 Protein receptors in protein-protein interactions

At the start of our study, three protein receptors were identified for coronaviruses including the aminopeptidase N (used by different alphacoronaviruses), the angiotensin-converting enzyme 2 (SARS-CoV and HCoV-NL63) and the carcinoembryonic antigen-related cell adhesion molecule 1 (MHV). These receptors will be discussed below in more detail.

##### ***Aminopeptidase N***

Aminopeptidase N (APN), also known as CD13, is a highly glycosylated, type II membrane protein with a molecular mass of approximately 160 kDa. It has a seahorse-shaped structure that consists of four domains (side, head, body and tail) and forms head-to-head dimers (Figure 1.6 A and B). APN belongs to the M1 family of zinc metallopeptidases which preferentially cleaves neutral amino acids, most notably alanine, off the N terminus of peptides (95). It is widely expressed in different tissues at variable expression levels, such as renal and intestinal epithelia, the nervous system (synaptic membranes and pericytes), myeloid cells (monocytes, macrophages and DCs) and fibroblast-like cells (synoviocytes) (96-97).

APN has been designated a “moonlighting enzyme” referring to the wide range of physiological processes the protein is involved in (98). According to the involvement

## Coronavirus spike-receptor interactions

of its catalytic activity, functions of mammalian APN are divided into peptidase-dependent and peptidase-independent activities (99). APN is involved in multiple peptide metabolism pathways associating with its catalytic activity. It is able to enhance pain sensation and influence mood by degrading pain-relief and mood-regulating neuropeptides (100). In addition, metabolism of the vasoconstrictive peptide angiotensin-III by APN leads to vasodilation and lower blood pressure (101). APN also mediates cell-cell adhesion by contacting with other cell surface proteins, a function which is independent of its peptidase activity (102-105).

APN was identified as the functional receptor for transmissible gastroenteritis virus (TGEV) in 1992 (66). Concurrently, human APN (hAPN) was identified as the receptor for HCoV-229E (69). Later on, other alphacoronaviruses were also shown to employ APN as functional receptors including porcine epidemic diarrhea virus (PEDV), porcine respiratory coronavirus (PRCV) and FCoV (57, 64, 106). APN from humans, pigs as well as other mammals share high structural similarity (107-109). Interestingly, feline APN (fAPN) can also serve as a receptor for the porcine (TGEV, PRCV), canine (CCoV) and human coronaviruses (HCoV-229E) (57). On the contrary, hAPN and pAPN only serve as receptors for HCoV-229E and TGEV/PRCV, respectively, but not for FCoV.

A structural study on mammalian APN demonstrated that the virus binding motifs (VBM) for different APN-binding coronaviruses cluster to three regions, termed as VBM1-3 (99, 110). HCoV-229E recognizes VBM1, TGEV recognizes VBM2, and FCoV and CCoV recognize both VBM2 and VBM3 (Figure 1.6C) (111-112). These three VBMs are located at the membrane-distal end of the APN molecule and are hence easily accessible for virus binding.

### Angiotensin-converting enzyme 2

Angiotensin-converting enzyme 2 (ACE2), a type I transmembrane glycoprotein consisting of 805 amino acids, belongs to the M2 family (clan MA) of metalloproteases

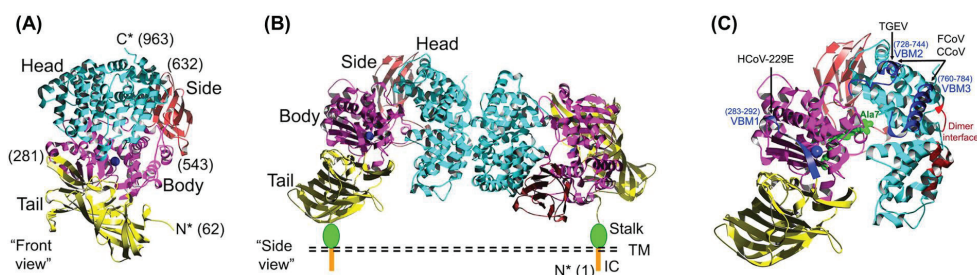


**Figure 1.6 Overall structure of APN.** (A) pAPN ectodomain (front view) contains four domains: head, side, body, and tail. (B) Proposed organization of a dimeric pAPN ectodomain on the cell surface (side view). (C) Structure of pAPN with the dimerization interface and coronavirus-binding sites indicated (side view) (112). This figure was taken from of Chen et al (99).

with a molecular mass of approximately 120 kDa (113). It is predominantly expressed in cardiomyocytes, kidney tubular epithelial cells and adult Leydig cells. It is also present in a wide variety of tissues at a lower expression level, particularly the colon and lung (113-116). Like its homolog ACE, ACE2 comprises two domains: the amino-terminal catalytic domain and the carboxy-terminal domain, which are related to its two categories of functions: the peptidase-dependent and peptidase-independent functions, respectively (117).

ACE2 contains a zinc metallopeptidase domain, which releases a single amino acid from the C-terminus of its substrate with a preference for hydrolysis between a proline and a C-terminal hydrophobic or basic residue (113, 115, 118). ACE2 is a counter regulator for ACE in the renin-angiotensin system (RAS) by degrading Ang II to heptapeptide Ang1-7, leading to vasodilatation and vasoprotection (119-121).

ACE2 was originally identified as the functional receptor for SARS-CoV (79). Overexpression of ACE2 provided non-permissive human cells the susceptibility to SARS-CoV. Receptor function of ACE2 appeared independent of the peptidase activity (79). ACE2 was also identified as a functional receptor for the alphacoronavirus

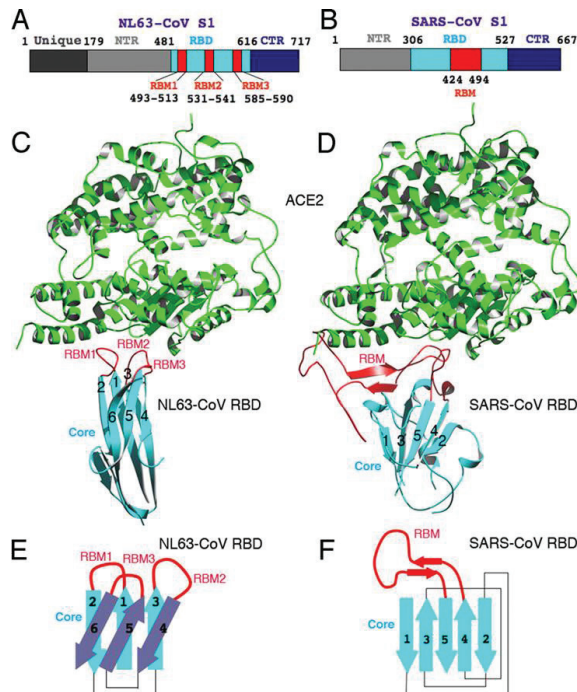


**Figure 1.7 Structural comparison of HCoV-NL63 and SARS-CoV RBDs. (A)** Domain structure of HCoV-NL63 S1. **(B)** Domain structure of SARS-CoV S1. **(C)** Structure of the NL63-RBD-ACE2 complex. **(D)** Structure of the SARS-RBD-ACE2 complex. **(E)** Schematic illustration of the topology of NL63-CoV RBD. **(F)** Schematic illustration of the topology of SARS-CoV RBD. This figure is taken from (123).

## ***Coronavirus spike-receptor interactions***

---

HCoV-NL63 (12-13) (71). Structural studies illustrate that NL63-RBD binds to ACE2 with an RBD composed of three discontinuous receptor binding motifs (RBMs), while SARS-RBD contacts ACE2 by just one RBM. Despite the low amino acid identity (14%) in the ACE2-binding site, the SARS-RBD and NL63-RBD demonstrated comparable binding affinity to human ACE2 and display an overlapping ACE2 binding site (71,122-123). Binding to the same virus-binding hotspot on a shared receptor indicates the convergent as well as divergent evolution strategies coronaviruses take during evolution from their ancestor coronavirus (71, 124) .

### ***Carcinoembryonic antigen-related cell adhesion molecule 1***

The carcinoembryonic antigen-related cell adhesion molecule 1 (CEACAM1), also known as BGP, C-CAM and CD66a, is grouped in the carcinoembryonic antigen-related cell adhesion molecule (CEACAM) family with orthologs in various mammalian species (125-126). Full-length CEACAM1 comprises an N-terminal, membrane-distal immunoglobulin variable-region-like (IgV-like) domain which is followed by up to three membrane-proximal immunoglobulin constant-region type-2-like (IgC2-like) domains. The IgV-like domain of CEACAM1 is relatively conserved among CEA-family members (127). CEACAM1 is expressed widely in different cell types such as epithelial cells, endothelial cells, various leukocytes as well as other cell types after induction (128-131).

CEACAM1 has been involved in various physiological processes associated with signal transduction and protein-protein interaction (128). It exhibits pro-angiogenic effects acting as a major effector of vascular endothelial growth factor (VEGF) and stimulus of the proliferation, chemotaxis and capillary-like tube formation of microvascular endothelial cells (132). Besides its functions in angiogenesis, CEACAM1 plays a role in the regulation of insulin by acting as a substrate for the insulin receptor (133).

CEACAM1 is hijacked as a receptor by several pathogens including bacteria as well as all MHV strains (75, 77, 125, 134). Murine CEACAM1 (mCEACAM1) is encoded by two alternative alleles, mCEACAM1a and mCEACAM1b, and mCEACAM1a is a much more efficient receptor for MHV than mCEACAM1b (135). A monoclonal antibody targeting the N-terminus of CEACAM1 blocked virus attachment to murine fibroblasts and infection of variant murine cell lines, and provided partial protection to infection of BABL/c mice. Different isoforms of CEACAM1 were shown to facilitate the infection of MHV-A59 (75-76, 136).

The NTD of the MHV S1 protein demonstrates high structural similarity with human galectin-3 and the rotavirus carbohydrate-binding VP4 protein, which may suggest common ancestry (137-138). However, the MHV S protein interacts with CEACAM1 exclusively via protein-protein interaction rather than by binding to its surface carbohydrates (44, 139). Sharing the same galectin-like fold with MHV S1-



NTD, the S1-NTDs of two other betacoronaviruses, HCoV-OC43 and BCoV, bind to 9-O-acetylated sialic acids as receptors for entry (73-74). MHV was proposed to have lost its sugar-binding activity due to a shortened 10-11 loop in the S1-NTD. The shared similarity between coronavirus S1-NTD and human galectins may indicate that the betacoronavirus S1-NTD originated from a host galectin and subsequently acquired different receptor usage specificities by divergent evolution (139).

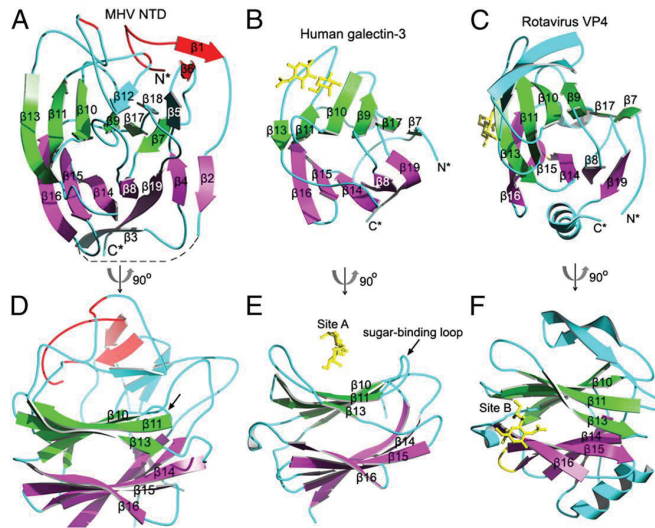


**Figure 1.8 Structural comparison of MHV S-NTD, human galectin and rotavirus VP4.** The structures of the MHV S1-NTD (A,D), human galectin-3 (B,E) and Rotavirus VP4 are shown (C,F) in two orientations. This figure is taken from (139).

### 3.2 Viral protein-host sugar interaction

Carbohydrates, either attached to glycoproteins or glycolipids, are complex molecules composed of various types of monosaccharides and present on almost all living cells. Their structural and functional diversity determines their complex and often indispensable roles in many biological and physiological processes at the molecular level. Viruses, including coronaviruses, are able to enter cells by interacting with terminal carbohydrate moieties, sialic acids.

#### Sialic acids

Sialic acids (SAs) are negatively charged monosaccharides prevalent on cell surface (140). They are in a family including about fifty derivatives of neuraminic acids that share a common nine-carbon (C1-9) backbone but carry various substituents at the amino or hydroxyl groups (141). All different substituents can be combined to obtain a large variety of SAs in the animal kingdom. N-Acetylneuraminic acid (Neu5Ac),

## ***Coronavirus spike-receptor interactions***

---

N-glycolylneuraminic acid (Neu5Gc) and N-acetyl-9-O-acetylneuraminic acid (Neu5,9Ac2) are the three most common terminal moieties on glycan chains of all vertebrate and many invertebrate cells. The distribution of different forms depends on cell types as well as the function of cells (141).

Due to their presence on the cell surface, SAs, either alone or in oligo- or polymeric form, play a crucial role in cell biology because of their accessibility to lectins (142-143). SAs can function in masking recognition sites of lectins or, contrarily, provide a biological target for recognition by lectins (141). SAs mask the penultimate galactose residues on carbohydrates for binding by galectins. Desialylation of proteins or cells leads to recognition by host galectins and subsequent degradation by the immune system. For example, malignant cells could be eliminated by the immune system after desialylation, which in turn could be prevented by oversialylation of these cells (144-145). Sialylation also confers better survival chances to microorganisms in the host which may lead to enhanced virulence (146). In contrast to masking, SAs are recognized by lectins of bacteria and viruses with influenza viruses as the best studied example (reviewed in (142)). SAs are also of great importance for the attachment of coronaviruses to target cells. Coronaviruses are able to recruit SAs but display differences in SA binding fine-specificity. The betacoronaviruses HCoV-OC43 and BCoV use the Neu5,9Ac2 as a functional receptor for entry (36, 37, 73), whereas the gammacoronavirus IBV recognizes  $\alpha$ 2,3-linked SA as an attachment factor (86). Apart from binding to the APN receptor, the alphacoronavirus TGEV S protein also has SA binding activity which was hypothesized to be a determinant for its enteric tropism (65).

### **3.3 Viral carbohydrate-host lectin interaction**

Lectins are a family of molecules that bind carbohydrate moieties mediated by their carbohydrate recognition domain (CRD) at the N-terminus of the extracellular domain (147). Lectins can act as friends or foes to the immune system. They can recognize and target pathogens for degradation. On the contrary, lectins, in particular C-type lectins expressed on antigen presenting cells, can be hijacked by pathogens to mediate their invasion into host cells (148-149) with one representative example, the C-type lectin DC-SIGN (150).

#### ***Dendritic cell-specific intercellular adhesion molecule-3-grabbing nonintegrin***

Dendritic cell (DC)-specific intercellular adhesion molecule (ICAM)-3-grabbing nonintegrin (DC-SIGN, CD209) is a mannose-binding, calcium dependent (C-type) lectin. It is a type II membrane protein comprising a carbohydrate recognition domain (CRD), a neck region and a transmembrane region which is followed by a cytoplasmic tail containing recycling and internalization motifs (150-151). By its neck-repeat domain, it assembles into tetramers, which increases the binding affinity

and specificity of the CRD to its ligands (152-153). DC-SIGN is mainly expressed on immature DCs (iDCs) present in peripheral tissues, or on mature or activated DCs (mDCs) in lymphoid tissues such as lymph nodes, tonsils and spleen at relatively low level (150).

DC-SIGN is a cell marker for DCs and has multiple functions, such as differentiation of DCs from monocytes guided by IL-4 (154), transendothelial migration of DCs through binding to ICAM-2, antigen uptake and T cell priming (155-157). In addition, it not only facilitates antigen uptake as a receptor, but also promotes the adhesion of DCs to T cells (150), endothelial cells (155, 158) and neutrophils (159-160). DC-SIGN is hijacked by a variety of pathogens including viruses, bacteria, fungi as well as several parasites as a mechanism to escape immune surveillance (154). The best studied virus that can recruit DC-SIGN for its own benefit is human immunodeficiency virus type 1 (HIV-1), which binds DC-SIGN through its mannose-rich glycans on the envelope glycoprotein gp120. By interacting with DC-SIGN on DCs, HIV-1 can enter and initiate infection directly (in-cis) (150,161) or it can be transferred to lymph nodes to infect CD4<sup>+</sup> T cells by interacting with its receptors CD4 and CCR5 (in-trans) (162). By either of these two pathways, HIV-1 manipulates DCs as a Trojan horse to escape from the host immune system and invade target cells (163).

Within the coronavirus family, several species have shown their capacity to infect cells via DC-SIGN as an entry portal. Overexpression of DC-SIGN, or its isoform L-SIGN, allows infection of several IBV strains in a SA-independent way (88). DC-SIGN and L-SIGN overexpression also allowed successful entry of SARS-CoV into non-permissive cell lines that lack ACE2 receptor expression (80-82). Furthermore, DC-SIGN was shown to be recruited by type I FIPV as a receptor for infection of monocytes (62). Overexpression of DC-SIGN conferred the infectivity of non-permissive cells to type I and II FIPVs and enhanced infection of permissive cells (164).

### **4. Outline of this thesis**

In order to initiate a successful infection, viruses need to bring their genomes across the cellular membrane into the cytoplasm. This process is initiated by binding of the virus to functional receptors on the cell surface. Given the importance of the receptors for virus entry, epidemiology and pathogenesis, we investigated the receptor usage of two coronavirus pathogens highly relevant for humans and cats, MERS-CoV and FCoV.

In chapter 2, we described the identification of the functional receptor for MERS-CoV. In chapter 3, we subsequently mapped the receptor binding domain within the MERS-CoV spike protein and assessed its potential to elicit neutralizing antibodies. In chapter 4, a microarray-based serological assay was developed using expressed and purified coronavirus S1 subunits, which has proven itself as a practical and convenient diagnostic method to study virus epidemiology, and to identify the animal reservoir of this zoonotic virus.

Except for studies associated with MERS-CoV, we also investigated the receptor usage of FCoVs. The macrophage-tropic FIPV has been shown to use DC-SIGN for entry. Considering that FIPV is a virulent mutant of FECV, we investigated whether the enterocyte-tropic FECV possesses the ability to recruit DC-SIGN for entry or gains this capacity during the transition from FECV to FIPV (Chapter 5).

In the final chapter, a summarizing discussion concerning the studies in this thesis is provided.

## References

1. Hudson CB, Beaudette FR. Infection of the Cloaca with the Virus of Infectious Bronchitis. *Science*. 1932;76(1958):34.
2. Beaudette FR, Hudson CB. Cultivation of the virus of infectious bronchitis. *J Am Vet Med Assoc*. 1937;90:51-8.
3. Almeida JD, Tyrrell DA. The morphology of three previously uncharacterized human respiratory viruses that grow in organ culture. *J Gen Virol*. 1967;1(2):175-8.
4. Hamre D, Procknow JJ. A new virus isolated from the human respiratory tract. *Proc Soc Exp Biol Med*. 1966;121(1):190-3.
5. McIntosh K, Dees JH, Becker WB, Kapikian AZ, Chanock RM. Recovery in tracheal organ cultures of novel viruses from patients with respiratory disease. *Proc Natl Acad Sci U S A*. 1967;57(4):933-40.
6. McIntosh K, Kapikian AZ, Turner HC, Hartley JW, Parrott RH, Chanock RM. Seroepidemiologic studies of coronavirus infection in adults and children. *Am J Epidemiol*. 1970;91(6):585-92.
7. Tyrrell DA, Almeida JD, Cunningham CH, Dowdle WR, Hofstad MS, McIntosh K, et al. Coronaviridae. *Intervirology*. 1975;5(1-2):76-82.
8. Weiss SR, Navas-Martin S. Coronavirus pathogenesis and the emerging pathogen severe acute respiratory syndrome coronavirus. *Microbiol Mol Biol Rev*. 2005;69(4):635-64.
9. Ksiazek TG, Erdman D, Goldsmith CS, Zaki SR, Peret T, Emery S, et al. A novel coronavirus associated with severe acute respiratory syndrome. *N Engl J Med*. 2003;348(20):1953-66.
10. Peiris JS, Lai ST, Poon LL, Guan Y, Yam LY, Lim W, et al. Coronavirus as a possible cause of severe acute respiratory syndrome. *Lancet*. 2003;361(9366):1319-25.
11. Drosten C, Gunther S, Preiser W, van der Werf S, Brodt HR, Becker S, et al. Identification of a novel coronavirus in patients with severe acute respiratory syndrome. *N Engl J Med*. 2003;348(20):1967-76.
12. Fouchier RA, Hartwig NG, Bestebroer TM, Niemeyer B, de Jong JC, Simon JH, et al. A previously undescribed coronavirus associated with respiratory disease in humans. *Proc Natl Acad Sci U S A*. 2004;101(16):6212-6.
13. van der Hoek L, Pyrc K, Jebbink MF, Vermeulen-Oost W, Berkhout RJ, Wolthers KC, et al. Identification of a new human coronavirus. *Nat Med*. 2004;10(4):368-73.
14. Woo PC, Lau SK, Chu CM, Chan KH, Tsoi HW, Huang Y, et al. Characterization and complete genome sequence of a novel coronavirus, coronavirus HKU1, from patients with pneumonia. *J Virol*. 2005;79(2):884-95.
15. de Groot RJ, Baker SC, Baric RS, Brown CS, Drosten C, Enjuanes L, et al. Middle East respiratory syndrome coronavirus (MERS-CoV): announcement of the Coronavirus Study Group. *J Virol*. 2013;87(14):7790-2.
16. Guan Y, Zheng BJ, He YQ, Liu XL, Zhuang ZX, Cheung CL, et al. Isolation and characterization of viruses related to the SARS coronavirus from animals in southern China. *Science*. 2003;302(5643):276-8.
17. Ge XY, Li JL, Yang XL, Chmura AA, Zhu G, Epstein JH, et al. Isolation and characterization of a bat SARS-like coronavirus that uses the ACE2 receptor. *Nature*. 2013;503(7477):535-8.
18. Tu C, Cramer G, Kong X, Chen J, Sun Y, Yu M, et al. Antibodies to SARS coronavirus in civets.

## ***Coronavirus spike-receptor interactions***

---

---

- Emerg Infect Dis. 2004;10(12):2244-8.
19. Pedersen NC. A review of feline infectious peritonitis virus infection: 1963-2008. *J Feline Med Surg*. 2009;11(4):225-58.
  20. Poland AM, Vennema H, Foley JE, Pedersen NC. Two related strains of feline infectious peritonitis virus isolated from immunocompromised cats infected with a feline enteric coronavirus. *J Clin Microbiol*. 1996;34(12):3180-4.
  21. Vennema H, Poland A, Foley J, Pedersen NC. Feline infectious peritonitis viruses arise by mutation from endemic feline enteric coronaviruses. *Virology*. 1998;243(1):150-7.
  22. Drechsler Y, Alcaraz A, Bossong FJ, Collisson EW, Diniz PP. Feline coronavirus in multicat environments. *Vet Clin North Am Small Anim Pract*. 2011;41(6):1133-69.
  23. Benbacher L, Kut E, Besnardeau L, Laude H, Delmas B. Interspecies aminopeptidase-N chimeras reveal species-specific receptor recognition by canine coronavirus, feline infectious peritonitis virus, and transmissible gastroenteritis virus. *J Virol*. 1997;71(1):734-7.
  24. Burkard C, Verheije MH, Wicht O, van Kasteren SI, van Kuppeveld FJ, Haagmans BL, et al. Coronavirus cell entry occurs through the endo-/lysosomal pathway in a proteolysis-dependent manner. *PLoS Pathog*. 2014;10(11):e1004502.
  25. Pedersen NC. An update on feline infectious peritonitis: virology and immunopathogenesis. *Vet J*. 2014;201(2):123-32.
  26. Belouzard S, Millet JK, Licitra BN, Whittaker GR. Mechanisms of coronavirus cell entry mediated by the viral spike protein. *Viruses*. 2012;4(6):1011-33.
  27. Wertheim JO, Chu DK, Peiris JS, Kosakovsky Pond SL, Poon LL. A case for the ancient origin of coronaviruses. *J Virol*. 2013;87(12):7039-45.
  28. Lai MMC, Cavanagh D. The molecular biology of coronaviruses. *AdvVirus Res*. 1997;48:1-100.
  29. Tyrrell DAJ, Almeida JD, Berry DM, Cunningham CH, Hamre D, Hofstad MS, et al. Coronaviruses. *Nature*. 1968;220:650.
  30. Bosch BJ, van der Zee R, de Haan CA, Rottier PJ. The coronavirus spike protein is a class I virus fusion protein: structural and functional characterization of the fusion core complex. *J Virol*. 2003;77(16):8801-11.
  31. Cowley TJ, Weiss SR. Murine coronavirus neuropathogenesis: determinants of virulence. *J Neurovirol*. 2010;16(6):427-34.
  32. Krempf C, Schultze B, Laude H, Herrler G. Point mutations in the S protein connect the sialic acid binding activity with the enteropathogenicity of transmissible gastroenteritis coronavirus. *J Virol*. 1997;71(4):3285-7.
  33. Sanchez CM, Izeta A, Sanchez-Morgado JM, Alonso S, Sola I, Balasch M, et al. Targeted recombination demonstrates that the spike gene of transmissible gastroenteritis coronavirus is a determinant of its enteric tropism and virulence. *J Virol*. 1999;73(9):7607-18. Epub 1999/08/10. PubMed PMID: 10438851; PubMed Central PMCID: PMC104288.
  34. Callebaut PE, Pensaert MB. Characterization and isolation of structural polypeptides in haemagglutinating encephalomyelitis virus. *J Gen Virol*. 1980;48(1):193-204. Epub 1980/05/01. PubMed PMID: 7381432.
  35. King B, Potts BJ, Brian DA. Bovine coronavirus hemagglutinin protein. *Virus Res*. 1985;2(1):53-9.
  36. Vlasak R, Luytjes W, Leider J, Spaan W, Palese P. The E3 protein of bovine coronavirus is a receptor-destroying enzyme with acetylesterase activity. *J Virol*. 1988;62(12):4686-90.
  37. Vlasak R, Luytjes W, Spaan W, Palese P. Human and bovine coronaviruses recognize sialic

- acid-containing receptors similar to those of influenza C viruses. *Proc Natl Acad Sci U S A*. 1988;85(12):4526-9.
38. Stadler K, Masignani V, Eickmann M, Becker S, Abrignani S, Klenk HD, et al. SARS--beginning to understand a new virus. *Nat Rev Microbiol*. 2003;1(3):209-18.
  39. Perlman S, Netland J. Coronaviruses post-SARS: update on replication and pathogenesis. *Nat Rev Microbiol*. 2009;7(6):439-50.
  40. Bergmann CC, Lane TE, Stohlman SA. Coronavirus infection of the central nervous system: host-virus stand-off. *Nat Rev Microbiol*. 2006;4(2):121-32.
  41. Bisht H, Roberts A, Vogel L, Bukreyev A, Collins PL, Murphy BR, et al. Severe acute respiratory syndrome coronavirus spike protein expressed by attenuated vaccinia virus protectively immunizes mice. *Proc Natl Acad Sci U S A*. 2004;101(17):6641-6.
  42. Simmons G, Zmora P, Gierer S, Heurich A, Pohlmann S. Proteolytic activation of the SARS-coronavirus spike protein: cutting enzymes at the cutting edge of antiviral research. *Antiviral Res*. 2013;100(3):605-14.
  43. Heald-Sargent T, Gallagher T. Ready, set, fuse! The coronavirus spike protein and acquisition of fusion competence. *Viruses*. 2012;4(4):557-80.
  44. Kubo H, Yamada YK, Taguchi F. Localization of neutralizing epitopes and the receptor-binding site within the amino-terminal 330 amino acids of the murine coronavirus spike protein. *J Virol*. 1994;68(9):5403-10.
  45. Bonavia A, Zelus BD, Wentworth DE, Talbot PJ, Holmes KV. Identification of a receptor-binding domain of the spike glycoprotein of human coronavirus HCoV-229E. *J Virol*. 2003;77(4):2530-8.
  46. He Y, Zhou Y, Liu S, Kou Z, Li W, Farzan M, et al. Receptor-binding domain of SARS-CoV spike protein induces highly potent neutralizing antibodies: implication for developing subunit vaccine. *Biochem Biophys Res Commun*. 2004;324(2):773-81.
  47. Mou H, Raj VS, van Kuppeveld FJ, Rottier PJ, Haagmans BL, Bosch BJ. The receptor binding domain of the new Middle East respiratory syndrome coronavirus maps to a 231-residue region in the spike protein that efficiently elicits neutralizing antibodies. *J Virol*. 2013;87(16):9379-83.
  48. Madu IG, Roth SL, Belouzard S, Whittaker GR. Characterization of a highly conserved domain within the severe acute respiratory syndrome coronavirus spike protein S2 domain with characteristics of a viral fusion peptide. *J Virol*. 2009;83(15):7411-21.
  49. de Haan CA, Stadler K, Godeke GJ, Bosch BJ, Rottier PJ. Cleavage inhibition of the murine coronavirus spike protein by a furin-like enzyme affects cell-cell but not virus-cell fusion. *J Virol*. 2004;78(11):6048-54.
  50. de Haan CA, Haijema BJ, Schellen P, Wichgers Schreur P, te Lintelo E, Vennema H, et al. Cleavage of group 1 coronavirus spike proteins: how furin cleavage is traded off against heparan sulfate binding upon cell culture adaptation. *J Virol*. 2008;82(12):6078-83.
  51. Sturman LS, Ricard CS, Holmes KV. Proteolytic cleavage of the E2 glycoprotein of murine coronavirus: activation of cell-fusing activity of virions by trypsin and separation of two different 90K cleavage fragments. *J Virol*. 1985;56(3):904-11.
  52. Gombold JL, Hingley ST, Weiss SR. Fusion-defective mutants of mouse hepatitis virus A59 contain a mutation in the spike protein cleavage signal. *J Virol*. 1993;67(8):4504-12.
  53. Bos EC, Luytjes W, Spaan WJ. The function of the spike protein of mouse hepatitis virus strain A59 can be studied on virus-like particles: cleavage is not required for infectivity. *J Virol*. 1997;71(12):9427-33.

## ***Coronavirus spike-receptor interactions***

---

54. Epand RM. Fusion peptides and the mechanism of viral fusion. *Biochim Biophys Acta*. 2003;1614(1):116-21.
55. Belouzard S, Chu VC, Whittaker GR. Activation of the SARS coronavirus spike protein via sequential proteolytic cleavage at two distinct sites. *Proc Natl Acad Sci U S A*. 2009;106(14):5871-6.
56. Wicht O, Li W, Willems L, Meuleman TJ, Wubbolts RW, van Kuppeveld FJ, et al. Proteolytic activation of the porcine epidemic diarrhea coronavirus spike fusion protein by trypsin in cell culture. *J Virol*. 2014;88(14):7952-61.
57. Tresnan DB, Levis R, Holmes KV. Feline aminopeptidase N serves as a receptor for feline, canine, porcine, and human coronaviruses in serogroup I. *J Virol*. 1996;70(12):8669-74.
58. Desmarests LM, Theuns S, Roukaerts ID, Acar DD, Nauwynck HJ. Role of sialic acids in feline enteric coronavirus infections. *J Gen Virol*. 2014;95(Pt 9):1911-8.
59. Hegyi A, Kolb AF. Characterization of determinants involved in the feline infectious peritonitis virus receptor function of feline aminopeptidase N. *J Gen Virol*. 1998;79 ( Pt 6):1387-91.
60. Kolb AF, Hegyi A, Maile J, Heister A, Hagemann M, Siddell SG. Molecular analysis of the coronavirus-receptor function of aminopeptidase N. *Adv Exp Med Biol*. 1998;440:61-7.
61. Regan AD, Ousterout DG, Whittaker GR. Feline Lectin Activity Is Critical for the Cellular Entry of Feline Infectious Peritonitis Virus. *Journal of Virology*. 2010;84(15):7917-21.
62. Van Hamme E, Desmarests L, Dewerchin HL, Nauwynck HJ. Intriguing interplay between feline infectious peritonitis virus and its receptors during entry in primary feline monocytes. *Virus Research*. 2011;160(1-2):32-9.
63. Schwegmann-Wessels C, Herrler G. Sialic acids as receptor determinants for coronaviruses. *Glycoconj J*. 2006;23(1-2):51-8.
64. Delmas B, Gelfi J, Sjostrom H, Noren O, Laude H. Further characterization of aminopeptidase-N as a receptor for coronaviruses. *Adv Exp Med Biol*. 1993;342:293-8.
65. Schultze B, Krempl C, Ballesteros ML, Shaw L, Schauer R, Enjuanes L, et al. Transmissible gastroenteritis coronavirus, but not the related porcine respiratory coronavirus, has a sialic acid (N-glycolylneuraminic acid) binding activity. *J Virol*. 1996;70(8):5634-7.
66. Delmas B, Gelfi J, L'Haridon R, Vogel LK, Sjostrom H, Noren O, et al. Aminopeptidase N is a major receptor for the entero-pathogenic coronavirus TGEV. *Nature*. 1992;357(6377):417-20.
67. Oh JS, Song DS, Park BK. Identification of a putative cellular receptor 150 kDa polypeptide for porcine epidemic diarrhea virus in porcine enterocytes. *J Vet Sci*. 2003;4(3):269-75.
68. Li BX, Ge JW, Li YJ. Porcine aminopeptidase N is a functional receptor for the PEDV coronavirus. *Virology*. 2007;365(1):166-72.
69. Yeager CL, Ashmun RA, Williams RK, Cardellicchio CB, Shapiro LH, Look AT, et al. Human aminopeptidase N is a receptor for human coronavirus 229E. *Nature*. 1992;357(6377):420-2.
70. Jeffers SA, Hemmila EM, Holmes KV. Human coronavirus 229E can use CD209L (L-SIGN) to enter cells. *Adv Exp Med Biol*. 2006;581:265-9.
71. Hofmann H, Pyrc K, van der Hoek L, Geier M, Berkhout B, Pohlmann S. Human coronavirus NL63 employs the severe acute respiratory syndrome coronavirus receptor for cellular entry. *Proc Natl Acad Sci USA*. 2005;102(22):7988-93.
72. Hofmann H, Simmons G, Rennekamp AJ, Chaipan C, Gramberg T, Heck E, et al. Highly conserved regions within the spike proteins of human coronaviruses 229E and NL63 determine recognition of their respective cellular receptors. *Journal of virology*. 2006;80(17):8639-52.
73. Schultze B, Gross HJ, Brossmer R, Herrler G. The S protein of bovine coronavirus is a hemagglutinin



- recognizing 9-O-acetylated sialic acid as a receptor determinant. *J Virol.* 1991;65(11):6232-7.
74. Kunkel F, Herrler G. Structural and functional analysis of the surface protein of human coronavirus OC43. *Virology.* 1993;195(1):195-202.
  75. Dveksler GS, Pensiero MN, Cardellichio CB, Williams RK, Jiang GS, Holmes KV, et al. Cloning of the mouse hepatitis virus (MHV) receptor: expression in human and hamster cell lines confers susceptibility to MHV. *J Virol.* 1991;65(12):6881-91.
  76. Dveksler GS, Dieffenbach CW, Cardellichio CB, McCuaig K, Pensiero MN, Jiang GS, et al. Several members of the mouse carcinoembryonic antigen-related glycoprotein family are functional receptors for the coronavirus mouse hepatitis virus-A59. *J Virol.* 1993;67(1):1-8.
  77. Dveksler GS, Pensiero MN, Dieffenbach CW, Cardellichio CB, Basile AA, Elia PE, et al. Mouse hepatitis virus strain A59 and blocking antireceptor monoclonal antibody bind to the N-terminal domain of cellular receptor. *Proc Natl Acad Sci U S A.* 1993;90(5):1716-20.
  78. Wurzer WJ, Obojes K, Vlasak R. The sialate-4-O-acetylerases of coronaviruses related to mouse hepatitis virus: a proposal to reorganize group 2 Coronaviridae. *J Gen Virol.* 2002;83(Pt 2):395-402.
  79. Li W, Moore MJ, Vasileva N, Sui J, Wong SK, Berne MA, et al. Angiotensin-converting enzyme 2 is a functional receptor for the SARS coronavirus. *Nature.* 2003;426(6965):450-4.
  80. Jeffers SA, Tusell SM, Gillim-Ross L, Hemmila EM, Achenbach JE, Babcock GJ, et al. CD209L (L-SIGN) is a receptor for severe acute respiratory syndrome coronavirus. *Proc Natl Acad Sci U S A.* 2004;101(44):15748-53.
  81. Marzi A, Gramberg T, Simmons G, Moller P, Rennekamp AJ, Krumbiegel M, et al. DC-SIGN and DC-SIGNR interact with the glycoprotein of Marburg virus and the S protein of severe acute respiratory syndrome coronavirus. *J Virol.* 2004;78(21):12090-5.
  82. Chan VS, Chan KY, Chen Y, Poon LL, Cheung AN, Zheng B, et al. Homozygous L-SIGN (CLEC4M) plays a protective role in SARS coronavirus infection. *Nat Genet.* 2006;38(1):38-46.
  83. Raj VS, Mou H, Smits SL, Dekkers DH, Muller MA, Dijkman R, et al. Dipeptidyl peptidase 4 is a functional receptor for the emerging human coronavirus-EMC. *Nature.* 2013;495(7440):251-4.
  84. Wang Q, Qi J, Yuan Y, Xuan Y, Han P, Wan Y, et al. Bat origins of MERS-CoV supported by bat coronavirus HKU4 usage of human receptor CD26. *Cell Host Microbe.* 2014;16(3):328-37.
  85. Yang Y, Du L, Liu C, Wang L, Ma C, Tang J, et al. Receptor usage and cell entry of bat coronavirus HKU4 provide insight into bat-to-human transmission of MERS coronavirus. *Proc Natl Acad Sci USA.* 2014;111(34):12516-21.
  86. Winter C, Schwegmann-Wessels C, Cavanagh D, Neumann U, Herrler G. Sialic acid is a receptor determinant for infection of cells by avian Infectious bronchitis virus. *J Gen Virol.* 2006;87(Pt 5):1209-16.
  87. Wickramasinghe IN, van Beurden SJ, Weerts EA, Verheije MH. The avian coronavirus spike protein. *Virus Res.* 2014;194:37-48.
  88. Zhang Y, Buckles E, Whittaker GR. Expression of the C-type lectins DC-SIGN or L-SIGN alters host cell susceptibility for the avian coronavirus, infectious bronchitis virus. *Vet Microbiol.* 2012;157(3-4):285-93.
  89. Qu XX, Hao P, Song XJ, Jiang SM, Liu YX, Wang PG, et al. Identification of two critical amino acid residues of the severe acute respiratory syndrome coronavirus spike protein for its variation in zoonotic tropism transition via a double substitution strategy. *J Biol Chem.* 2005;280(33):29588-95.
  90. Edman P. A method for the determination of amino acid sequence in peptides. *Arch Biochem.*

## ***Coronavirus spike-receptor interactions***

---

- 1949;22(3):475.
91. Li F, Li W, Farzan M, Harrison SC. Structure of SARS coronavirus spike receptor-binding domain complexed with receptor. *Science*. 2005;309(5742):1864-8.
  92. Hou Y, Peng C, Yu M, Li Y, Han Z, Li F, et al. Angiotensin-converting enzyme 2 (ACE2) proteins of different bat species confer variable susceptibility to SARS-CoV entry. *Arch Virol*. 2010;155(10):1563-9.
  93. Hofmann M, Wyler R. Propagation of the virus of porcine epidemic diarrhea in cell culture. *J Clin Microbiol*. 1988;26(11):2235-9.
  94. Matsuyama S, Nagata N, Shirato K, Kawase M, Takeda M, Taguchi F. Efficient activation of the severe acute respiratory syndrome coronavirus spike protein by the transmembrane protease TMPRSS2. *J Virol*. 2010;84(24):12658-64.
  95. Hooper NM. Families of zinc metalloproteases. *FEBS Lett*. 1994;354(1):1-6. Epub 1994/10/31. doi: 0014-5793(94)01079-X [pii]. PubMed PMID: 7957888.
  96. Olsen J, Kokholm K, Noren O, Sjoström H. Structure and expression of aminopeptidase N. *Adv Exp Med Biol*. 1997;421:47-57.
  97. Riemann D, Hansen GH, Niels-Christiansen L, Thorsen E, Immerdal L, Santos AN, et al. Caveolae/lipid rafts in fibroblast-like synoviocytes: ectopeptidase-rich membrane microdomains. *Biochem J*. 2001;354(Pt 1):47-55.
  98. Jeffery CJ. Moonlighting proteins: old proteins learning new tricks. *Trends Genet*. 2003;19(8):415-7.
  99. Chen L, Lin YL, Peng G, Li F. Structural basis for multifunctional roles of mammalian aminopeptidase N. *Proc Natl Acad Sci USA*. 2012;109(44):17966-71.
  100. König M, Zimmer AM, Steiner H, Holmes PV, Crawley JN, Brownstein MJ, et al. Pain responses, anxiety and aggression in mice deficient in pre-proenkephalin. *Nature*. 1996;383(6600):535-8.
  101. Danziger RS. Aminopeptidase N in arterial hypertension. *Heart Fail Rev*. 2008;13(3):293-8.
  102. Chang YW, Chen SC, Cheng EC, Ko YP, Lin YC, Kao YR, et al. CD13 (aminopeptidase N) can associate with tumor-associated antigen L6 and enhance the motility of human lung cancer cells. *Int J Cancer*. 2005;116(2):243-52.
  103. Mina-Osorio P, Winnicka B, O'Connor C, Grant CL, Vogel LK, Rodriguez-Pinto D, et al. CD13 is a novel mediator of monocytic/endothelial cell adhesion. *J Leukoc Biol*. 2008;84(2):448-59.
  104. Mina-Osorio P, Shapiro LH, Ortega E. CD13 in cell adhesion: aminopeptidase N (CD13) mediates homotypic aggregation of monocytic cells. *J Leukoc Biol*. 2006;79(4):719-30.
  105. Salmi M, Jalkanen S. Cell-surface enzymes in control of leukocyte trafficking. *Nat Rev Immunol*. 2005;5(10):760-71.
  106. Dean GA, Olivry T, Stanton C, Pedersen NC. In vivo cytokine response to experimental feline infectious peritonitis virus infection. *Vet Microbiol*. 2003;97(1-2):1-12.
  107. Olsen J, Sjoström H, Noren O. Cloning of the pig aminopeptidase N gene. Identification of possible regulatory elements and the exon distribution in relation to the membrane-spanning region. *FEBS letters*. 1989;251(1-2):275-81.
  108. Look AT, Ashmun RA, Shapiro LH, Peiper SC. Human myeloid plasma membrane glycoprotein CD13 (gp150) is identical to aminopeptidase N. *The Journal of clinical investigation*. 1989;83(4):1299-307.
  109. Watt VM, Yip CC. Amino acid sequence deduced from a rat kidney cDNA suggests it encodes the Zn-peptidase aminopeptidase N. *The Journal of biological chemistry*. 1989;264(10):5480-7.
  110. Reguera J, Santiago C, Mudgal G, Ordone D, Enjuanes L, Casasnovas JM. Structural bases of

- coronavirus attachment to host aminopeptidase N and its inhibition by neutralizing antibodies. *PLoS Pathog.* 2012;8(8):e1002859.
111. Wentworth DE, Holmes KV. Molecular determinants of species specificity in the coronavirus receptor aminopeptidase N (CD13): influence of N-linked glycosylation. *J Virol.* 2001;75(20):9741-52.
  112. Tusell SM, Schittone SA, Holmes KV. Mutational analysis of aminopeptidase N, a receptor for several group 1 coronaviruses, identifies key determinants of viral host range. *J Virol.* 2007;81(3):1261-73.
  113. Tipnis SR, Hooper NM, Hyde R, Karran E, Christie G, Turner AJ. A human homolog of angiotensin-converting enzyme: Cloning and functional expression as a captopril-insensitive carboxypeptidase. *J Biol Chem.* 2000;275(43):33238-43.
  114. Gallagher PE, Ferrario CM, Tallant EA. Regulation of ACE2 in cardiac myocytes and fibroblasts. *Am J Physiol Heart Circ Physiol.* 2008;295(6):H2373-9.
  115. Donoghue M, Hsieh F, Baronas E, Godbout K, Gosselin M, Stagliano N, et al. A novel angiotensin-converting enzyme-related carboxypeptidase (ACE2) converts angiotensin I to angiotensin 1-9. *Circ Res.* 2000;87(5):E1-9.
  116. Douglas GC, O'Bryan MK, Hedger MP, Lee DK, Yarski MA, Smith AI, et al. The novel angiotensin-converting enzyme (ACE) homolog, ACE2, is selectively expressed by adult Leydig cells of the testis. *Endocrinology.* 2004;145(10):4703-11.
  117. Kuba K, Imai Y, Ohto-Nakanishi T, Penninger JM. Trilogy of ACE2: a peptidase in the renin-angiotensin system, a SARS receptor, and a partner for amino acid transporters. *Pharmacol Ther.* 2010;128(1):119-28.
  118. Vickers C, Hales P, Kaushik V, Dick L, Gavin J, Tang J, et al. Hydrolysis of biological peptides by human angiotensin-converting enzyme-related carboxypeptidase. *J Biol Chem.* 2002;277(17):14838-43.
  119. Santos RA, Frezard F, Ferreira AJ. Angiotensin-(1-7): blood, heart, and blood vessels. *Curr Med Chem Cardiovasc Hematol Agents.* 2005;3(4):383-91.
  120. Ferrario CM. Angiotensin-converting enzyme 2 and angiotensin-(1-7): an evolving story in cardiovascular regulation. *Hypertension.* 2006;47(3):515-21.
  121. Turner AJ, Hiscox JA, Hooper NM. ACE2: from vasopeptidase to SARS virus receptor. *Trends Pharmacol Sci.* 2004;25(6):291-4.
  122. Li W, Zhang C, Sui J, Kuhn JH, Moore MJ, Luo S, et al. Receptor and viral determinants of SARS-coronavirus adaptation to human ACE2. *EMBO J.* 2005;24(8):1634-43.
  123. Wu K, Li W, Peng G, Li F. Crystal structure of NL63 respiratory coronavirus receptor-binding domain complexed with its human receptor. *Proc Natl Acad Sci U S A.* 2009;106(47):19970-4.
  124. Li F. Receptor Recognition Mechanisms of Coronaviruses: a Decade of Structural Studies. *J Virol.* 2014;89(4):1954-64.
  125. Beauchemin N, Draber P, Dveksler G, Gold P, Gray-Owen S, Grunert F, et al. Redefined nomenclature for members of the carcinoembryonic antigen family. *Exp Cell Res.* 1999;252(2):243-9.
  126. Zebhauser R, Kammerer R, Eisenried A, McLellan A, Moore T, Zimmermann W. Identification of a novel group of evolutionarily conserved members within the rapidly diverging murine Cea family. *Genomics.* 2005;86(5):566-80.
  127. Gray-Owen SD, Blumberg RS. CEACAM1: contact-dependent control of immunity. *Nat Rev Immunol.* 2006;6(6):433-46.
  128. Kuespert K, Pils S, Hauck CR. CEACAMs: their role in physiology and pathophysiology. *Curr Opin Cell Biol.* 2006;18(5):565-71.

## ***Coronavirus spike-receptor interactions***

---

---

129. Prall F, Nollau P, Neumaier M, Haubeck HD, Drzeniek Z, Helmchen U, et al. CD66a (BGP), an adhesion molecule of the carcinoembryonic antigen family, is expressed in epithelium, endothelium, and myeloid cells in a wide range of normal human tissues. *J Histochem Cytochem.* 1996;44(1):35-41.
130. Odin P, Obrink B. Quantitative determination of the organ distribution of the cell adhesion molecule cell-CAM 105 by radioimmunoassay. *Exp Cell Res.* 1987;171(1):1-15.
131. Kammerer R, Hahn S, Singer BB, Luo JS, von Kleist S. Biliary glycoprotein (CD66a), a cell adhesion molecule of the immunoglobulin superfamily, on human lymphocytes: structure, expression and involvement in T cell activation. *Eur J Immunol.* 1998;28(11):3664-74.
132. Ergun S, Kilik N, Ziegeler G, Hansen A, Nollau P, Gotze J, et al. CEA-related cell adhesion molecule 1: a potent angiogenic factor and a major effector of vascular endothelial growth factor. *Mol Cell.* 2000;5(2):311-20.
133. Soni P, Al-Hosaini KA, Fernstrom MA, Najjar SM. Cell adhesion properties and effects on receptor-mediated insulin endocytosis are independent properties of pp120, a substrate of the insulin receptor tyrosine kinase. *Mol Cell Biol Res Commun.* 1999;1(2):102-8.
134. Hauck CR, Agerer F, Muenzner P, Schmitter T. Cellular adhesion molecules as targets for bacterial infection. *Eur J Cell Biol.* 2006;85(3-4):235-42.
135. Ohtsuka N, Yamada YK, Taguchi F. Difference in virus-binding activity of two distinct receptor proteins for mouse hepatitis virus. *J Gen Virol.* 1996;77 ( Pt 8):1683-92.
136. Williams RK, Jiang GS, Holmes KV. Receptor for mouse hepatitis virus is a member of the carcinoembryonic antigen family of glycoproteins. *Proc Natl Acad Sci U S A.* 1991;88(13):5533-6.
137. Dormitzer PR, Sun ZY, Wagner G, Harrison SC. The rhesus rotavirus VP4 sialic acid binding domain has a galectin fold with a novel carbohydrate binding site. *EMBO J.* 2002;21(5):885-97.
138. Seetharaman J, Kanigsberg A, Slaaby R, Leffler H, Barondes SH, Rini JM. X-ray crystal structure of the human galectin-3 carbohydrate recognition domain at 2.1-Å resolution. *J Biol Chem.* 1998;273(21):13047-52.
139. Peng G, Sun D, Rajashankar KR, Qian Z, Holmes KV, Li F. Crystal structure of mouse coronavirus receptor-binding domain complexed with its murine receptor. *Proc Natl Acad Sci U S A.* 2011;108(26):10696-701.
140. Varki A. Diversity in the sialic acids. *Glycobiology.* 1992;2(1):25-40.
141. Schauer R. Sialic acids: fascinating sugars in higher animals and man. *Zoology (Jena).* 2004;107(1):49-64.
142. Kelm S, Schauer R. Sialic acids in molecular and cellular interactions. *Int Rev Cytol.* 1997;175:137-240.
143. Muhlenhoff M, Eckhardt M, Gerardy-Schahn R. Polysialic acid: three-dimensional structure, biosynthesis and function. *Curr Opin Struct Biol.* 1998;8(5):558-64.
144. Lamari FN, Karamanos NK. Separation methods for sialic acids and critical evaluation of their biologic relevance. *J Chromatogr B Analyt Technol Biomed Life Sci.* 2002;781(1-2):3-19.
145. Schauer R. Sialic acids as regulators of molecular and cellular interactions. *Current opinion in structural biology.* 2009;19(5):507-14.
146. Vimr E, Lichtensteiger C. To sialylate, or not to sialylate: that is the question. *Trends Microbiol.* 2002;10(6):254-7.
147. Lam SK, Ng TB. Lectins: production and practical applications. *Appl Microbiol Biotechnol.* 2010;89(1):45-55.

148. Cambi A, Figdor CG. Dual function of C-type lectin-like receptors in the immune system. *Curr Opin Cell Biol.* 2003;15(5):539-46.
149. Cambi A, Koopman M, Figdor CG. How C-type lectins detect pathogens. *Cell Microbiol.* 2005;7(4):481-8.
150. Geijtenbeek TB, Torensma R, van Vliet SJ, van Duijnhoven GC, Adema GJ, van Kooyk Y, et al. Identification of DC-SIGN, a novel dendritic cell-specific ICAM-3 receptor that supports primary immune responses. *Cell.* 2000;100(5):575-85.
151. Kwon DS, Gregorio G, Bitton N, Hendrickson WA, Littman DR. DC-SIGN-mediated internalization of HIV is required for trans-enhancement of T cell infection. *Immunity.* 2002;16(1):135-44.
152. Mitchell DA, Fadden AJ, Drickamer K. A novel mechanism of carbohydrate recognition by the C-type lectins DC-SIGN and DC-SIGNR. Subunit organization and binding to multivalent ligands. *J Biol Chem.* 2001;276(31):28939-45.
153. Frison N, Taylor ME, Soilleux E, Bousser MT, Mayer R, Monsigny M, et al. Oligolysine-based oligosaccharide clusters: selective recognition and endocytosis by the mannose receptor and dendritic cell-specific intercellular adhesion molecule 3 (ICAM-3)-grabbing nonintegrin. *J Biol Chem.* 2003;278(26):23922-9.
154. Svaiger U, Anderlueh M, Jeras M, Obermajer N. C-type lectin DC-SIGN: an adhesion, signalling and antigen-uptake molecule that guides dendritic cells in immunity. *Cell Signal.* 2010;22(10):1397-405.
155. Geijtenbeek TB, Krooshoop DJ, Bleijs DA, van Vliet SJ, van Duijnhoven GC, Grabovsky V, et al. DC-SIGN-ICAM-2 interaction mediates dendritic cell trafficking. *Nat Immunol.* 2000;1(4):353-7.
156. Ludwig IS, Lekkerkerker AN, Depla E, Bosman F, Musters RJ, Depraetere S, et al. Hepatitis C virus targets DC-SIGN and L-SIGN to escape lysosomal degradation. *J Virol.* 2004;78(15):8322-32.
157. Cambi A, Gijzen K, de Vries I J, Torensma R, Joosten B, Adema GJ, et al. The C-type lectin DC-SIGN (CD209) is an antigen-uptake receptor for *Candida albicans* on dendritic cells. *Eur J Immunol.* 2003;33(2):532-8.
158. Garcia-Vallejo JJ, van Liempt E, da Costa Martins P, Beckers C, van het Hof B, Gringhuis SI, et al. DC-SIGN mediates adhesion and rolling of dendritic cells on primary human umbilical vein endothelial cells through LewisY antigen expressed on ICAM-2. *Mol Immunol.* 2008;45(8):2359-69.
159. van Gisbergen KP, Geijtenbeek TB, van Kooyk Y. Close encounters of neutrophils and DCs. *Trends Immunol.* 2005;26(12):626-31.
160. van Gisbergen KP, Sanchez-Hernandez M, Geijtenbeek TB, van Kooyk Y. Neutrophils mediate immune modulation of dendritic cells through glycosylation-dependent interactions between Mac-1 and DC-SIGN. *J Exp Med.* 2005;201(8):1281-92.
161. Geijtenbeek TB, Kwon DS, Torensma R, van Vliet SJ, van Duijnhoven GC, Middel J, et al. DC-SIGN, a dendritic cell-specific HIV-1-binding protein that enhances trans-infection of T cells. *Cell.* 2000;100(5):587-97.
162. Arrighi JF, Pion M, Garcia E, Escola JM, van Kooyk Y, Geijtenbeek TB, et al. DC-SIGN-mediated infectious synapse formation enhances X4 HIV-1 transmission from dendritic cells to T cells. *J Exp Med.* 2004;200(10):1279-88.
163. van Kooyk Y, Appelmelk B, Geijtenbeek TB. A fatal attraction: *Mycobacterium tuberculosis* and HIV-1 target DC-SIGN to escape immune surveillance. *Trends Mol Med.* 2003;9(4):153-9.
164. Regan AD, Whittaker GR. Utilization of DC-SIGN for Entry of Feline Coronaviruses into Host Cells. *Journal of Virology.* 2008;82(23):11992-6.



# CHAPTER 2

## Dipeptidyl peptidase 4 is a functional receptor for the emerging human coronavirus-EMC

**V. Stalin Raj<sup>1,a</sup>, Huihui Mou<sup>2,a</sup>, Saskia L. Smits<sup>1,7</sup>, Dick H.W. Dekkers<sup>3</sup>, Marcel A. Müller<sup>4</sup>, Ronald Dijkman<sup>6</sup>, Doreen Muth<sup>4</sup>, Jeroen A.A. Demmers<sup>3</sup>, Ali Zaki<sup>5</sup>, Ron A.M. Fouchier<sup>1</sup>, Volker Thiel<sup>6</sup>, Christian Drosten<sup>4</sup>, Peter J.M. Rottier<sup>2</sup>, Albert D.M.E. Osterhaus<sup>1</sup>, Berend Jan Bosch<sup>2,b</sup> & Bart L. Haagmans<sup>1,b</sup>**

1 Department of Viroscience, Erasmus Medical Center, Rotterdam, the Netherlands

2 Virology Division, Department of Infectious Diseases & Immunology, Faculty of Veterinary Medicine, Utrecht University, Utrecht, the Netherlands

3 Proteomics Department, Erasmus Medical Center, Rotterdam, the Netherlands

4 Institute of Virology, University of Bonn Medical Centre, Bonn, Germany

5 Virology Laboratory, Dr Soliman Fakeeh Hospital, Jeddah, Kingdom of Saudi Arabia

6 Institute of Immunobiology, Kanton Hospital St. Gallen, St. Gallen, Switzerland.

7 Viroclinics Biosciences BV, Rotterdam, the Netherlands

a V.S.R and H.M. contributed equally to this work.

b B.J.B. and B.L.H contributed equally to this work.

*Nature, 2013 Mar 14;495(7440):251-4.*



### **Abstract**

Most human coronaviruses (CoVs) cause mild upper respiratory tract disease but may be associated with more severe pulmonary disease in immunocompromised individuals<sup>1</sup>. SARS-CoV on the other hand caused severe lower respiratory disease with nearly 10% mortality and evidence of systemic spread. Recently, another coronavirus (HCoV-EMC) was identified in patients with severe and sometimes lethal lower respiratory tract infection<sup>2,3</sup>. Viral genome analysis revealed close relatedness to CoVs found in bats<sup>4</sup>. Here we identify dipeptidyl peptidase 4 (DPP4) - also known as CD26 - as a functional receptor for HCoV-EMC. DPP4 specifically co-purified with the receptor binding S1 domain of the HCoV-EMC spike protein from lysates of susceptible Huh-7 cells. Antibodies directed against DPP4 inhibited HCoV-EMC infection of primary human bronchial epithelial cells and Huh-7 cells. Expression of human and bat (*Pipistrellus pipistrellus*) DPP4 in non-susceptible COS-7 cells enabled infection by HCoV-EMC. The use of the evolutionary conserved DPP4 protein from different species as a functional receptor provides clues about HCoV-EMC's host range potential. In addition, it will contribute critically to our understanding of the pathogenesis and epidemiology of this emerging human CoV, and may facilitate the development of intervention strategies.



Coronaviruses (CoVs) infect a wide range of mammals and birds. Their tropism is primarily determined by the ability of the spike (S) entry protein to bind to a cell surface receptor. Coronaviruses have zoonotic potential due to the adaptability of their S protein to receptors of other species, most notably demonstrated by SARS-CoV<sup>5</sup>, the causative agent of the SARS epidemic, which likely originated from bats<sup>6</sup>. Recently, a new CoV – named HCoV-EMC – has been identified in thus far nine patients with five fatalities that suffered from severe respiratory illness, in some cases accompanied with renal dysfunction<sup>2,3,7</sup>. Genetically the virus bears resemblance to bat CoVs HKU4 and 5 and - based on phylogenetic analysis using a small fragment of the virus – to a bat CoV found in *Pipistrellus pipistrellus* in the Netherlands<sup>4</sup>. In recent years molecular surveillance studies revealed the existence of at least 60 novel bat CoVs, including relatives of SARS-CoV<sup>8</sup>. As the human cases do not seem to originate from transmission from one source, the epidemiology of HCoV-EMC may be explained by a somehow concealed circulation in the human population or by the repeated introduction from an intermediate animal host. For a better understanding of the biology of this novel CoV, timely identification of the receptor could reveal important clues to its zoonotic transmission potential and pathogenesis and to the design of possible intervention strategies. Two types of CoV protein receptors have been identified; the Betacoronavirus mouse hepatitis virus uses immunoglobulin related carcinoembryonic antigen-related cell adhesion molecules (CEACAM)<sup>9</sup> to enter cells whereas for several Alpha- and Betacoronaviruses two peptidases have been identified as receptors: aminopeptidase N (APN, CD13) for HCoV-229E and several animal CoVs<sup>10, 11</sup> and angiotensin converting enzyme 2 (ACE2) for SARS-CoV<sup>12</sup>. In addition, sialic acid may act as a receptor for some CoVs<sup>13</sup>.

Our initial experiments indicated that HCoV-EMC does not use ACE2 as an entry receptor<sup>14</sup>. Therefore we first examined whether the amino-terminal receptor binding spike domain S1 binds to cells and investigated its correlation with cell susceptibility. We expressed the S1 domain fused to the Fc region of human IgG, yielding a recombinant disulfide bonded dimer of approximately 280 kDa (Supplementary Fig.1). Highly specific binding was observed to African green monkey kidney (Vero) and human liver (Huh-7) cells by immunofluorescence and FACS analysis, while kidney cells of the *Pipistrellus pipistrellus* bat showed intermediate staining (Fig. 1). No S1 binding was detectable to COS-7 African green monkey kidney cells (Fig 1b). Furthermore, no specific binding to any of these cells was observed with a feline CoV S1 domain, while feline cells (***Felis catus*** whole fetus, FCWF) showed strong reactivity (Supplementary Table.1). Binding of HCoV-EMC S1 was shown to correlate with susceptibility to HCoV-EMC infection and with viral genome detection in the culture medium of infected cells (Fig 1). The HCoV-EMC S1 domain was demonstrated also to bind to cells from other species but its overall reactivity was more restricted compared to that observed for SARS-CoV S1 (Supplementary Table 1).

## Coronavirus spike-receptor interactions

In order to identify the cell surface protein(s) binding to S1 we affinity isolated proteins from Vero and Huh-7 cells using the S1-Fc chimeric proteins. The HCoV-EMC S1-Fc protein - but not SARS-CoV S1-Fc - extracted a protein of ~110 kDa when analyzed under non-reducing conditions from Huh-7 cell lysates (Fig. 2a). Mass spectrometric analysis identified this protein as dipeptidyl peptidase 4 (DPP4 or DPP IV, also called CD26; Supplementary Fig. 2). Similar results were obtained using Vero cells (data not shown). We subsequently produced soluble (i.e. non membrane-anchored) forms of DPP4 and ACE2 and found that the HCoV-EMC S1-Fc protein bound the former but not the latter while the opposite was seen with the SARS-S1-Fc protein (Fig. 2b). Soluble DPP4, but not soluble ACE2, inhibited infection of Vero cells by HCoV-EMC (Supplemental Fig. 3). Moreover, transient expression of human DPP4 in the non-susceptible COS-7 cells rendered these cells susceptible to binding the HCoV-EMC S1-Fc protein to their surface (Supplementary Fig. 4). These data indicate a direct and specific binding of HCoV-EMC S1 to human DPP4.

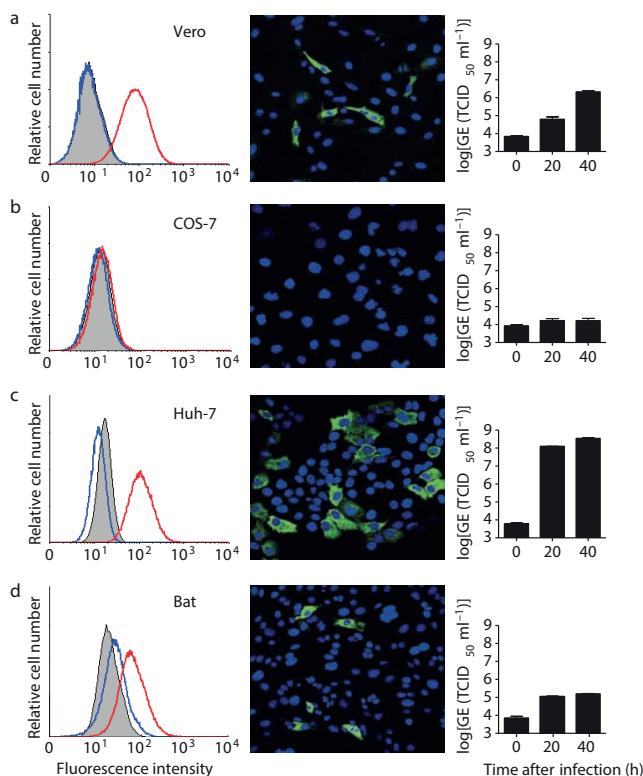


**Figure 1 Binding of HCoV-EMC S1 to cells is correlated with infection of HCoV-EMC.** Shown in the left panels are the FACS analyses of HCoV-EMC S1-Fc binding (red line) to Vero (a), COS-7 (b), Huh-7 (c) and bat cells (d). A feline CoV S1-Fc protein (blue line) and mock-incubated cells (black line) were used as controls. In the middle panels HCoV-EMC infected cells are visualized using an antiserum that recognizes the nonstructural protein nsp4. In the right panels, HCoV-EMC RNA levels in supernatants of the infected cells at 0, 20 and 40 h after infection were quantified using a TaqMan assay and expressed as genome equivalents GE (TCID<sub>50</sub>/ml). Error bars, s.e.m.

The DPP4 protein displays high amino acid sequence conservation across different species, including the sequence we obtained from *Pipistrellus pipistrellus* bat cells (Supplementary Fig. 5), particularly towards the carboxy-terminal end (Supplementary Fig. 6). Next, we tested surface expression of DPP4 on susceptible and non-susceptible cells employing a polyclonal human DPP4 antiserum. The specific reactivity of the anti-DPP4 serum with human and bat DPP4 was demonstrated by staining of human and bat DPP4 transfected cells (Fig. 3a). Expression of bat DPP4 in COS-7 cells allowed HCoV-EMC S1-Fc cell surface binding (Fig. 3a). Consistent with their susceptibility to HCoV-EMC infection and with the HCoV-EMC S1 cell surface binding, Vero and Huh-7 cells expressed high levels of DPP4 on their surface as judged by antibody reactivity, bat cells displayed low level antibody binding whereas COS-7 cells did not show any significant binding (Fig. 3b). Thus, DPP4 cell surface expression on the cell lines was consistent with HCoV-EMC S1 cell surface binding and with susceptibility to HCoV-EMC infection. The relevance of these observations was enforced by the finding that DPP4 expression was also found in primary human bronchiolar epithelial cell cultures (Fig. 3c) and in human bronchial lung tissue (Fig. 3d), in both instances localized to the apical surfaces of non-ciliated (tubulin-IV negative) cells. In addition, HCoV-EMC infection of human bronchiolar epithelial cell cultures appeared localized to the non-ciliated cells that express DPP4 (Fig. 3e).

To determine whether DPP4 essentially contributes to infection, susceptible cells were preincubated with polyclonal DPP4 antiserum prior to virus inoculation. Infection of Huh-7 cells was blocked by this serum but not by control serum or ACE2

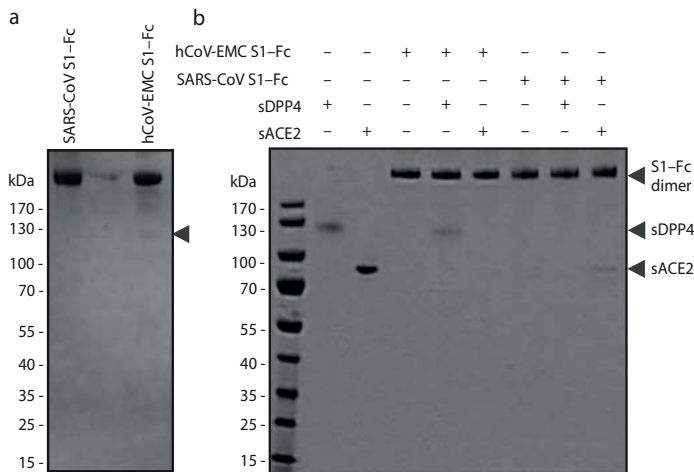


**Figure 2 HCoV-EMC S1 binding to DPP4.** (a) Huh-7 cell lysates were incubated with HCoV-EMC and SARS-CoV S1-Fc proteins and affinity-isolated proteins were subjected to protein electrophoresis under non-reducing conditions. The arrowhead indicates the position of the ~110 kDa DPP4 protein specifically isolated using the HCoV-EMC S1-Fc protein. (b) HCoV-EMC and SARS-CoV S1-Fc proteins were mock-incubated or incubated with soluble DPP4 (sDPP4) or soluble ACE2 (sACE2) followed by Protein A Sepharose affinity isolation and subjected to protein electrophoresis under non-reducing conditions.

## Coronavirus spike-receptor interactions

antibodies as evidenced by a strong reduction of virus infection, of virus excretion and of virus-induced cytopathic effects (Fig. 4a and Supplementary Fig. 7). In addition, infection of primary bronchiolar epithelial cells was blocked by the DPP4 antibodies in a dose dependent manner (Fig. 4b). We next examined whether DPP4 expression confers susceptibility to HCoV-EMC infection. COS-7 cells transfected with the human DPP4 expression plasmid – but not with the empty plasmid – were efficiently infected by HCoV-EMC as demonstrated by the presence of viral non-structural proteins in the cells (Fig 4c) and of viral RNA (Fig 4d) and infectious virus in the cell supernatants (not shown). Likewise, expression of bat DPP4 in COS-7 cells conferred susceptibility to the virus although to a lesser extent (Fig. 4c). Transfection

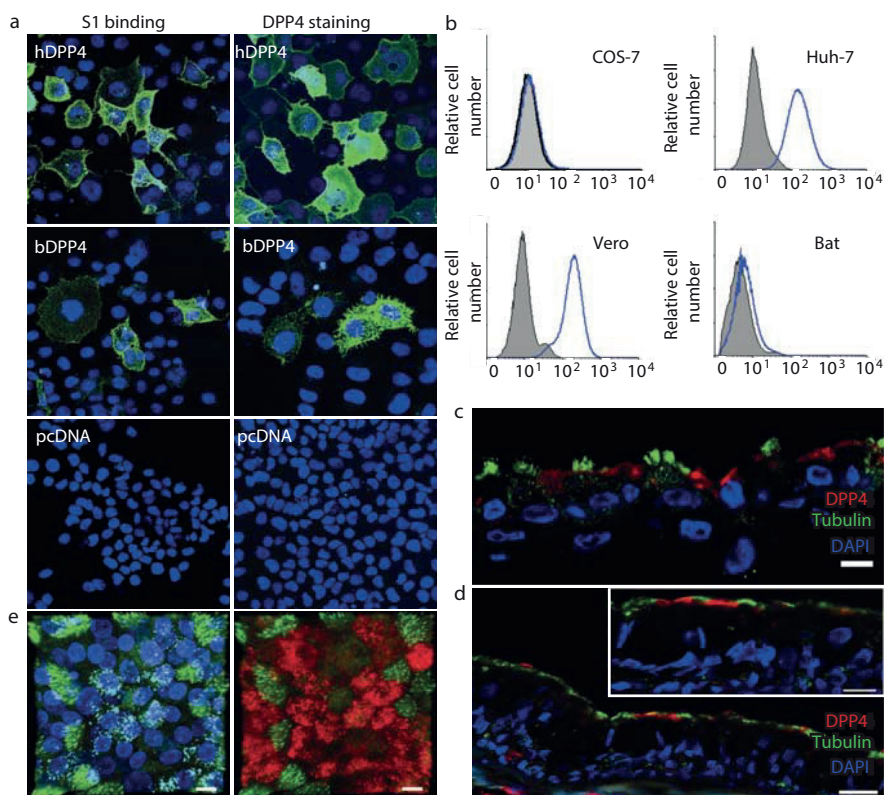


**Figure 3** DPP4 is present on HCoV-EMC susceptible cell lines and human bronchiolar epithelial cells. **(a)** COS-7 cells transfected with plasmids encoding human DPP4 (hDPP4), bat DPP4 (bDPP4) or a control plasmid (pcDNA) were tested for S1 binding and staining with a polyclonal antiserum against DPP4. **(b)** Similarly COS-7, Huh-7, Vero and bat cells were tested for reactivity with the same antiserum against DPP4 (blue lines) or with a control normal goat serum (gray peak). DPP4 expression (red) was also found in primary human bronchiolar epithelial cell cultures **(c)** and human bronchiolar tissue **(d)** and appeared localized to the apical surfaces of non-ciliated cells that do not express  $\beta$ -tubulin IV. **(e)** Double stranded viral RNA (cyan) was detected in HCoV-EMC infected primary human bronchiolar epithelial cell cultures and appeared localized to non-ciliated cells that do not express  $\beta$ -tubulin IV. Stainings were performed using antibodies directed against  $\beta$ -tubulin IV (ciliated cells; green), DPP4 (red), dsRNA (HCoV-EMC; cyan), and DAPI (cell nucleus; blue). Scale bar is 10  $\mu$ m.

## DPP4 is a functional receptor for MERS-CoV

of human DPP4 in non susceptible cells of different species origin (feline, murine and canine) did also permit infection with HCoV-EMC (Supplementary Fig. 8a), whereas other human CoVs such as HCoV-NL63, -229E and -OC43 were not able to infect hDPP4 transfected cells (Supplementary Fig. 8b-d). Collectively, our data demonstrate that DPP4 of human and bat origin acts as a functional receptor for HCoV-EMC.

After ACE2 and APN, DPP4 is the third exopeptidase to be discovered as a receptor for CoVs. DPP4 is a multifunctional 766 amino acids long type-II transmembrane glycoprotein presented in a dimeric form on the cell surface. It preferentially cleaves N-terminal Xaa-Pro dipeptides from hormones and chemokines thereby regulating their bioactivity<sup>15</sup>. Yet the use of peptidases by coronaviruses may be more related to their abundant presence on epithelial and endothelial tissues – the primary tissues of CoV infection - rather than to their proteolytic activity which in case of APN and ACE2 appeared not critical for infection<sup>11, 12</sup>. Consistently, HCoV-EMC infection could not be blocked by the DPP4 inhibitors Sitagliptin, Vildagliptin, Saxagliptin or P32/98 (Supplementary Fig. 9). DPP4 also plays a major role in glucose metabolism

2

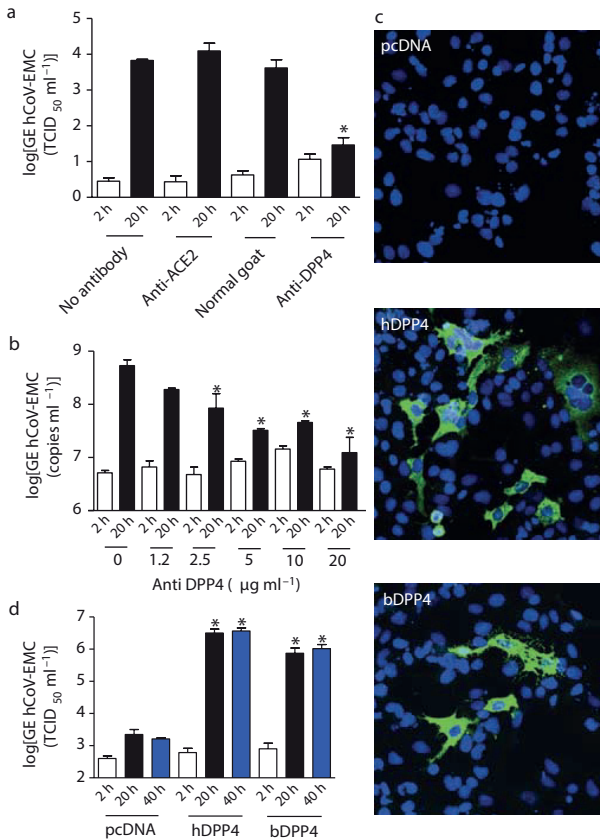


**Figure 4 DPP4 is essential for virus infection.** (a) Inhibition of HCoV-EMC infection of Huh-7 cells by antibodies to DPP4. Supernatants collected at 2 h (open bars) and 20 h (closed bars) were tested for presence of HCoV-EMC RNA using a TaqMan assay. Results representative of three different experiments are shown as  $\Delta$ Ct values (One Way Anova test, \* $P < 0.05$ ;  $n = 3$  per group). (b) Infection of human primary bronchiolar epithelial cells is blocked by the DPP4 antibodies in a dose-dependent manner and samples were analyzed at 2 h (open bars) and 20 h (closed bars) post infection (One Way Anova test, \* $P < 0.05$ ;  $n = 3$  per group). (c) COS-7 cells transfected with plasmids encoding human DPP4 (hDPP4), bat DPP4 (bDPP4) or a control plasmid (pcDNA) were inoculated with HCoV-EMC at a multiplicity of infection of 1 and left for 1 hour. Cells were washed twice and stained at 8 h after infection or (d) supernatant collected at 2 h (open bars), 20 h (closed bars) and 40 h (blue bars) was tested for presence of HCoV-EMC RNA using a TaqMan assay. Results representative of three different experiments are expressed as GE (TCID<sub>50</sub>/ml) values (One Way Anova test, \* $P < 0.05$ ;  $n = 4$  per group). All error bars represent s.e.m.

## ***Coronavirus spike-receptor interactions***

---

by its degradation of incretins and has been further implicated in T-cell activation, chemotaxis modulation, cell adhesion, apoptosis, and regulation of tumorigenicity<sup>15, 16</sup>. In humans it is primarily expressed on the epithelial cells in kidney, small intestine, liver and prostate, and on activated leukocytes while it occurs as a soluble form in the circulation<sup>15,16</sup>. At present little is known about the tropism of HCoV-EMC *in vivo*; the virus has been detected only in upper respiratory swabs, urine, sputum and tracheal aspirate<sup>2,3</sup>. Our observation of DPP4 being expressed on non-ciliated bronchial epithelial cells together with its reported expression in the kidney is consistent with clinical manifestations of HCoV-EMC infection. It is important to note that most respiratory viruses, including SARS-CoV<sup>17</sup>, have a marked tropism for ciliated cells that are more widely distributed along the upper and lower respiratory tract.

The epidemiological history of HCoV-EMC remains enigmatic. As for SARS-CoV and HCoV-NL63<sup>18</sup>, a bat origin possibly combined with the existence of an intermediate animal reservoir seems feasible. In view of the evolutionary conservation of DPP4 and HCoV-EMC's ability to employ bat DPP4 as a functional receptor such host species switching would not be surprising. Adaptive mutations in the SARS-CoV S1 domain allowing improved binding to human ACE2 have been noted explaining – at least in part – the zoonotic transmission event<sup>19,20</sup>. Further in depth characterization of the binding interface of HCoV-EMC S1 and DPP4 may shed light on the possible adaptive processes of this virus or related CoVs utilizing DPP4 in novel host species.

Variations in soluble DPP4 levels in serum have been reported as clinically relevant in a number of pathophysiological conditions including type-2 diabetes mellitus and virus infections<sup>15,16</sup>. It will be important to investigate whether and how varying soluble DPP4 levels affect HCoV-EMC pathogenesis. Downregulation of ACE2 expression after SARS-CoV infection has been shown to contribute to the severity of disease<sup>21</sup> consistent with the protective role of soluble ACE2 in lung injury<sup>22</sup>. Given the importance of DPP4 in regulation of chemokine and cytokine responses<sup>15</sup> one may speculate that *in vivo* downregulation of the HCoV-EMC receptor may potentially influence the pathogenesis of this virus. Preliminary findings *in vitro*, however, indicate that S1 binding to DPP4 did not result in significant downregulation of DPP4 or of the DPP4 enzymatic activity on Huh7 cells (not shown), possibly due to the observed active recycling of DPP4 from the plasma membrane<sup>15</sup>. Manipulation of DPP4 levels or development of inhibitors that target the binding interface between the S1 domain and receptor *in vivo* may provide therapeutic opportunities to combat HCoV-EMC infection. In addition, future studies should address the development of effective vaccines, including those that elicit antibodies that prevent HCoV-EMC's binding to DPP4.

### Methods

**Protein expression.** A plasmid encoding HCoV-EMC S1-Fc was generated by ligating a fragment encoding the S1 domain (residues 1-747) 3'-terminally to a fragment encoding the Fc domain of human IgG into the pCAGGS expression vector. Likewise, an S1-Fc expression plasmid was made for the SARS-CoV domain S1 subunit (isolate CUHK-W1: residues 1-676), the FIPV S1 domain (isolate 79-1146; residues 1-788) and the human ACE2 ectodomain (sACE2; residues 1-614). Fc chimeric proteins were expressed by transfection of the expression plasmids into HEK-293T cells and affinity purified from the culture supernatant using Protein A Sepharose beads (GE Healthcare). Purified ACE2-Fc was cleaved with thrombin and soluble ACE2 was purified by gel-filtration chromatography. A DPP4 expression vector was generated by cloning the full-length human DPP4 gene into the pCAGGS or the pcDNA3 vector. A plasmid encoding the ectodomain of human DPP4 was generated by ligating a fragment encoding residues 39-766 of human DPP4 into a pCD5 expression vector<sup>23</sup> encoding the signal sequence of CD5 and an OneSTrEP affinity tag (IBA GmbH). Soluble DPP4 ectodomain was prepared by transfection of the expression plasmid into HEK-293T cells and affinity-purification from the culture supernatant using Strep-Tactin sepharose beads (IBA GmbH). S1 binding of cells was measured by incubating  $2.5 \times 10^5$  cells with 15  $\mu\text{g/ml}$  of S1-Fc followed by incubation with FITC or DyLight488 labeled goat-anti-human IgG antibody and

analysis by flow cytometry.

**Affinity-purification and detection of DPP4.** Huh-7 cells were washed twice with ice-cold PBS, scraped off the plastic with a rubber policeman, pelleted and lysed in ice-cold lysis buffer (0.3% n-decyl- $\beta$ -D-maltopyranoside in PBS) containing protease inhibitors (Roche Complete Mini and phenylmethylsulfonyl fluoride) at a final density of  $\sim 2.5 \times 10^7$  cells/mL. The supernatants of centrifuged cell lysates were precleared with protein A sepharose beads after which 10  $\mu\text{g}$  of S1-Fc and 100  $\mu\text{l}$  protein A sepharose beads (50% v/v) was added to 1ml of cell lysate and incubated for 1h at 4°C under rotation. Beads were washed thrice with lysis buffer and once with PBS and subjected to protein electrophoresis (NoVEX® 4-12% Tris-Glycine gradient gel, Invitrogen) under non-reducing conditions. A distinct  $\sim 110\text{kDa}$  protein co-purified with HCoV-EMC-S1-Fc was visualized by GelCodeBlue staining, excised from the gel, incubated with trypsin and analysed by mass spectrometry.

**Mass spectrometry and data analysis.** The distinct  $\sim 110\text{kDa}$  protein which co-purified with HCoV-EMC-S1-Fc was excised from the gel and subjected to in-gel reduction with dithiothreitol, alkylation with chloroacetamide and digestion with trypsin (Promega, sequencing grade), essentially as described by Van den Berg et al<sup>24</sup>. Alternatively, affinity-isolated proteins were reduced and alkylated on beads similarly as described above. Nanoflow LC-MS/MS was performed on either an 1100 series capillary LC system (Agilent Technologies) coupled to an LTQ-Orbitrap

## ***Coronavirus spike-receptor interactions***

---

XL mass spectrometer (Thermo), or an EASY-nLC coupled to a Q Exactive mass spectrometer (Thermo), operating in positive mode and equipped with a nanospray source. Peptide mixtures were trapped on a ReproSil C18 reversed phase column (Dr Maisch GmbH; column dimensions 1.5 cm × 100 µm, packed in-house) at a flow rate of 8 µl/min. Peptide separation was performed on ReproSil C18 reversed phase column (Dr Maisch GmbH; column dimensions 15 cm × 50 µm, packed in-house) using a linear gradient from 0 to 80% B (A = 0.1 % formic acid; B = 80% (v/v) acetonitrile, 0.1 % formic acid) in 70 or 120 min and at a constant flow rate of 200 nl/min. The column eluent was directly sprayed into the ESI source of the mass spectrometer. Mass spectra were acquired in continuum mode; fragmentation of the peptides was performed in data-dependent mode by CID or HCD. Peak lists were automatically created from raw data files using the Mascot Distiller software (version 2.3; MatrixScience) or Proteome Discoverer (version 1.3; Thermo). The Mascot algorithm (version 2.2; MatrixScience, UK) was used for searching against a Uniprot database (release 2012\_10.fasta, taxonomy: Homo sapiens, or Chlorocebus sabaeus). The peptide tolerance was set to 10 ppm and the fragment ion tolerance was set to 0.8 Da for CID spectra (LTQ-Orbitrap) or to 20 mmu for HCD (Q Exactive) spectra). A maximum number of 2 missed cleavages by trypsin were allowed and carbamidomethylated cysteine and oxidized methionine were set as fixed and variable modifications, respectively.

***Blocking of HCoV-EMC replication by DPP4 antiserum.*** Huh-7 and primary airway epithelial cells (triplicates of one donor) were pre-incubated with antibodies to DPP4 (polyclonal goat-anti DPP4 immunoglobulin, R&D systems) in a range of 0-20 µg/ml. Cells were infected with HCoV-EMC, incubated for 1 hour at 37°C, washed and subsequently incubated with medium containing the respective antibody concentrations. Supernatants were collected at 2 h and 20 h and were analysed for the presence of HCoV-EMC RNA using a real-time Taqman assay.

***Human bronchial epithelial cultures and confocal microscopy analysis.*** Human bronchial lung tissue was obtained from patients (age >18 years old) who underwent surgical lung resection in their diagnostic pathway for any pulmonary disease and that gave informed consent. This was done in accordance with local regulation of the Kantonal Hospital St.Gallen, Switzerland, as part of the St. Gallen Lung Biopsy Biobank (SGLBB) which received approval by the ethics committee of the Kanton St. Gallen (EKSG 11/044, 27 April 2011; and EKSG 11/103, 23 September 2011).

Primary human bronchial epithelial cultures were generated as previously described<sup>25</sup>. Human bronchial epithelial cultures were maintained for 1-2 months until pseudostratified and fully differentiated epithelia were obtained. Human bronchial tissue or human bronchial epithelial cultures were fixed with 4% PFA (FormaFix) for 30 minutes at room temperature (RT). The fixed human bronchial tissue or cultures were mounted in Tissue-Tek® OCT medium and snap frozen in liquid nitrogen, from



which 10  $\mu$ M horizontal sections were made. The cryosections were immunostained using the procedure as described<sup>25</sup>, using mouse monoclonal antibody anti- $\beta$ -tubulin IV (Sigma) and goat anti hDPP4 polyclonal antibody (R&D Systems) as primary antibodies, and Dylight 488 labeled, anti-mouse IgG (H+L) and Dylight 549 labeled, anti-goat IgG (H+L) as secondary antibodies (Jackson ImmunoResearch). Counterstaining was done with DAPI (Invitrogen). Fluorescent images were acquired using EC Plan-Neofluor 40x/1.30 Oil DIC M27 or EC Plan-Neofluor 63x/1.30 Oil DIC M27 objectives on a Zeiss LSM 710 confocal microscope. Image capture, analysis and processing were performed using the ZEN 2010 (Zeiss) software packages.

HCoV-EMC infected human bronchial epithelial cultures were fixed with 4% PFA (FormaFix) for 30 minutes at room temperature (RT). Fixed cultures were immunostained using the procedure as described<sup>25</sup>, with mouse monoclonal antibody anti-dsRNA (J2, English & Scientific Consulting Bt.) and goat anti hDPP4 polyclonal antibody (R&D Systems) as primary antibodies, and Dylight 488 labeled, anti-mouse IgG (H+L) and Dylight 549 labeled, anti-goat IgG (H+L) as secondary antibodies (Jackson ImmunoResearch). The rabbit monoclonal anti- $\beta$ -tubulin conjugated with Alexafluor 647 (9F3, cell signaling) was applied as tertiary antibody. Counterstaining was done with DAPI (Invitrogen). Z-stack images were acquired using a EC Plan-Neofluor 63x/1.40 Oil DIC M27 objective on a Zeiss LSM 710 confocal microscope from which a 3D reconstruction was made using maximum intensity projection. Image capture, analysis and processing were performed using the ZEN 2010 (Zeiss) and Imaris (Bitplane Scientific Software) software packages.

***DPP4 enzymatic activity.*** DPPIV activity was measured on live cells using DPPIV/CD26 Assay kit for Biological Samples (Enzo Life sciences). Briefly, Vero cells ( $1 \times 10^4$  cells/well) were grown in 96 well plates, washed twice with PBS, incubated with or without inhibitor (20 $\mu$ g/ml) for 10 min after which H-Gly-Pro-AMC substrate was added and incubated for 10 min. Fluorescence intensity was measured at 380/460 nm using Tecan Infinite F200.

***Cloning and expression of human and bat DPP4.*** Total RNA was isolated from Huh-7 and PipNi/1 cells using RNeasy mini kit (Qiagen) and cDNAs were synthesized by using the Superscript reverse transcriptase (Life Technologies). The complete DPP4 genes were amplified using Pfu Ultra II fusion HS DNA polymerase (Stratagene) and cloned into the pcDNA 3.1 (+) expression vector (Life technologies). After sequencing, alignment was performed using ClustalW in the MEGA 5.0 software package ([www.megasoftware.net](http://www.megasoftware.net)) and the trees were constructed by using the neighbor-joining method with p-distance (gap/missing data treatment; complete deletion) and 1,000 bootstrap replicates as in MEGA 5.0 pcDNA plasmids containing the human or bat DPP4 or the empty pcDNA plasmid were transfected into COS-7 cells using lipofectamine 2000 (Life technologies). After 24 hours incubation cells were stained with both goat anti-human DPP4 polyclonal antibody (R&D system) and a rabbit anti-goat IgG-FITC antibody (Sigma).

## ***Coronavirus spike-receptor interactions***

---

---

***Virus infection, RNA extraction and quantitative RT-PCR.*** Virus stocks of HCoV-EMC were prepared as described earlier<sup>4</sup>. Vero, COS7, Huh-7 and kidney cells of the *Pipistrellus pipistrellus* bat cells<sup>14</sup> were inoculated with HCoV-EMC for 1 h and incubated with medium containing 1% fetal bovine serum. Formaldehyde fixed cells were stained using rabbit-anti-SARS-CoV nsp4 antibodies that are cross reactive for HCoV-EMC, according to standard protocols using a FITC-conjugated swine-anti-rabbit antibody as a second step. RNA from 200 µl of culture supernatant was isolated with the Magnapure LC total nucleic acid isolation kit (Roche) and eluted in 100 µl. HCoV-EMC RNA was quantified on the ABI prism 7700, with the TaqMan® Fast Virus 1-Step Master Mix (Applied Biosystems) using 20 µl isolated RNA, 1× Taqman mix, 0.5U uracil-N-glycosylase, 45 pmol forward primer (5'-GGGTGTACCTCTTAATGCCAATTC-3'), 45 pmol reverse primer (5'-TCTGTCCTGTCTCCGCCAAT-3') and 5 pmol probe (5'-FAM-ACCCCTGCGCAAATGCTGGG-BHQ1-3'). Amplification parameters were 5 min at 50°C, 20 sec at 95°C, and 45 cycles of 3 s at 95°C, and 30 sec at 60°C. RNA dilutions isolated from an HCoV-EMC stock were used as a standard. HCoV-NL63, HCoV-229E and HCoV-OC43 quantitative PCRs were routinely performed at the diagnostics Department of Viroscience at the Erasmus MC Rotterdam.

***Statistics.*** We compared the mean Ct values and log GE HCoV-EMC using One Way Anova with Post test Bonferroni. Statistical analysis was performed with Prism 4.0 (Graphpad).

## **Acknowledgments**

We thank Dr. Eric Snijder (LUMC, Leiden, The Netherlands) for providing the anti-SARS-CoV nsp4 antibody, Eveline Kindler, Hula Jónsdóttir, Dr. Regulo Rodriguez (Institute of Pathology, Kantonal Hospital St.Gallen), Theo Bestebroer, Suzan Pas, Georgina Arron, Monique van Velzen and Werner Ouwendijk for technical assistance. This work was supported by a fellowship from China Scholarship Council to H.M. The study was financed by the European Union FP7 project EMPERIE (contract number 223498), ANTIGONE (contract number 278976), the Swiss National Science Foundation (31003A\_132898) and the 3R Research Foundation Switzerland (Project 128-11). C.D. was supported by the German Research Foundation (DFG grant DR 772/3-1, KA1241/18-1) and the German Ministry of Education and Research (BMBF SARS II).

## **Authors contributions**

B.J.B., V.S.R and B.L.H. designed and coordinated the study. V.S.R., H.M., S.L.S., D.H.W.D., M.A.M., R.D., D.M., B.J.B., and B.L.H conducted the experiments. A.Z., provided the virus, R.A.M.F., J.A.A.D., V.T., C.D., A.D.M.E.O, and P.J.M.R. supervised part of the experiments. All authors contributed to the interpretations and conclusions presented. B.J.B. and B.L.H. wrote the manuscript, A.D.M.E.O, and P.J.M.R. participated in editing it.

## **Author information**

The *Pipistrellus pipistrellus* bat DPP4 sequence was deposited into GenBank under accession no. KC249974. Reprints and permissions information is available at [nature.com/reprints](http://nature.com/reprints). The authors declare no competing financial interests. Readers are welcome to comment on the online version of the paper. Correspondence and requests for materials should be addressed to B.J.B (([b.j.bosch@uu.nl](mailto:b.j.bosch@uu.nl)) and B.L.H. ([b.haagmans@erasmusmc.nl](mailto:b.haagmans@erasmusmc.nl)).

### **References**

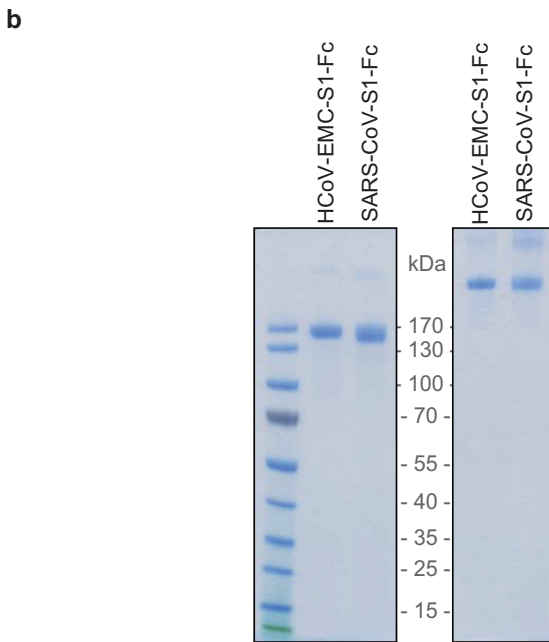
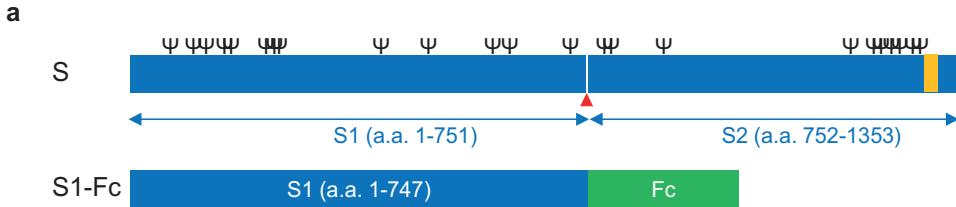
1. Weiss, S. R. & Navas-Martin, S. Coronavirus pathogenesis and the emerging pathogen severe acute respiratory syndrome coronavirus. *Microbiol. Mol. Biol. Rev.* 69, 635-664 (2005).
2. Zaki, A. M., van Boheemen, S., Bestebroer, T. M., Osterhaus, A. D. & Fouchier, R. A. Isolation of a novel coronavirus from a man with pneumonia in Saudi Arabia. *N. Engl. J. Med.* 367, 1814-1820 (2012).
3. Bermingham, A. et al. Severe respiratory illness caused by a novel coronavirus, in a patient transferred to the United Kingdom from the Middle East, September 2012. *Euro Surveill.* 17, 20290 (2012).
4. van Boheemen, S. et al. Genomic characterization of a newly discovered coronavirus associated with acute respiratory distress syndrome in humans. *MBio* 3, 10.1128/mBio.00473-12 (2012).
5. Graham, R. L. & Baric, R. S. Recombination, reservoirs, and the modular spike: mechanisms of coronavirus cross-species transmission. *J. Virol.* 84, 3134-3146 (2010).
6. Li, W. et al. Bats are natural reservoirs of SARS-like coronaviruses. *Science* 310, 676-679 (2005).
7. Source WHO ([http://www.who.int/csr/disease/coronavirus\\_infections/InterimRevisedSurveillanceRecommendations\\_nCoVInfection\\_28Nov12u.pdf](http://www.who.int/csr/disease/coronavirus_infections/InterimRevisedSurveillanceRecommendations_nCoVInfection_28Nov12u.pdf)).
8. Quan, P. L. et al. Identification of a severe acute respiratory syndrome coronavirus-like virus in a leaf-nosed bat in Nigeria. *MBio* 1, e00208-10 (2010).
9. Williams, R. K., Jiang, G. S. & Holmes, K. V. Receptor for mouse hepatitis virus is a member of the carcinoembryonic antigen family of glycoproteins. *Proc. Natl. Acad. Sci. U. S. A.* 88, 5533-5536 (1991).
10. Yeager, C. L. et al. Human aminopeptidase N is a receptor for human coronavirus 229E. *Nature* 357, 420-422 (1992).
11. Delmas, B. et al. Aminopeptidase N is a major receptor for the entero-pathogenic coronavirus TGEV. *Nature* 357, 417-420 (1992).
12. Li, W. et al. Angiotensin-converting enzyme 2 is a functional receptor for the SARS coronavirus. *Nature* 426, 450-454 (2003).
13. Schultze, B. & Herrler, G. Bovine coronavirus uses N-acetyl-9-O-acetylneuraminic acid as a receptor determinant to initiate the infection of cultured cells. *J. Gen. Virol.* 73 ( Pt 4), 901-906 (1992).
14. Müller, M. et al. Human Coronavirus EMC does not require the SARS-Coronavirus receptor and maintains broad replicative capability in mammalian cell lines. (in press, mBio).
15. Lambeir, A. M., Durinx, C., Scharpe, S. & De Meester, I. Dipeptidyl-peptidase IV from bench to bedside: an update on structural properties, functions, and clinical aspects of the enzyme DPP IV. *Crit. Rev. Clin. Lab. Sci.* 40, 209-294 (2003).
16. Boonacker, E. & Van Noorden, C. J. The multifunctional or moonlighting protein CD26/DPPIV. *Eur. J. Cell Biol.* 82, 53-73 (2003).
17. Sims, A. C., Burkett, S. E., Yount, B. & Pickles, R. J. SARS-CoV replication and pathogenesis in an in vitro model of the human conducting airway epithelium. *Virus Res.* 133, 33-44 (2008).
18. Huynh, J. et al. Evidence Supporting a Zoonotic Origin of Human Coronavirus Strain NL63. *J. Virol.* 86, 12816-12825 (2012).
19. Wu, K., Peng, G., Wilken, M., Geraghty, R. J. & Li, F. Mechanisms of host receptor adaptation by severe acute respiratory syndrome coronavirus. *J. Biol. Chem.* 287, 8904-8911 (2012).
20. Li, F., Li, W., Farzan, M. & Harrison, S. C. Structure of SARS coronavirus spike receptor-binding

## ***DPP4 is a functional receptor for MERS-CoV***

---

- domain complexed with receptor. *Science* 309, 1864-1868 (2005).
21. Kuba, K. et al. A crucial role of angiotensin converting enzyme 2 (ACE2) in SARS coronavirus-induced lung injury. *Nat. Med.* 11, 875-879 (2005).
  22. Imai, Y. et al. Angiotensin-converting enzyme 2 protects from severe acute lung failure. *Nature* 436, 112-116 (2005).
  23. Bosch, B. J. et al. Recombinant soluble, multimeric HA and NA exhibit distinctive types of protection against pandemic swine-origin 2009 A(H1N1) influenza virus infection in ferrets. *J. Virol.* 84, 10366-10374 (2010).
  24. van den Berg, D. L. et al. An Oct4-centered protein interaction network in embryonic stem cells. *Cell. Stem Cell.* 6, 369-381 (2010).
  25. Dijkman, R., Koekkoek, S. M., Molenkamp, R., Schildgen, O. & van der Hoek, L. Human bocavirus can be cultured in differentiated human airway epithelial cells. *J. Virol.* 83, 7739-7748 (2009).

**Supplementary Information**



**Supplementary Figure 1. HCoV-EMC spike (S) protein and S1-Fc expression.** (a) Schematic representation of the HCoV-EMC S and S1-Fc fusion protein. Position of the predicted N-glycosylation sites ( $\Psi$ ; predicted by the NetNGlyc server) and TM domain (yellow bar; predicted by the TMHMM server) are indicated in the full-length S protein. The border between the S1 and S2 subunits is marked by the presence of a predicted furin cleavage site (red triangle; predicted by the ProP 1.0 server). (b) Analysis of purified EMC-S1-Fc and SARS-S1-Fc proteins. One microgram of purified EMC-S1-Fc and SARS-S1-Fc proteins was analysed on a NovEX® 4-12% Tris-Glycine gradient gel under reducing (left) and non-reducing (right) conditions, and stained with GelCodeBlue reagent. Position and sizes of the marker proteins are indicated.

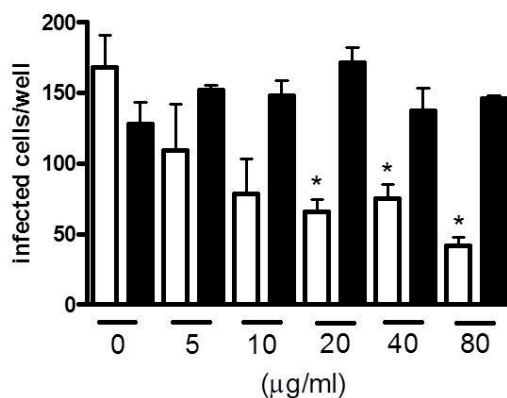
## DPP4 is a functional receptor for MERS-CoV

1 MKTPWKVLLG LLGAAALVTI ITVPVLLNK **GTDDATADSR KTYTLTDYLK**  
51 NTYRLKLYSL **RWISDHEYLY KQENNILVFN** AEYGNSSVFL ENSTFDEFHG  
101 SINDYSISPD GQFILLEINY VKQWR**HSYTA SYDIYDLNKR** QLITEERIPN  
151 NTQWVTWSPV GHK**LAYVWNN DIYVKIEPNL PSYRITWTGK** EDIIYNGITD  
201 WYEEEEVFSA YSALWWSPNG TFLAYAQFND TEVPLIEYSF YSDESLQYPK  
251 **TVRVYPKAG AVNPTVKFFV** VNTDSLSSVT NATSIQITAP ASMLIGDHYL  
301 CDVTWATQER **ISLQWLRRIQ** NYSVMDICDY DESSGR**WNCL VARQHIEMST**  
351 **TGWVGRFRPS** EPHFTLDGNS FYK**IISNEEG YRHICYFQID KKDCTFITGK**  
401 TWEVIGIEAL TSDYLYYISN EYKGMPPGGRN LYK**IQLSDYT KVTCLSCELN**  
451 **PERCQYYSVS FSKEAKYYQL** R**CSGPGPLPLY TLHSSVNDKG** LRVLEDNSAL  
501 **DKMLQNVQMP SKKLDIFIILN** ETKFWYQ**MIL PPHFDKSKKY PLLLDVYAGP**  
551 **CSQKADTVFR** LNWAYTYLAST ENIIVASFDG R**SGYQGDKI MHAINRRLGT**  
601 **FEVEDQIEAA RQFSKMGFVD** NKR**IAIWGWS YGGYVTSMVL** GSGSGVFK**CG**  
651 **IAVAPVSRWE YYDSVYTERY** M**GLPTPEDNL DHYRNSTVMS** RAENFKQVEY  
701 LLIHGTADDN VHFQQAQIS KALVDVGVD**F QAMWYDDEDH** GIASSTAHQH  
751 IYTHMSHF**IK QCFSLP**

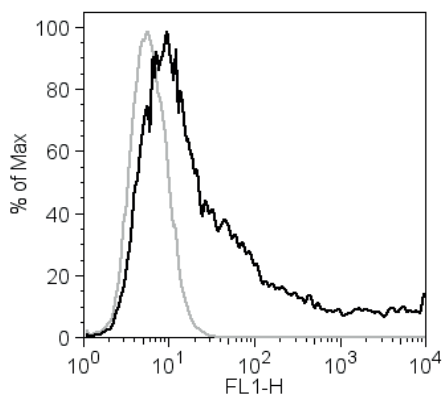
**Supplementary Figure 2. DPP4-derived tryptic fragments as determined by mass spectrometry.** Shown is the human DPP4 protein sequence (NCBI RefSeq: NP\_001926.2) with the tryptic fragments corresponding to DPP4 obtained from the ~110 kDa band (Fig. 2A of main text) indicated in red.

2

## Coronavirus spike-receptor interactions



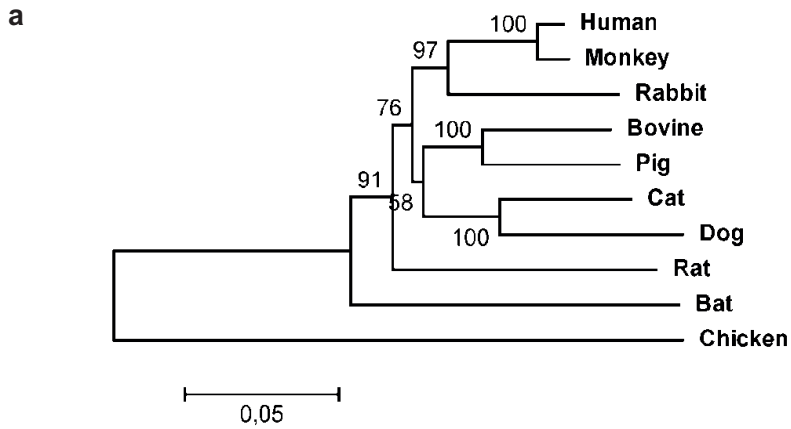
**Supplementary Figure 3. Soluble DPP4, but not soluble ACE2, inhibits HCoV-EMC infection.** HCoV-EMC was preincubated with the indicated concentrations of soluble DPP4 (sDPP4; white bars) or soluble ACE2 (sACE2; black bars). VERO cells were subsequently inoculated for 1 hour with the virus-protein mixes. Cells were washed and the number of infected cells per well was counted 8 hours post infection after immunofluorescence staining (One Way Anova test, \* $P < 0.05$ ;  $n = 3$  per group). Error bars indicate s.e.m.



**Supplementary Figure 4. HCoV-EMC S1-Fc binding to cells.** Binding of HCoV-EMC S1-Fc proteins to COS-7 cells transfected with control pCAGGS (grey line) or with pCAGGS-DPP4 (black line) expression plasmid, analyzed by flow cytometry.



## DPP4 is a functional receptor for MERS-CoV

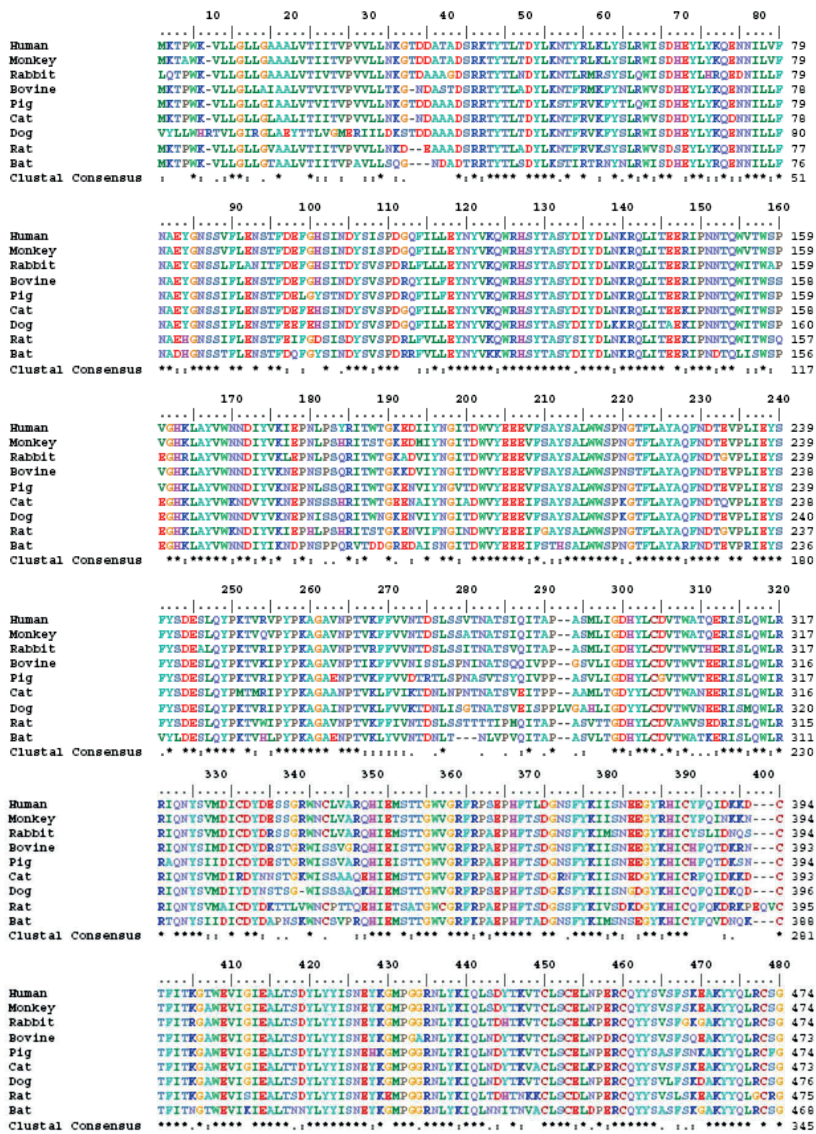


**b**

Species	UniProt accession nr.	protein identity (%)
Homo sapiens ( Human)	P27487	82,2
Macaca mulatta (Monkey)	F6VRB0	82,0
Bos taurus (Bovine)	P81425	81,4
Sus scrofa (Pig)	P22411	81,3
Oryctolagus cuniculus (Rabbit)	G1T1C1	81,4
Felis catus (Cat)	Q9N2I7	80,2
Rattus norvegicus (Rat)	P14740	78,6
Canis familiaris (Dog)	F1PP08	77,3
Gallus gallus (Chicken)	F1NDK7	63,1

**Supplementary Figure 5. Phylogenetic analysis of DPP4.** Phylogenetic tree of DPP4 from different species by amino acid sequence analysis using neighbor joining (**a**) and percentage identity of bat DPP4 compared to that of different species (**b**).

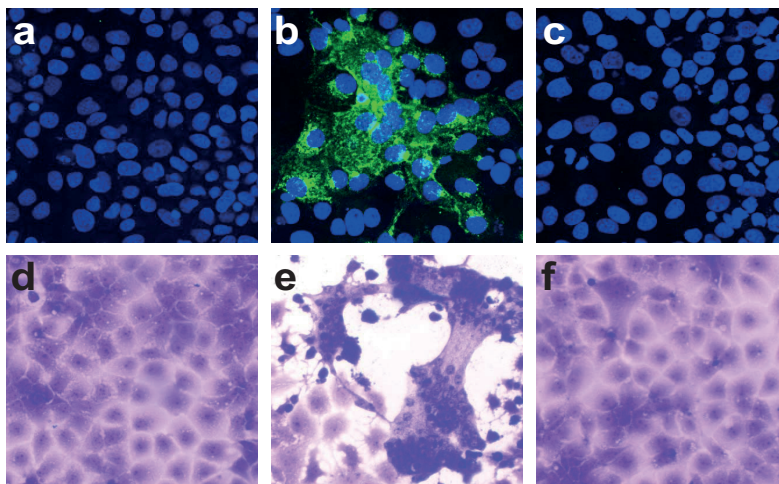
# Coronavirus spike-receptor interactions



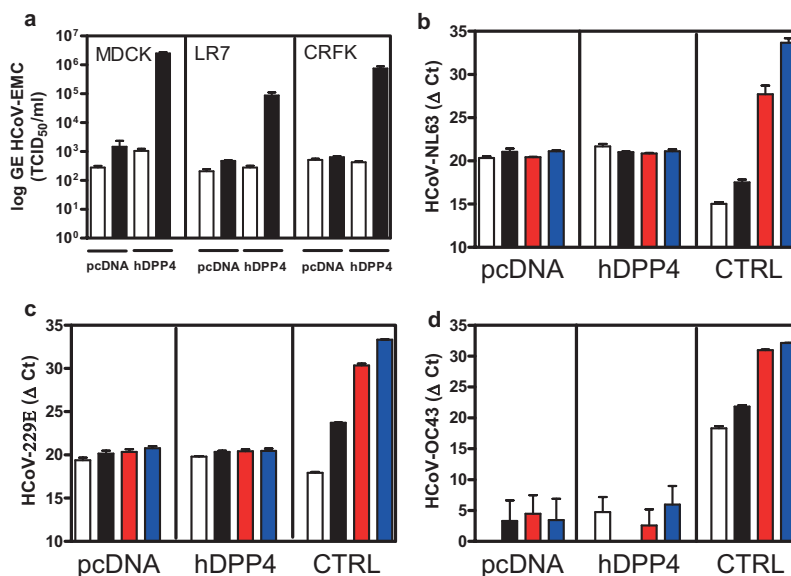
Supplementary Figure 6. Alignment of amino acid DPP4 sequences from different species. UniProt accession numbers used are mentioned under Supplementary Figure 5.



## Coronavirus spike-receptor interactions

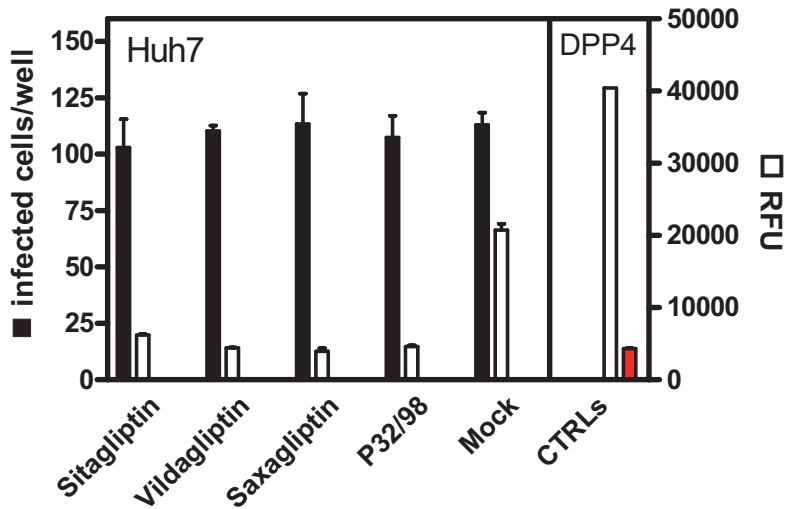


**Supplementary Figure 7. Inhibition of HCoV-EMC infection of Huh-7 cells by antibodies to DPP4.** Mock inoculated cells (a,d), or cells inoculated with HCoV-EMC in the presence of normal goat serum (b,e) or anti DPP4 antibodies (c,f) were fixed at 20h (a-c) or 40 h p.i. (d-f) and stained for viral antigen (a-f) or with crystal violet (d-f).



**Supplementary Figure 8. DPP4 is not essential for infection with other HCoVs.** LR7 (a), CRFK (a) and MDCK (a-d) cells transfected with plasmids encoding human DPP4 (hDPP4) or a control plasmid (pcDNA) were inoculated with HCoV-EMC (a), HCoV-NL63 (b), HCoV-229E (c) or HCoV-OC43 (d) and left for 1 hour. Controls in the panels b-d included Vero cells infected with HCoV-NL63 or human embryonic lung cells infected with HCoV-229E (c) or HCoV-OC43 (d). Cells were washed twice and supernatant collected at 2 h (open bars), 20 h (closed bars), 72 h (red bars) or 120 hrs (blue bars) was tested for presence of HCoV-EMC RNA using a TaqMan assay. Results are expressed as GE (TCID<sub>50</sub>/ml) values or ΔCt.

## DPP4 is a functional receptor for MERS-CoV



**Supplementary Figure 9. Effect of DPP4 enzyme inhibitors on HCoV-EMC infection.** Vero cells were treated with the indicated inhibitors at a concentration of 20  $\mu\text{g/ml}$  for 1 h and subsequently inoculated with HCoV-EMC by adding the virus. At 8 h p.i. cells were fixed and infected cells visualized (closed bars). Enzymatic activity of DPP4 on the cells (open bars) and of the recombinant DPP4 control (open bar) or substrate only (red bar) is depicted as relative fluorescence units (RFU).

## Coronavirus spike-receptor interactions

Supplementary Table 1. Surface binding efficiencies of EMC-, SARS- and FIPV-S1-Fc proteins to cells of different species as analyzed by flow cytometry.

Species:	Cell line:	Binding efficiency S1-Fc proteins		
		EMC	SARS	FIPV
<i>Bos primigenius</i> (cow)	MDBK	-	+++	-
<i>Canis familiaris</i> (dog)	MDCK	-	+	-
<i>Mesocricetus auratus</i> (hamster)	BHK21	-	++	-
	CHO	-	+++	-
<i>Felis catus</i> (cat)	CRFK	-	++	++++
	FCWF	-	++	+++
	FEA	-	+	+++
<i>Homo sapiens</i> (human)	293T	+/-	++	
	A549	-	++	-
	Huh-7	+++++	++++	-
	HeLa	-	+	-
<i>Sus scrofa</i> (pig)	LLC-PK1	+	++	-
	PD-5	-	++	-
<i>Cercopithecus aethiops</i> (African green monkey)	VERO E6	+	+++	-
	VERO 81	++	++	-
	COS7	-	++	-
	MARC145	-	++	-
<i>Macaca mulatta</i> (rhesus monkey)	LLC-MK2	+/-	++	-
<i>Mus musculus</i> (mouse)	LR7	-	-	-
<i>Oryctolagus cuniculus</i> (rabbit)	RK-13	-	+++	-

***DPP4 is a functional receptor for MERS-CoV***

---





# CHAPTER 3

## The receptor binding domain of the new MERS coronavirus maps to a 231-residue region in the spike protein that efficiently elicits neutralizing antibodies

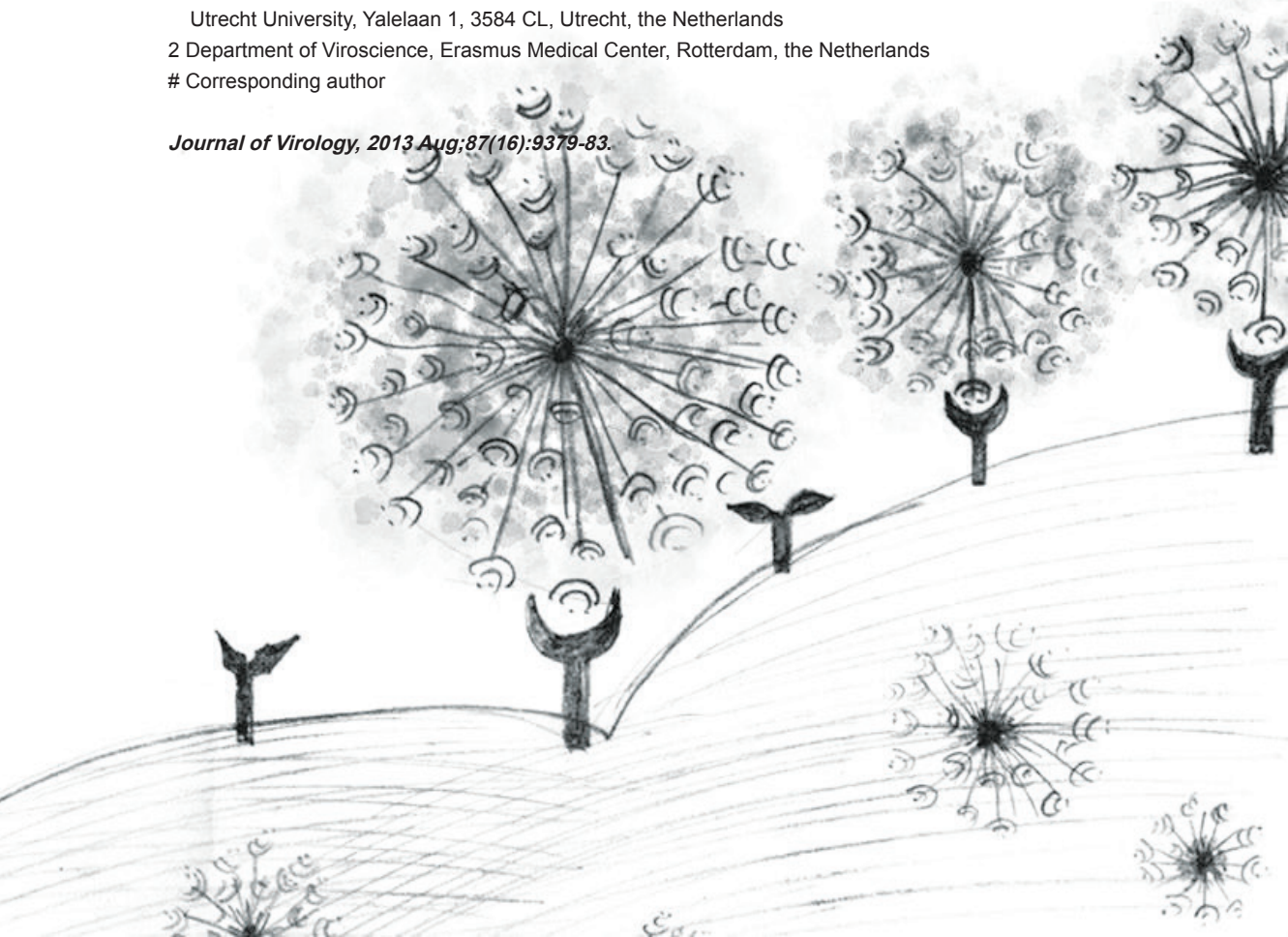
Huihui Mou<sup>1</sup>, V. Stalin Raj<sup>2</sup>, Frank J.M. van Kuppeveld<sup>1</sup>, Peter J.M. Rottier<sup>1</sup>, Bart L. Haagmans<sup>2</sup> and Berend Jan Bosch<sup>1</sup>#

1 Department of Infectious Diseases and Immunology, Virology Division, Faculty of Veterinary Medicine, Utrecht University, Yalelaan 1, 3584 CL, Utrecht, the Netherlands

2 Department of Viroscience, Erasmus Medical Center, Rotterdam, the Netherlands

# Corresponding author

*Journal of Virology*, 2013 Aug;87(16):9379-83.



### **Abstract**

The spike (S) protein of the recently emerged human coronavirus (MERS-CoV) mediates infection by binding to the cellular receptor dipeptidyl peptidase 4 (DPP4). Here we mapped the receptor-binding domain in the S protein to a 231-amino acid fragment (residues 358-588) by evaluating the interaction of spike truncation variants with receptor expressing cells and soluble DPP4. Antibodies to this domain - much less so to the preceding N-terminal region - efficiently neutralize MERS-CoV infection.

Just 10 years following the outbreak of the severe respiratory acute syndrome coronavirus (SARS-CoV) the world is confronted with yet another deadly human coronavirus. The virus, first provisionally called human coronavirus-EMC (hCoV-EMC) (1, 2) but now named MERS-CoV, referring to its emergence in the Middle-East and to the respiratory syndrome it causes, belongs to the betacoronavirus genus lineage 2c (3). As of June 7<sup>th</sup> 2013, 55 cases have been laboratory confirmed including 31 deaths, all from - or linked to - the Arabian Peninsula (4). Like with SARS-CoV, patients affected by MERS-CoV suffer from severe and often lethal lower respiratory tract infection. The epidemiology of MERS-CoV is still enigmatic, but the geographical distribution of epidemiologically unlinked individuals points to intermittent, zoonotic transmission from a - so far unknown - animal source, whereas a number of reported clusters indicate limited human-to-human spread (5).

The main determinant of coronavirus tropism is the viral spike (S) protein as it mediates binding to a cell-surface receptor. The MERS-CoV S protein, a 1353 amino acid type I membrane glycoprotein, assembles into trimers that constitute the spikes or peplomers on the surface of the enveloped coronavirus particle. The protein combines the two essential entry functions, namely that of host receptor binding and membrane fusion, which are attributed to the N-terminal (S1, residues 1-751) and C-terminal (S2, residues 752-1353) half of the S protein, respectively (Fig.1a). Recently we have identified dipeptidyl peptidase 4 (DPP4, also known as CD26), expressed in the human lung, as a functional receptor for MERS-CoV(6). Importantly, MERS-CoV can also use the evolutionary conserved DPP4 of other species, most notably that of bats(6, 7).

Coronaviruses bind to receptors via independently folded, generally about 150-300 residues long receptor binding domains (RBD) present in their S1 subunit, of which the location within S1 can vary (8-10). Thus, for the betacoronavirus mouse hepatitis virus (MHV) the binding to its CEACAM receptor (11) has been mapped to the N-terminal ~300 amino acids of the spike protein (12, 13) whereas for the SARS-CoV - of the same genus - binding to the ACE2 receptor (14) maps to residues 323-502 of S1 (15, 16) (Fig.1a). Identification of the RBD can hence help the development of monoclonal antibodies and vaccines for the treatment and prevention of infection. The RBD is the most important target for neutralizing antibodies (12, 17, 18) preventing virus-receptor interaction.

We previously used the S1 domain of MERS-CoV fused to the Fc-region of human IgG to demonstrate the interaction of S1 with DPP4-expressing cells and with soluble, i.e. non membrane-anchored DPP4 (6). To identify the receptor binding domain in the MERS-CoV S1 subunit, we generated S1-Fc protein chimera's with truncations at the C-terminus and N-terminus of the S1 domain. We considered a three domain structure of the MERS-CoV S1 protein (residues 1-357, 358-588 and 589-747) based on the predicted location and structure of the RBD of two other betacoronaviruses, MHV and SARS-CoV (12, 13, 15, 16), of which the homologous regions for MERS-

## Coronavirus spike-receptor interactions

CoV S map to the residues 18-351 and 379-580, respectively (Fig.1b). In addition, a soluble form of human DPP4 (residues 39-766) was made, which was C-terminally tagged with the Fc region. These proteins were expressed in HEK-293T cells after transfection of the respective expression plasmids and subsequently affinity-purified from the cell culture supernatant using protein A sepharose beads as described(6). The Fc region of purified sDPP4-Fc was proteolytically removed using trypsin (data not shown). First, we analyzed the S1-Fc proteins and C-terminal S1 truncations thereof for their ability to interact with sDPP4 using a co-purification assay. sDPP4 was efficiently co-purified by the S1-Fc variants encompassing residues 1-588 and 1-747 whereas the 1-357 S1-Fc variant was unable to bind sDPP4 (Fig.2a). We next generated an S1-Fc variant comprising residues 358-588, a region homologous to the ACE2 receptor binding domain in SARS-CoV S1 (Fig.2a). This S1-Fc truncation variant efficiently bound soluble DPP4, indicating that the DPP4 receptor binding domain is located within the 358-588 residues domain of the MERS-CoV spike protein.

We subsequently tested the ability of these S1-Fc variants to bind to HEK-293T cells transiently expressing DPP4 by using flow cytometry. The S1-Fc variants

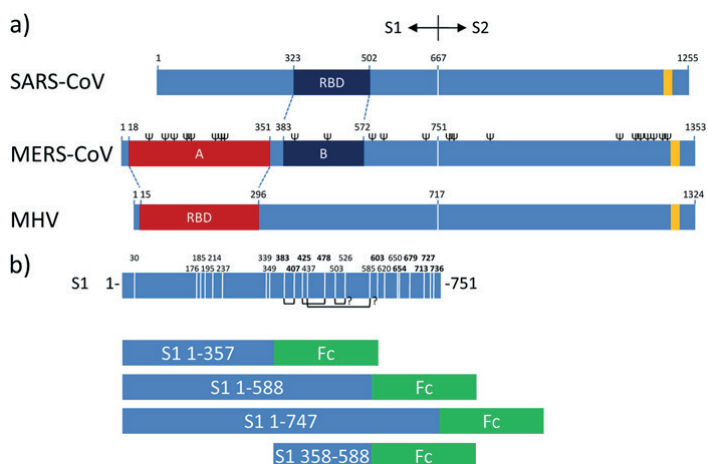


**Figure 1. Receptor binding domains in betacoronavirus spike proteins and S1-Fc expression constructs.** (a) Schematic representation of the betacoronaviruses SARS-CoV, MERS-CoV S and MHV (strain A59) spike (S) protein sequence (drawn to scale) aligned at the S1-S2 junction. The known receptor binding domain in the S1 subunit of MHV and SARS-CoV S proteins and their corresponding homologous regions in MERS-CoV S as defined by ClustalW alignment are indicated. Positions of the transmembrane domain (yellow bar; predicted by the TMHMM server) and of the predicted N-glycosylation sites (Ψ; predicted by the NetNGlyc server, only shown for the MERS-CoV S) are indicated. The border between the S1 and S2 subunits of the spike protein is represented by a vertical white line. (b) upper panel, schematic presentation of the MERS-CoV S1 subunit (residues 1-751) sequence. Cysteine positions in S1 subunit are indicated by vertical white lines with corresponding amino acid positions on top. Positions of cysteines highly conserved among betacoronaviruses S1 proteins are in bold. Predicted disulfide bond connections inferred from the structure of the SARS-CoV receptor binding domain are presented as connecting black lines underneath. Lower panel, domains of the MERS-CoV S1 subunit expressed as Fc chimeras.

encompassing residues 1-588 and 358-588 bound to DPP4-expressing HEK-293T cells with efficiencies comparable to the full-length S1 protein whereas no binding was observed with the 1-357 S1-Fc variant (Fig.2b). These data show the 358-588 amino acids S1 region to be essential and sufficient for binding to DPP4-expressing cells, consistent with the results of the sDPP4 interaction study.

To confirm the observed interactions in a more biological assay we analyzed the ability of the S1-Fc variants to prevent MERS-CoV infection. Thus, Huh-7 cells were preincubated with the different S1-Fc variants before being inoculated with the MERS-CoV. We found that the variants encompassing residues 1-747 and 358-588, but not the 1-357 S1-Fc variant, inhibited infection (Fig.2c).

Finally polyclonal antibodies were raised in rabbits against the 1-747, 1-357 and 358-588 S1-Fc variants (Davids Biotechnology GmbH, Germany). The sera, which displayed equal ELISA titers towards its antigen (1:300.000, data not shown), were tested for their ability to neutralize virus infectivity. Antibodies raised against the 358-588 S1-Fc variant efficiently neutralized virus infectivity, superior to those raised against the 1-747 and 1-357 S1-Fc variants (Fig.2d). This indicates that neutralizing epitopes within S1 are primarily localized to the RBD region. The elicited antibodies are likely to block the interaction of the spike protein with DPP4 thereby neutralizing MERS-CoV infectivity. Of note, antibodies raised against the MERS-CoV-S RBD did not cross-neutralize SARS-CoV infection (data not shown). The results demonstrate the potential of S1 protein and of the 358-588 S1 polypeptide as subunit vaccines with a high biosafety profile compared to vaccines based on inactivated viruses or live-attenuated virus.

Except for the betacoronavirus MHV, which binds to its CEACAM receptor through a domain in the N-terminal part of its S1 protein, the RBDs of all other coronaviruses that engage protein receptors and that have been mapped occur in the C-terminal portion of the S1 subunit (Fig.3). Examples also include the alphacoronaviruses binding to ACE2 (hCoV-NL63) and APN (e.g. TGEV, hCoV-229E) (10, 19-25). In this study we have experimentally mapped the RBD of MERS-CoV to a 231-amino acid fragment (residues 358-588) within the spike protein. This domain nicely corresponds with the S1 region recently anticipated to interact with the DPP4 receptor on the basis of theoretical S1 structure predictions (26). The RBD in the MERS-CoV S1 protein localizes in the same region where the SARS-CoV S protein interacts with its ACE2 receptor (26). The SARS-CoV RBD structure displays a 5-stranded  $\beta$ -sheet core structure ( $\beta$ 1-4 and  $\beta$ 7) maintaining the overall domain conformation, and a long extended loop containing two anti-parallel  $\beta$ -sheets ( $\beta$ 5 and  $\beta$ 6) responsible for receptor binding(16). Intriguingly, compared to SARS-CoV, the RBD of MERS-CoV contains a relatively conserved core domain but a highly variable loop region, tentatively explaining the differential receptor usage(26). Crystallization and structure analysis of this MERS-CoV RBD region in complex with DPP4 will give detailed insight into the virus-receptor binding interface.

## Coronavirus spike-receptor interactions

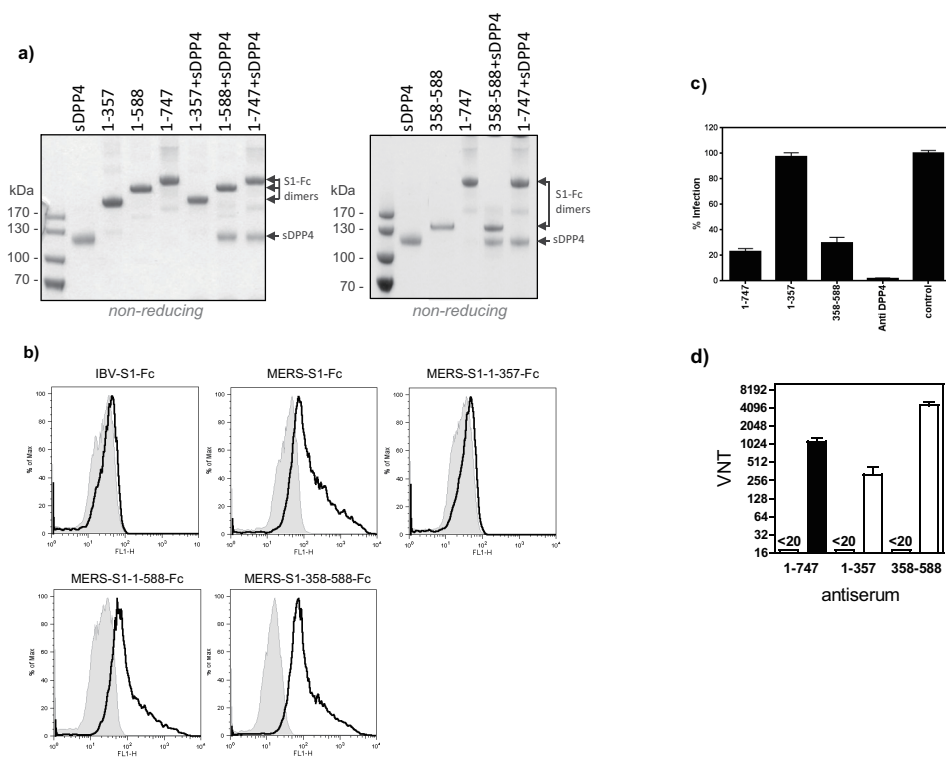


**Figure 2. The DPP4 binding domain is located within residues 358-588 of the MERS-CoV spike protein and efficiently elicits neutralizing antibodies. (a)** S1-Fc chimeric proteins and soluble DPP4 (sDPP4) receptor were expressed from HEK-293T cells and purified from the culture supernatant. S1-Fc proteins were mixed with sDPP4 followed by protein A sepharose affinity isolation, analyzed on a NovEX® 4-12% Tris-Glycine gradient gel under non-reducing conditions, and stained with GelCodeBlue reagent. Position of the S1-Fc proteins - running as dimers under non-reducing conditions due to an Fc interchain disulphide bond - and sDPP4 as well as the sizes of the marker proteins are indicated. Individual proteins were loaded as controls. **(b)** Binding of MERS-CoV S1-Fc proteins to DPP4 expressing cells.  $2.5 \times 10^5$  HEK-293T cells transfected with control pCAGGS (grey shaded area) or with pCAGGS-DPP4 (black line) expression plasmid were incubated with 15  $\mu\text{g/ml}$  of the indicated S1-Fc followed by incubation with DyLight488 labeled goat-anti-human IgG antibody and analysis by flow cytometry. An Fc-chimera containing the S1 of infectious bronchitis virus (IBV-S1-Fc) was taken along as a negative control. **(c)** Inhibition of MERS-CoV infection by S1-Fc 1-747, 1-357 and 358-588 variants. Huh7 cells were preincubated with 40  $\mu\text{g/ml}$  S1-Fc 1-747, 1-357 or 358-588 for 0.5 h prior to virus inoculation (1 h), all at RT. Mock incubated cells (control) and cells incubated with a DPP4 polyclonal antibody (anti-DPP4) were taken along as controls. Following incubation at 37° C for 8 hours, infected cells were detected by immunofluorescence and infection was quantified (relative to control). The experiment was carried out twice and the data of one representative experiment are shown. Error bars indicate standard error of the mean. **(d)** Neutralization of MERS-CoV infection by rabbit antisera raised against the S1-Fc 1-747, 1-357 and 358-588 variants. Virus (200 pfu) was premixed 1:1 with serial dilutions of sera obtained (open bars) or after immunization (closed bars) prior to inoculation onto VERO cells and virus infection was monitored by the occurrence of CPE at 72 hours post infection. Virus neutralization titers (VNT) were determined in quadruplicate as the highest serum dilutions that completely prevent CPE. The experiment was carried out twice and the data of one representative experiment are shown. Error bars indicate standard error of the mean.

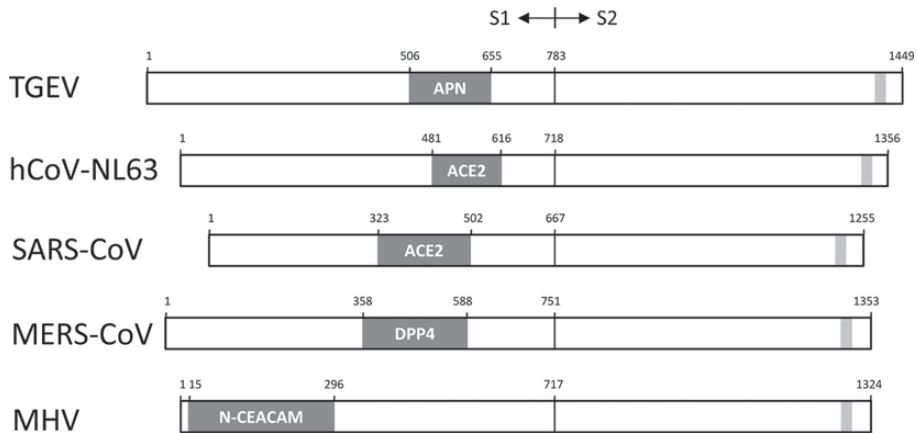


**Figure 3. Localization of receptor-binding domains in coronavirus spike proteins.** Schematic presentation of the spike proteins of the alphacoronaviruses TGEV and hCoV-NL63 and of the betacoronaviruses SARS-CoV, MERS-CoV and MHV (drawn to scale), aligned at the S1-S2 junction. Blue boxes represent the receptor-binding domains (RBD) and indicate the engaged receptor. The RBD of TGEV, hCoV-NL63, SARS-CoV and MHV have been confirmed by crystallography (12, 15, 22, 26). Grey boxes indicate the transmembrane domain. Sequence IDs: TGEV (ABG89335.1), hCoV-NL63 (NC\_005831.2), SARS-CoV (NP\_828851.1), MERS-CoV (AFS88936.1), MHV (NC\_001846.1).

## Acknowledgements

We thank Ger Arkesteijn and Laura de Vries (UU, Utrecht, The Netherlands) for experimental support. This work was supported by a fellowship from China Scholarship Council to H.M. The study was financed by the European Union FP7 projects EMPERIE (contract number 223498) and ANTIGONE (contract number 278976).

### **References**

1. Zaki, A. M., S. van Boheemen, T. M. Bestebroer, A. D. Osterhaus, and R. A. Fouchier. 2012. Isolation of a novel coronavirus from a man with pneumonia in Saudi Arabia. *N. Engl. J. Med.* 367:1814-1820.
2. van Boheemen, S., M. de Graaf, C. Lauber, T. M. Bestebroer, V. S. Raj, A. M. Zaki, A. D. Osterhaus, B. L. Haagmans, A. E. Gorbalenya, E. J. Snijder, and R. A. Fouchier. 2012. Genomic characterization of a newly discovered coronavirus associated with acute respiratory distress syndrome in humans. *MBio.* 3:10.1128/mBio.00473-12.
3. de Groot, R. J., S. C. Baker, R. S. Baric, C. S. Brown, C. Drosten, L. Enjuanes, R. A. Fouchier, M. Galiano, A. E. Gorbalenya, Z. Memish, S. Perlman, L. L. Poon, E. J. Snijder, G. M. Stephens, P. C. Woo, A. M. Zaki, M. Zambon, and J. Ziebuhr. 2013. Middle East Respiratory Syndrome Coronavirus (MERS-CoV); Announcement of the Coronavirus Study Group. *J. Virol.*
4. Source WHO. [http://www.who.int/csr/don/2013\\_06\\_07/en/index.html](http://www.who.int/csr/don/2013_06_07/en/index.html) .
5. Health Protection Agency (HPA) UK Novel Coronavirus Investigation team. 2013. Evidence of person-to-person transmission within a family cluster of novel coronavirus infections, United Kingdom, February 2013. *Euro Surveill.* 18:20427.
6. Raj, V. S., H. Mou, S. L. Smits, D. H. Dekkers, M. A. Muller, R. Dijkman, D. Muth, J. A. Demmers, A. Zaki, R. A. Fouchier, V. Thiel, C. Drosten, P. J. Rottier, A. D. Osterhaus, B. J. Bosch, and B. L. Haagmans. 2013. Dipeptidyl peptidase 4 is a functional receptor for the emerging human coronavirus-EMC. *Nature.* 495:251-254.
7. Muller, M. A., V. S. Raj, D. Muth, B. Meyer, S. Kallies, S. L. Smits, R. Wollny, T. M. Bestebroer, S. Specht, T. Suliman, K. Zimmermann, T. Binger, I. Eckerle, M. Tschapka, A. M. Zaki, A. D. Osterhaus, R. A. Fouchier, B. L. Haagmans, and C. Drosten. 2012. Human coronavirus EMC does not require the SARS-coronavirus receptor and maintains broad replicative capability in mammalian cell lines. *MBio.* 3:10.1128/mBio.00515-12.
8. Graham, R. L., and R. S. Baric. 2010. Recombination, reservoirs, and the modular spike: mechanisms of coronavirus cross-species transmission. *J. Virol.* 84:3134-3146.
9. Li, W., S. K. Wong, F. Li, J. H. Kuhn, I. C. Huang, H. Choe, and M. Farzan. 2006. Animal origins of the severe acute respiratory syndrome coronavirus: insight from ACE2-S-protein interactions. *J. Virol.* 80:4211-4219.
10. Li, F. 2012. Evidence for a common evolutionary origin of coronavirus spike protein receptor-binding subunits. *J. Virol.* 86:2856-2858.
11. Williams, R. K., G. S. Jiang, and K. V. Holmes. 1991. Receptor for mouse hepatitis virus is a member of the carcinoembryonic antigen family of glycoproteins. *Proc. Natl. Acad. Sci. U. S. A.* 88:5533-5536.
12. Kubo, H., Y. K. Yamada, and F. Taguchi. 1994. Localization of neutralizing epitopes and the receptor-binding site within the amino-terminal 330 amino acids of the murine coronavirus spike protein. *J. Virol.* 68:5403-5410.
13. Peng, G., D. Sun, K. R. Rajashankar, Z. Qian, K. V. Holmes, and F. Li. 2011. Crystal structure of mouse coronavirus receptor-binding domain complexed with its murine receptor. *Proc. Natl. Acad. Sci. U. S. A.* 108:10696-10701.
14. Li, W., M. J. Moore, N. Vasilieva, J. Sui, S. K. Wong, M. A. Berne, M. Somasundaran, J. L. Sullivan, K. Luzuriaga, T. C. Greenough, H. Choe, and M. Farzan. 2003. Angiotensin-converting enzyme 2 is a functional receptor for the SARS coronavirus. *Nature.* 426:450-454.



15. Wong, S. K., W. Li, M. J. Moore, H. Choe, and M. Farzan. 2004. A 193-amino acid fragment of the SARS coronavirus S protein efficiently binds angiotensin-converting enzyme 2. *J. Biol. Chem.* 279:3197-3201.
16. Li, F., W. Li, M. Farzan, and S. C. Harrison. 2005. Structure of SARS coronavirus spike receptor-binding domain complexed with receptor. *Science.* 309:1864-1868.
17. Bonavia, A., B. D. Zelus, D. E. Wentworth, P. J. Talbot, and K. V. Holmes. 2003. Identification of a receptor-binding domain of the spike glycoprotein of human coronavirus HCoV-229E. *J. Virol.* 77:2530-2538.
18. He, Y., Y. Zhou, S. Liu, Z. Kou, W. Li, M. Farzan, and S. Jiang. 2004. Receptor-binding domain of SARS-CoV spike protein induces highly potent neutralizing antibodies: implication for developing subunit vaccine. *Biochem. Biophys. Res. Commun.* 324:773-781.
19. Breslin, J. J., I. Mork, M. K. Smith, L. K. Vogel, E. M. Hemmila, A. Bonavia, P. J. Talbot, H. Sjostrom, O. Noren, and K. V. Holmes. 2003. Human coronavirus 229E: receptor binding domain and neutralization by soluble receptor at 37 degrees C. *J. Virol.* 77:4435-4438.
20. Hofmann, H., G. Simmons, A. J. Rennekamp, C. Chaipan, T. Gramberg, E. Heck, M. Geier, A. Wegele, A. Marzi, P. Bates, and S. Pohlmann. 2006. Highly conserved regions within the spike proteins of human coronaviruses 229E and NL63 determine recognition of their respective cellular receptors. *J. Virol.* 80:8639-8652.
21. Delmas, B., J. Gelfi, R. L'Haridon, L. K. Vogel, H. Sjostrom, O. Noren, and H. Laude. 1992. Aminopeptidase N is a major receptor for the entero-pathogenic coronavirus TGEV. *Nature.* 357:417-420.
22. Reguera, J., D. Ordone, C. Santiago, L. Enjuanes, and J. M. Casasnovas. 2011. Antigenic modules in the N-terminal S1 region of the transmissible gastroenteritis virus spike protein. *J. Gen. Virol.* 92:1117-1126.
23. Reguera, J., C. Santiago, G. Mudgal, D. Ordone, L. Enjuanes, and J. M. Casasnovas. 2012. Structural bases of coronavirus attachment to host aminopeptidase N and its inhibition by neutralizing antibodies. *PLoS Pathog.* 8:e1002859.
24. Yeager, C. L., R. A. Ashmun, R. K. Williams, C. B. Cardellichio, L. H. Shapiro, A. T. Look, and K. V. Holmes. 1992. Human aminopeptidase N is a receptor for human coronavirus 229E. *Nature.* 357:420-422.
25. Godet, M., J. Grosclaude, B. Delmas, and H. Laude. 1994. Major receptor-binding and neutralization determinants are located within the same domain of the transmissible gastroenteritis virus (coronavirus) spike protein. *J. Virol.* 68:8008-8016.
26. Jiang, S., L. Lu, L. Du, and A. K. Debnath. 2013. A predicted receptor-binding and critical neutralizing domain in S protein of the novel human coronavirus HCoV-EMC. *J. Infect.* 66:464-466.



# CHAPTER 4

## Specific serology for emerging human coronaviruses by protein microarray.

**C Reusken<sup>1,2</sup>, H Mou<sup>1,3</sup>, G J Godeke<sup>1,2</sup>, L van der Hoek<sup>4</sup>, B Meyer<sup>5</sup>, M A Müller<sup>5</sup>, B Haagmans<sup>6</sup>, R de Sousa<sup>2</sup>, N Schuurman<sup>3</sup>, U Dittmer<sup>7</sup>, P Rottier<sup>3</sup>, A Osterhaus<sup>6</sup>, C Drosten<sup>5</sup>, B J Bosch<sup>3</sup>, M Ko opmans<sup>2,6</sup>**

1 These authors contributed equally to this work

2 Centre for Infectious Disease Control, Division Virology, National Institute for Public Health and the Environment, Bilthoven, the Netherlands

3 Department of Infectious Diseases and Immunology, Utrecht University, Faculty of Veterinary Medicine, Utrecht, the Netherlands

4 Laboratory of Experimental Virology, Department of Medical Microbiology, Center for Infection and Immunity Amsterdam, Academic Medical Center, University of Amsterdam, Amsterdam, the Netherlands

5 Institute of Virology, University of Bonn Medical Centre, Bonn, Germany

6 Department of Viroscience, Erasmus Medical Centre, Rotterdam, the Netherlands

7 Institute for Virology, University Hospital Essen, University of Duisburg-Essen, Essen, Germany

*Eurosurveill. 2013 Apr 4;18(14):20441.*



### **Abstract**

We present a serological assay for the specific detection of IgM and IgG antibodies against the emerging human coronavirus hCoV-EMC and the SARS-CoV based on protein microarray technology. The assay uses the S1 receptor-binding subunit of the spike protein of hCoV-EMC and SARS-CoV as antigens. The assay has been validated extensively using putative cross-reacting sera of patient cohorts exposed to the four common hCoVs and sera from convalescent patients infected with hCoV-EMC or SARS-CoV.

## **Introduction**

In 2012, a novel human betacoronavirus (hCoV-EMC) emerged in the Middle-East region [1, 2]. At the end of March 2013, 17 confirmed cases of hCoV-EMC infection and a small number of probable cases had been reported to the World Health Organization (WHO). Nine confirmed cases were reported by the Kingdom of Saudi Arabia (KSA), two by Qatar, two by Jordan, three by the United Kingdom (UK) and one by the United Arab Emirates [2-9]. The second and third case reported by the UK resulted from person-to-person transmission after contact with the first case, a family member who returned to the UK from Pakistan and KSA with respiratory complaints due to an infection with hCoV-EMC [10]. Person-to-person transmission may also have been involved in two clusters in KSA and a hospital cluster in Jordan [2, 8]. Fifteen confirmed cases have presented with severe acute respiratory infection (SARI), in some cases accompanied by acute renal failure [11-13]. Eleven patients have died, five have recovered and one is still receiving intensive care at the time of reporting [4, 9]. One confirmed contact case in the UK and one confirmed case in KSA presented with mild illness, and the clinical manifestations appeared milder in unconfirmed but probable cases in the hospital cluster in Jordan as well [2, 4, 8, 14]. It is important to understand the full spectrum of illness associated with this new human infection, and to determine how that relates to infectivity and the ability to transmit the virus, as well as to outcomes of diagnostic tests.

The emergence of this novel hCoV lead to an international collaborative laboratory response resulting in the rapid availability of diagnostic real-time reverse transcription polymerase chain reaction (RT-PCR) assays, implemented world-wide in various diagnostic laboratories [15-17]. Successful use of PCR-based diagnostics relies on timing and technique of sampling, against knowledge about kinetics of viremia and shedding of virus during the course of an infection. Investigations into epidemiologically linked clinical cases in KSA and Jordan demonstrated that not in all symptomatic patients within a cluster viral RNA could be detected by RT-PCR, similar to what has been described for SARS and other infectious diseases [2, 14]. For diagnosis of hCoV-EMC infection, virus detection by RT-PCR during the acute phase may be less sensitive as samples from the lower respiratory tracts (tracheal aspirates, bronchoalveolar lavage) are necessary for optimal detection by RT-PCR, and these are not as readily available as upper respiratory tract samples [1, 12, 22]. In patients with SARS-associated SARI, in particular those seen more than 14 days after onset of symptoms, serological testing was imperative to complement RT-PCR findings for adequate diagnosis. In addition to diagnostic applications, serology is essential for the monitoring of the evolution of an outbreak, including (retrospective) studies of asymptomatic/ mild cases and animal reservoir identification. [16, 18-21].

Currently an immunofluorescence assay (IFA) using hCoV-EMC infected Vero B4 cells is available through the Institute for Virology of the University of Bonn [16]. However, as the authors caution, this assay may generate false-positive results due

## ***Coronavirus spike-receptor interactions***

---

to the global co-circulation of four hCoVs namely hCoV-NL63, hCoV-OC43, hCoV-229E and hCoV-HKU1 (at present, the fifth SARS-CoV is assumed not to circulate in the human population). Cross reactivity to conserved viral proteins limits the use of such whole virus-based IFAs, especially as antibodies against coronaviruses within a genus are generally known to cross react [4, 23]. Therefore, the European Centre for Disease Prevention and Control (ECDC) advised not to screen patients by regular IFA if second stage serology is not conducted [4]. For confirmation, virus neutralization assays are the gold standard, but these are difficult to implement and are not widely available. Therefore, there is a need for alternative methods.

Here, we describe the use of antigen-microarrays to measure antibodies directed against the receptor binding spike domain S1 of hCoV- EMC and SARS-CoV. The most variable immunogenic CoV antigen is the amino-terminal S1 subunit of the spike protein, which exhibits at most only some 30% amino acid identity between human CoV isolates (data not shown). We describe a specific serological tool, distinguishing cross-reactivity with the four common hCoVs belonging to the same genus as hCoV-EMC and SARS-CoV (genus Betacoronavirus, hCoV-OC43, hCoV-HKU1), and to the genus Alphacoronavirus (hCoV-NL63 and hCoV-229E).

## **Results**

***Testing antigen quality.*** The amino-terminal receptor binding spike domain S1 of hCoV-EMC and SARS-CoV were spotted in serial dilutions (1:2 - 1:8) on nitrocellulose slides and incubated with two-fold serial dilutions (1:20 - 1:640) of sera from hCoV-EMC infected macaques, a rabbit immunized with hCoV-EMC S1 or a SARS-CoV infected patient. All sera showed high-level IgG reactivity with their homologous S1 antigen while only background reactivity was observed with the heterologous antigen. Pre-immune serum of macaque and rabbit were non-reactive (table 1). Based on these observations it was concluded that the antigens as printed on the array slides were intact and with proper conformation for immuno-reactivity with homologous antibodies.

***Validation of protein array.*** To analyse the specificity of the microarray for detection of hCoV-EMC and SARS-CoV IgM and IgG antibodies, the reactivity of a cohort of human sera submitted to the RIVM for whooping cough diagnostics was tested. The cohort consisted of 72 sera of non-exposed patients, ranging from 0-95 years in age. This cohort represents the putative cross-reacting potential in the Dutch population, as previous studies in the Dutch population have shown high seroprevalences for one or more of the four common hCoVs [26, 27]. The sera were tested for IgM and IgG reactivity with the hCoV-EMC and SARS-CoV antigens at dilutions 1:20 and 1:40 (table 1, figure 1). The observed reactivity was low. Based on these results an arbitrary cut-off was set at 5,000 for IgM and at 10,000 for IgG measurements.

## **Serological assay for detection of emerging HCoVs**

The specificity of the micro-array was confirmed using serum samples from children with known recent exposure and antibody responses to one of the four common hCoVs, including the betacoronaviruses OC43 and HKU1. Sera were tested at dilutions 1:20 and 1:160, with one serum for each hCoV tested in a two-fold dilution series of 1:20- 1:640. None of the 14 sera showed reactivity above background, for either IgG or IgM, with the hCoV-EMC and SARS-CoV antigens (Table 1, figure 1 and 2).

Subsequently, the array was tested with a single serum sample taken in week three of illness of a patient infected with hCoV-EMC [28], and convalescent serum samples of two patients taken during the SARS-CoV epidemic. The serum of the hCoV-EMC patient showed a clear positive, reactivity for IgG with EMC S1 in the dilution range 1:20- 1: 20,480, declining only at dilutions 1:5120 and higher. The IgM reactivity of the hCoV-EMC serum with EMC antigen was saturated in the dilution range 1:20- 1:80 with declining, but clearly positive, levels of reactivity at higher dilutions. No reactivity was observed with SARS antigen for either IgG or IgM.

The two SARS-CoV sera SARS-1 and SARS-2 gave a clear positive reaction with the SARS antigen for IgG at dilutions 1:20-1:80 and 1:20-1:160 respectively, with no reactivity for IgM given the chosen cut-off. No reactivity was observed with the EMC antigen (Table 1, figure 1 and 2).

**Serological diagnosis.** Convalescent sera from three patients with severe respiratory complaints and a travel history to the Middle-East were tested using the newly developed microarray. None of the patients showed positive reactivity for IgM or IgG with EMC-S1.

**Table 1. Summary results of the validation of the hCoV-EMC and SARS-CoV S1 protein micro-array.**

Sera	Number	hCoV-EMC Ag <sup>a,b</sup>		SARS-CoV Ag <sup>a,b</sup>	
		IgG	IgM	IgG	IgM
<i>Human</i>					
population sera human	72	neg	neg	neg	neg
hCoV-OC43 human	6	neg	neg	neg	neg
hCoV-229E human	3	neg	neg	neg	neg
hCoV-NL63 human	3	neg	neg	neg	neg
hCoV-HKU1 human	2	neg	neg	neg	neg
hCoV-EMC human	1	pos	pos.	neg	neg
SARS-CoV human	2	neg	neg	pos	neg.
<i>Animal</i>					
pre-immunization rabbit	1	neg	n.t.	neg	n.t.
hCoV-EMC post-immunization rabbit	1	pos	n.t.	neg	n.t.
pre-infection macaque	1	neg	n.t.	neg	n.t.
hCoV-EMC post-infection macaque	2	pos	n.t.	neg	n.t.

**a** Ag is S1 antigen.

**b** neg = negative reactivity; pos = positive reactivity; n.t. = not tested. Reactivity was scored based on the arbitrary set cut-off.

# Coronavirus spike-receptor interactions

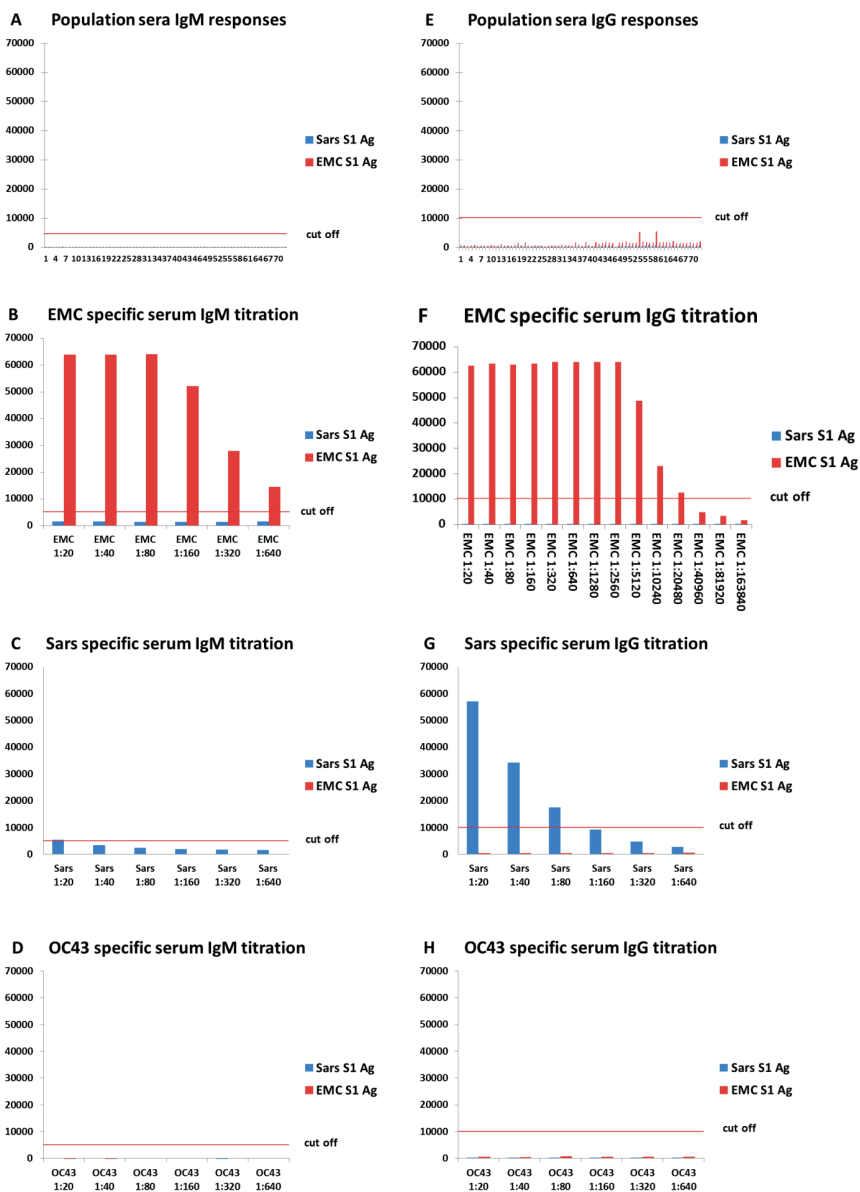


**Figure 1.** IgM and IgG reactivity of two-step serially diluted sera with hCoV-EMC S1- (EMC S1 Ag, red bars) and SARS-CoV S1- (SARS S1 Ag, blue bars) spotted microarrays (n=89). Sera: 72 population sera 1:20 diluted (panel A (IgM) and E (IgG)), hCoV-EMC (panel B (IgM) and F (IgG)), SARS-CoV serum SARS-1 (panel C (IgM) and G (IgG)) and hCoV-OC43 (panel D (IgM) and H (IgG)). Panels C and G are representative for all SARS-CoV sera tested (n=2). Panels D and H are representative for all common hCoV sera tested (n=14). X-axes denote serum numbers (panel A and E) or serum dilutions: two-step serial dilutions, starting dilution 1:20. Y-axes denote the measured median spot foreground fluorescence intensities.



## Serological assay for detection of emerging HCoVs

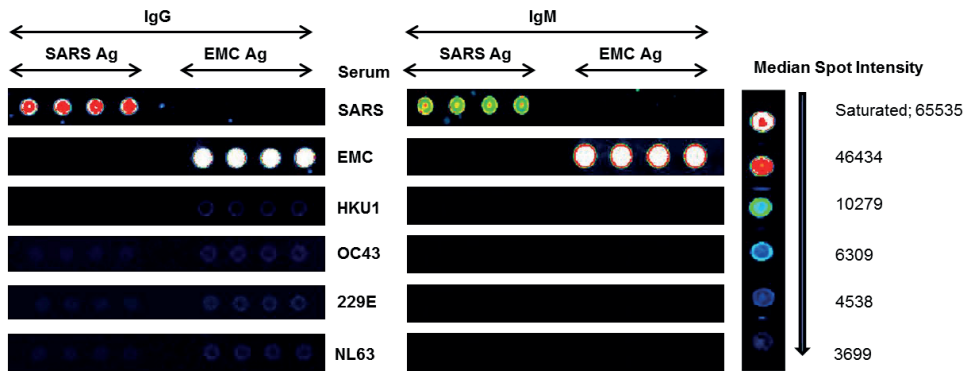


**Figure 2. Representative pictures of the protein microarray analysis of convalescent sera from patients infected with the six known hCoVs.** Vertically from top to bottom: Incubation with sera containing antibodies to SARS-CoV, hCoV-EMC, hCoV-HKU1, hCoV-OC43, hCoV-229E and hCoV-NL63. IgG (left panel) and IgM (right panel) reactivity of the six sera to SARS-CoV and hCoV-EMC S1protein (SARS Ag and EMC Ag respectively). Colours reflect median spot intensity as shown in the legend on the right. Antigens spotted in quadruplicate with dilution factor 1:2; sera dilution factor 1:20. Ag: antigen.

### **Discussion**

Here we present a protein microarray-based serological test for the confirmation of hCoV-EMC and SARS-CoV infections. A major obstacle in the development of detection tools for novel, emerging viruses is the availability of sufficient, well-defined negative and positive sera for the assessment of the specificity and sensitivity of the assays. Nevertheless, results so far suggest that the microarray seems highly specific for the detection of IgM and IgG antibodies against these emerging hCoVs, with no false-positive reactivity in 72 population sera and 14 sera known to be positive for one of the four widely circulating hCoVs -OC43, -HKU1, -229E and -NL63. Preferably high titer samples were used for assay validation, however the exact titers of the antibodies against the common hCoVs in the latter validation cohort were not known.

However, previous studies from the Netherlands have found that - by the age of 30 months- more than 50% of children seroconverted to one or more of the alpha (hCoV-NL63, hCoV-229E) - or betacoronaviruses (hCoV-OC43, hCoV-HKU1), and seropositivity reached 100% by 10 years of age for alphacoronaviruses [26, 27]. The seroprevalence for betacoronaviruses was not specifically tested in the Netherlands, but found to be 91% in adults in the US [30]. Therefore, the absence of false-positives in our population samples is strong evidence for the specificity of the method. IgG and IgM antibodies to hCoV-EMC and IgG to SARS-CoV were clearly detectable in positive patient sera. However due to the absence of a larger number of available positive patient sera, determination of the sensitivity of the assay in relation to viral loads, clinical manifestation and phase of infection needs more investigation. For this essential clinical validation, the international sharing of positive sera by (national) laboratories in possession of such sera is a prerequisite.

Currently, WHO and ECDC recommend the collection of paired serum samples, preferably from the acute and convalescent phase, of all cases under investigation as serological testing might be necessary to confirm infection when clinical presentation and epidemiology suggest an infection with hCoV-EMC despite negative PCR results [4, 22]. In addition serology is needed for contact investigations and source tracking. A two-staged serological approach is recommended, which proved effective in a contact investigation of an hCoV-EMC infection treated in Germany using IFA with virus -infected cells for screening and as second-stage tests recombinant Spike and Nucleocapsid transfected cells and virus neutralization tests [28]. Our protein micro-array enables specific, one-stage, high-throughput testing, with the benefit of minimal sample requirement. For other applications, we have used dried blood spots for testing, which greatly facilitates shipping of samples (De Bruin et al. manuscript in prep.).

The serological assay presented here is available and of great value for human and animal population screening, both necessary to gain insight in the epidemiology of

the novel hCoV. The array format can be modified to identify primary and intermediate animal reservoirs by simple adaptation of the conjugate used to visualize reactivity on the array as demonstrated for other applications (Freidl et al. manuscript in prep.). Our assay is available to aid diagnosis in individual patients, for confirmatory testing of positive tests and for (large-scale) contact studies.

### Methods

**Protein expression.** Plasmids encoding the amino-terminal receptor binding spike domain S1 of hCoV-EMC and SARS-CoV fused to the Fc part of human IgG were expressed in HEK-293T cells and S1-Fc proteins were purified from the culture supernatant by protein-A chromatography as described [24]. Purified S1-Fc was cleaved by thrombin on the beads at the thrombin cleavage site introduced at the S1-Fc junction. Soluble S1 was subsequently purified by gel-filtration chromatography and concentrated using Amicon Ultra-0.5 filter (Merck, Darmstadt, Germany).

**Preparation and testing of microarrays.** Purified hCoV-EMC S1 and SARS-CoV S1 were spotted in quadruplicate in two drops of 333 pL each in a twofold dilution series ranging from 1:2-1:8 (starting at 200 ug/ml for undiluted antigen) on 16-pad nitro-cellulose coated slides (Fast Slides, Maine Manufacturing, Grand Blanc, Michigan, USA) using a non-contact Piezorray spotter (PerkinElmer, Waltham, MA, USA) as described earlier [25]. Slides were pre-treated with Blotto-blocking buffer to avoid non-specific binding as described [25]. Dilutions of serum in Blotto containing 0.1 % Surfact-Amps 20 (thermo Fisher Scientific Inc.) were transferred in a volume of 90 µl to the slides and incubated for 1 h at 37 °C in a moist chamber. Sera tested for the presence of IgM were treated with Gullisorb (Meridian Bioscience, Inc. Cincinnati, OH, USA) to eliminate rheumatoid factor and immune IgG, which can interfere with IgM assays. Upon washing, goat anti-human IgG (Fc-fragment specific) or IgM (Fc5µ-fragment specific) conjugated with Dylight649-fluorescent dye (Jackson Immuno Research, West Grove, PA, USA) was incubated for 1 h at 37 °C in a moist chamber. After washing with buffer and water, the slides were dried. Fluorescence signals were quantified by a ScanArray Gx Plus microarray scanner (PerkinElmer) using an adaptive circle (diameter 80-200 µM) with a saturated signal at 65535. Median spot fluorescence foreground (background subtracted) intensity was determined using ScanArray Express vs 4.0 software.

**Sera.** For validation experiments the following serum samples were used. All sera were stored at -20 °C or -80 °C prior to testing.

- Anonymized serum samples from 72 persons ranging in age from 0.1 year to 95.3 years sampled during 2008. These sera had been sent to the Dutch National Institute for Public Health and the Environment (RIVM) for routine Bordetella pertussis serology, thus representing a cohort biased towards patients with non influenza-like respiratory symptoms. Anonymized use of serum from the RIVM

## ***Coronavirus spike-receptor interactions***

---

was covered by the rules of the code of conduct for proper use of human tissue of the Dutch Federation of Medical Scientific Associations.

- Anonymized serum samples of 10 children, ages ranging from 9-14 months, known to be positive for antibodies to one of the four common hCoVs, as determined by comparative ELISA using N antigen at a dilution factor of 1:200 [26, 27]. Samples were obtained in 2001, have been stored at -80°C and were chosen from this age group because antibodies in this age group most likely result from single exposures [27]. Two hCoV-HKU1, two hCoV-OC43, three hCoV-229E and three hCoV-NL63 IgG positive sera were used.

- Three anonymized hCoV-OC43 positive sera (including one paired sampled) from patients with virologically (PCR) and serologically (IgG IFA) confirmed infection, and one hCoV-OC43 IgG positive serum as described in [28].

- Serum samples of two cynomolgus macaques infected with hCoV-EMC (virus stock obtained as described [29]) taken at 28 days post infection, including a pre-infection serum.

- A serum sample of a rabbit immunized with hCoV-EMC S1 taken 28 days post immunization, including a pre-infection serum.

- One serum sample of a hCoV-EMC infected patient who was treated for SARI in a hospital in Essen, Germany taken at day 20 after onset of illness. This serum had an IgG titre of 1:10,000 and an IgM titre of 1:1,000 as determined by IFA on cells infected with hCoV-EMC and an IgM and IgG titer of > 1:320 as determined by IFA on cells expressing recombinant S protein [16, 28, 29].

- Convalescent serum samples of two SARS-CoV infected patients. Serum SARS-1 was taken 3.5 years after disease. It had an IgG titer of 1:160 and no IgM titer as determined by IFA on cells expressing recombinant S protein [28]. Serum SARS-2 was taken 36 days after onset of illness with an IgG titre of 1:1000 in IFA and 1:1600 in ELISA. No IgM titre was found by IFA (M. Niedrig pers. comm.).

- Convalescent serum samples of three patients with severe respiratory complaints who had travelled to KSA, Dubai and Dubai/Qatar within 10 days before the onset of illness, and therefore had been tested to exclude hCoV-EMC by RT-PCR, as recommended by WHO.

All human sera were collected in accordance with the ethical principles set out in the declaration of Helsinki; Macaque and rabbit sera were collected in compliance with Dutch laws on animal handling and welfare.

### References

1. Zaki AM, van Boheemen S, Bestebroer TM, Osterhaus AD, Fouchier RA. Isolation of a novel coronavirus from a man with pneumonia in Saudi Arabia. *The New England journal of medicine*. 2012;367(19):1814-20.
2. WHO. (GAR): Background and summary of novel coronavirus infection- as of 21 December 2012. 2012 [cited 2013 0208]; Available from: [http://www.who.int/csr/disease/coronavirus\\_infections/update\\_20121221/en/index.html](http://www.who.int/csr/disease/coronavirus_infections/update_20121221/en/index.html).
3. WHO. Global Alert and Response (GAR): Novel coronavirus infection- update 16 February 2013. 2013 [cited 2013 0219]; Available from: [http://www.who.int/csr/don/2013\\_02\\_16/en/index.html](http://www.who.int/csr/don/2013_02_16/en/index.html).
4. ECDC. Rapid Risk Assessment: Severe respiratory disease associated with a novel coronavirus, 19 February 2013. 2013 [cited 2013 0219]; Available from: <http://www.ecdc.europa.eu/en/publications/Publications/novel-coronavirus-rapid-risk-assessment-update.pdf>.
5. WHO. Global Alert and Response (GAR): Novel coronavirus infection- update 21 February 2013. 2013 [cited 2013 0219]; Available from: [http://www.who.int/csr/don/2013\\_02\\_16/en/index.html](http://www.who.int/csr/don/2013_02_16/en/index.html).
6. WHO. Global Alert and Response (GAR): Novel coronavirus infection- update 06 March 2013. 2013 [cited 2013 0307]; Available from: [http://www.who.int/csr/don/2013\\_03\\_06/en/index.html](http://www.who.int/csr/don/2013_03_06/en/index.html).
7. WHO. Global Alert and Response (GAR): Novel coronavirus infection- update 12 March 2013. 2013 [cited 2013 0314]; Available from: [http://www.who.int/csr/don/2013\\_03\\_12/en/index.html](http://www.who.int/csr/don/2013_03_12/en/index.html).
8. WHO. Global Alert and Response (GAR): Novel coronavirus infection- update 23 March 2013. 2013 [cited 2013 0314]; Available from: [http://www.who.int/csr/don/2013\\_03\\_23/en/index.html](http://www.who.int/csr/don/2013_03_23/en/index.html).
9. WHO. Global Alert and Response (GAR): Novel coronavirus infection- update 26 March 2013. 2013 [cited 2013 0327]; Available from: [http://www.who.int/csr/don/2013\\_03\\_26/en/index.html](http://www.who.int/csr/don/2013_03_26/en/index.html).
10. Pebody RG. The Health Protection Agency (HPA) UK Novel Coronavirus Investigation team. Evidence of person-to-person transmission within a family cluster of novel coronavirus infections, United Kingdom, February 2013. *Euro Surveill*. 2013;18(11).
11. Albarrak AM, Stephens GM, Hewson R, Memish ZA. Recovery from severe novel coronavirus infection. *Saudi medical journal*. 2012;33(12):1265-9.
12. Bermingham A, Chand MA, Brown CS, Aarons E, Tong C, Langrish C, et al. Severe respiratory illness caused by a novel coronavirus, in a patient transferred to the United Kingdom from the Middle East, September 2012. *Euro Surveill*. 2012;17(40):20290.
13. Pebody RG, Chand MA, Thomas HL, Green HK, Boddington NL, Carvalho C, et al. The United Kingdom public health response to an imported laboratory confirmed case of a novel coronavirus in September 2012. *Euro Surveill*. 2012;17(40):20292.
14. Anonymous. Novel coronavirus-East.Med. (7): Saudi Arabia, UK, Germany. *ProMED mail*. 2013;archivenumber 20130221.1554109.
15. Corman VM, Eckerle I, Bleicker T, Zaki A, Landt O, Eschbach-Bludau M, et al. Detection of a novel human coronavirus by real-time reverse-transcription polymerase chain reaction. *Euro Surveill*. 2012;17(39).
16. Corman V, Muller M, Costabel U, Timm J, Binger T, Meyer B, et al. Assays for laboratory confirmation of novel human coronavirus (hCoV-EMC) infections. *Euro Surveill*. 2012;17(49).
17. Palm D, Pereyaslov D, Vaz J, Broberg E, Zeller H, Gross D, et al. Laboratory capability for molecular detection and confirmation of novel coronavirus in Europe, November 2012. *Euro Surveill*. 2012;17(49).

## ***Coronavirus spike-receptor interactions***

---

---

18. Ng LF, Wong M, Koh S, Ooi EE, Tang KF, Leong HN, et al. Detection of severe acute respiratory syndrome coronavirus in blood of infected patients. *J Clin Microbiol.* 2004;42(1):347-50.
19. Chen W, Xu Z, Mu J, Yang L, Gan H, Mu F, et al. Antibody response and viraemia during the course of severe acute respiratory syndrome (SARS)-associated coronavirus infection. *Journal of medical microbiology.* 2004;53(Pt 5):435-8.
20. Guan Y, Zheng BJ, He YQ, Liu XL, Zhuang ZX, Cheung CL, et al. Isolation and characterization of viruses related to the SARS coronavirus from animals in southern China. *Science.* 2003;302(5643):276-8.
21. Prevalence of IgG antibody to SARS-associated coronavirus in animal traders--Guangdong Province, China, 2003. *MMWR Morbidity and mortality weekly report.* 2003;52(41):986-7.
22. WHO. Laboratory testing for novel coronavirus; Interim recommendations, 21 December 2012. 2012 [cited 2013 0314]; Available from: [http://www.who.int/csr/disease/coronavirus\\_infections/LaboratoryTestingNovelCoronavirus\\_21Dec12.pdf](http://www.who.int/csr/disease/coronavirus_infections/LaboratoryTestingNovelCoronavirus_21Dec12.pdf).
23. Drosten C. Recommendations regarding serological testing novel coronavirus-EMC. 2013 [cited 2013 0221]; Available from: <http://www.virology-bonn.de/index.php?id=40>.
24. Raj VS, Mou H, Smits SL, Dekkers DH, Muller MA, Dijkman R, et al. Dipeptidyl peptidase 4 is a functional receptor for the emerging human coronavirus-EMC. *Nature.* 2013;495(7440):251-4.
25. Koopmans M, de Bruin E, Godeke GJ, Friesema I, van Gageldonk R, Schipper M, et al. Profiling of humoral immune responses to influenza viruses by using protein microarray. *Clin Microbiol Infect.* 2012;18(8):797-807.
26. Dijkman R, Jebbink MF, El Idrissi NB, Pyrc K, Muller MA, Kuijpers TW, et al. Human coronavirus NL63 and 229E seroconversion in children. *J Clin Microbiol.* 2008;46(7):2368-73.
27. Dijkman R, Jebbink MF, Gaunt E, Rossen JW, Templeton KE, Kuijpers TW, et al. The dominance of human coronavirus OC43 and NL63 infections in infants. *J Clin Virol.* 2012;53(2):135-9.
28. Buchholz U, Müller MA, Nitsche A, Sanewski A, Wevering N, Bauer-Balci T, et al. Contact investigation of a case of human novel coronavirus infection treated in a German hospital, October-November 2012. *Euro Surveill.* 2013;18(8).
29. van Boheemen S, de Graaf M, Lauber C, Bestebroer TM, Raj VS, Zaki AM, et al. Genomic characterization of a newly discovered coronavirus associated with acute respiratory distress syndrome in humans. *mBio.* 2012;3(6).
30. Severance EG, Bossis I, Dickerson FB, Stallings CR, Origoni AE, Sullens A, et al. Development of a nucleocapsid-based human coronavirus immunoassay and estimates of individuals exposed to coronavirus in a U.S. metropolitan population. *Clin Vaccine Immunol.* 2008;15(12):1805-10.







# CHAPTER 5

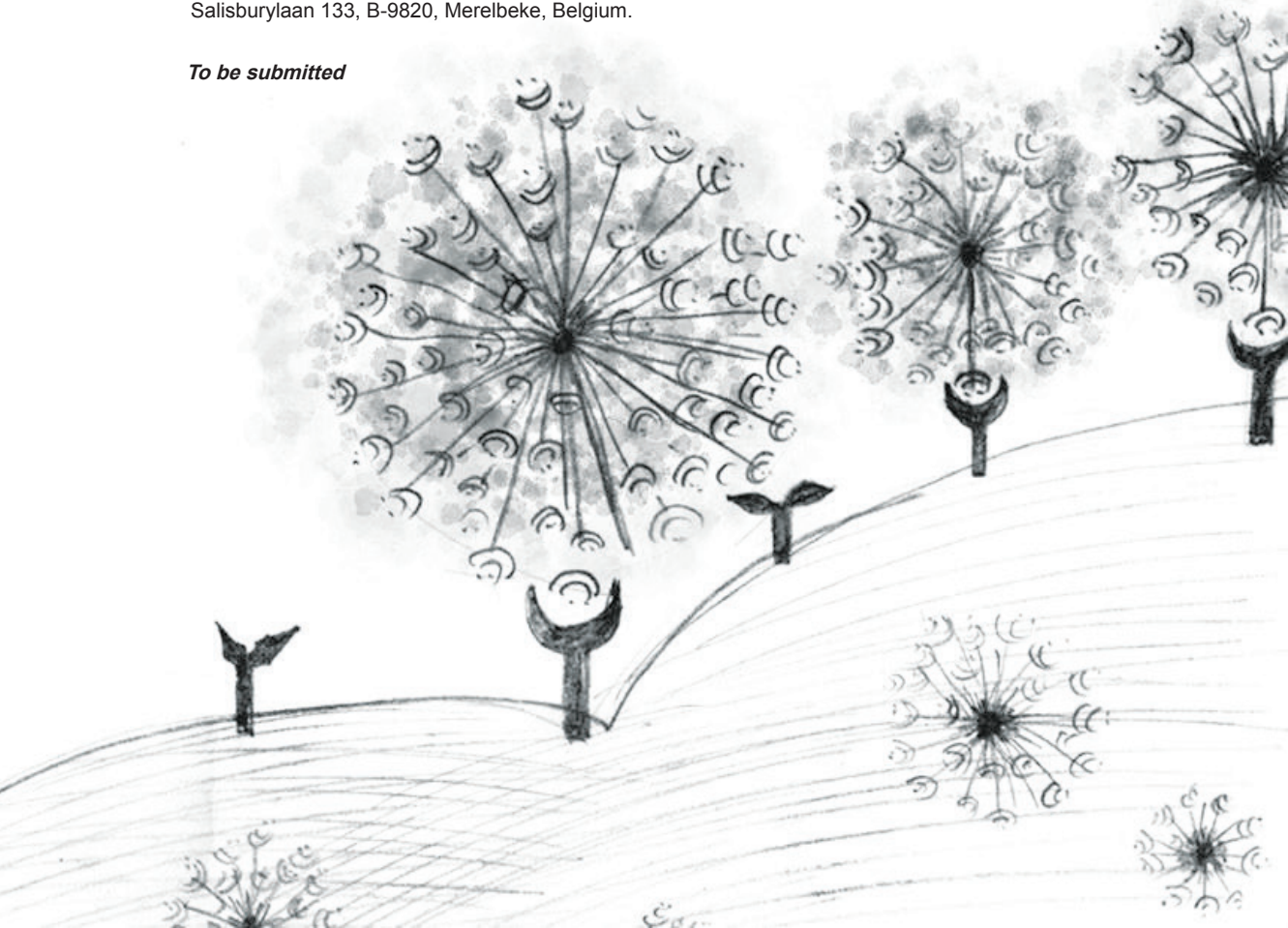
## An S protein mutation adapting feline enteric coronavirus to using DC-SIGN for cell entry does not confer macrophage tropism

Huihui Mou<sup>1</sup>, Lowiese M.B. Desmarets<sup>2</sup>, Frank J. M. van Kuppeveld<sup>1</sup>, Herman F. Egberink<sup>1</sup>, Hans J. Nauwynck<sup>2</sup>, Peter J. M. Rottier<sup>1</sup>, Berend-Jan Bosch<sup>1#</sup>

1 Department of Infectious Diseases and Immunology, Virology Division, Faculty of Veterinary Medicine, Utrecht University, 3508 TD Utrecht, The Netherlands.

2 Department of Virology, Parasitology and Immunology, Faculty of Veterinary Medicine, Ghent University, Salisburylaan 133, B-9820, Merelbeke, Belgium.

*To be submitted*



### **Abstract**

Feline enteric coronavirus (FECV) causes clinically mild or unapparent enteric infection in cats but does occasionally convert by mutation into a highly virulent form, the systemically replicating feline infectious peritonitis virus (FIPV), its tropism concomitantly changing from enterocytes to macrophages. Serotype I FIPV has been suggested to infect macrophages via the Dendritic Cell-Specific Intercellular adhesion molecule-3-Grabbing Non-integrin (DC-SIGN), a C-type lectin restricted to monocyte-derived cells, as a receptor. Whether the parental type I FECV has an intrinsic capacity or does require adaptation to utilize DC-SIGN as a receptor is unknown. To address this question, cell lines stably expressing feline DC-SIGN (fDC-SIGN) were created but this did not or hardly render feline embryonic fibroblast (FEA) cells and felis catus whole fetus (FCWF) cells susceptible to serotype I FECV strain UCD. However, introduction of fDC-SIGN into human hepatoma (Huh7) cells, which are naturally already somewhat susceptible to FECV UCD due perhaps to the expression of an orthologue receptor for the virus, clearly enhanced the infection. Subsequent passaging of FECV UCD in fDC-SIGN-Huh7 (fHuh7) cells yielded a virus, FECV UCDp that had become highly infectious to fHuh7 cells as well as to fDC-SIGN-FEA (fFEA) and fDC-SIGN-FWCF (fFCWF) cells in a DC-SIGN dependent manner. Sequencing of FECV UCDp revealed two amino acid substitutions (D142G and D317H) in the S1 receptor binding subunit of the viral spike (S) protein. By using S-pseudotyped viruses we demonstrated the mutation D317H to be responsible for the fDC-SIGN mediated cell entry enhancement and to correlate with an altered S cleavage pattern. Yet, the adaptive mutations acquired did not confer to FECV UCDp the capacity to infect macrophages, suggesting that alternative mutations in FECV are required both for this tropism switch and for the pathotype change to FIPV.

## **Introduction**

Coronaviruses (CoVs) are a group of enveloped, positive-strand RNA viruses that can infect a wide variety of mammals and birds causing respiratory and enteric diseases (1). The coronaviral spike (S) glycoprotein, trimers of which form the characteristic spikes on the virion, is a major determinant of host and tissue tropism as well as of pathogenesis. It is a type I membrane glycoprotein of ~200kDa, which is highly N-glycosylated with complex and high mannose sugars. The S protein mediates virus entry by facilitating receptor binding and membrane fusion through its S1 and S2 domains, respectively.

A remarkable characteristic of coronaviruses is their potential to change host, tissue or cell tropism, which they achieve by adapting their S glycoprotein to alternative receptors, and which often gives rise to a severe infection with potentially lethal outcome. One such example of a host tropism switch is the severe acute respiratory syndrome coronavirus (SARS-CoV) which caused the SARS epidemic in 2003 by making its way to humans from an animal reservoir (2). Another intriguing example, in this case of a tissue/cell tropism switch, is the feline coronavirus (FCoV), which can suddenly change within an infected cat from an enteric to a systemic replicating pathogen (3).

Together with canine coronavirus (CCoV) and transmissible gastroenteritis virus (TGEV), FCoV belongs to the alphacoronavirus 1 species within the alphacoronavirus genus. FCoVs are divided into two serotypes, serotype I and serotype II, based on different genetic and antigenic features of their S proteins (4). Type I FCoVs, which are the most prevalent in the field, have a distinctive feline S protein while the more sporadic type II FCoVs occasionally emerge by recombination of type I FCoVs with CCoVs when these viruses meet in a common host and as a result of which the feline virus acquires from its canine counterpart the S gene and some flanking genome sequences (5). Both FCoV serotypes are further divided into two pathotypes: feline enteric coronavirus (FECV) and feline infectious peritonitis virus (FIPV) (6). FECVs are widely prevalent particularly in multi-cat households and spread through the fecal-oral route (7-8). Their replication in intestinal epithelia causes a mild or clinically unapparent infection. In contrast, FIPVs primarily infect monocytes and macrophages leading to systemic and often lethal infections.

According to the internal mutation theory, the virulent FIPVs arise from avirulent FECVs through the acquisition of mutations that enable the efficient replication in monocytes and macrophages (9-11). Sequence comparisons of type I FECV and FIPV strains have pointed towards mutations within the spike gene (12-13), yet, functional and mechanistic relevance of these mutations for the pathotype switch is lacking.

## ***Coronavirus spike-receptor interactions***

---

Type II FIPV, but not type I FIPV, was shown to utilize the feline aminopeptidase N (fAPN) as a functional receptor for cell entry and can be efficiently propagated in vitro (5). Type I and II FIPV can both utilize the dendritic cell (DC)-specific intercellular adhesion molecule (ICAM) grabbing non-integrin (DC-SIGN) to enter cells. DC-SIGN is a calcium dependent (C-type) lectin that binds high-mannose carbohydrates on glycoproteins or glycolipids of pathogens. It has been shown to augment the entry of different enveloped viruses such as human immunodeficiency virus, Ebola virus and Hepatitis C virus as well as a number of coronaviruses (14-17). For FCoV, stable expression of feline DC-SIGN (fDC-SIGN) on Crandell feline kidney (CRFK) cells significantly enhanced the infection of both cell-adapted serotype I FIPV Black strain and serotype II FIPV strains (18). Moreover, the infection of FIPV type I and II in feline dendritic cells could be inhibited by mannan, a competitor of DC-SIGN binding. Furthermore, infection of the in vivo targeted monocytes by the FIPV type I Black strain and, to a lesser extent, by serotype II FIPV was demonstrated to be dependent on DC-SIGN expression (19). The receptor for the enteric serotype I FECV is unknown. However, DC-SIGN can be excluded as a candidate receptor for infection of enterocytes based on the lack of expression on these target cells.

In view of the important role of DC-SIGN in FIPV infection of monocytes and considering the observations with DC-SIGN expressing cell lines, we questioned whether FECV has the intrinsic capacity to utilize DC-SIGN as a receptor or needs to adapt to this receptor to convert to its FIPV pathotype. To address this question, we established cell lines stably expressing fDC-SIGN and assessed the replication characteristics of type I FECV infection on these cells.

## Results

**Creation of cell lines stably expressing feline DC-SIGN.** To enable selection of appropriate cell lines for our study we first tested the susceptibility of some cells for type I and type II FIPVs. Using immunofluorescence staining against FCoV nucleocapsid protein as an indicator we found feline embryonic fibroblasts (FEA) cells to be susceptible to the type I FIPV Black strain and the type II FIPV 79-1146 strain, while felis catus whole fetus (FCWF) cells could only be infected by the FIPV 79-1146 strain (data not shown). Intriguingly, human hepatoma (Huh7) cells were susceptible to the FIPV Black strain but not to the type II FIPV, suggesting these cells to express a human receptor orthologue for type I FCoV. In view of these differential susceptibilities Huh7, FEA and FCWF cell lines stably expressing feline DC-SIGN (fDC-SIGN) were generated using retroviral transduction and puromycin selection. Cell surface expression of fDC-SIGN on the resulting fDC-SIGN-Huh7 (fHuh7), fDC-SIGN-FEA (fFEA) and fDC-SIGN-FCWF (fFCWF) was confirmed by immunofluorescence staining (Fig.1).

**fDC-SIGN is able to increase FECV I infection in a cell type dependent manner.** We then tested the effect of fDC-SIGN expression on entry of a serotype I FECV. For this we used the serotype I FECV strain UCD which can be propagated on a recently generated FECV-susceptible feline intestinal epithelial cell line (20). Inoculation of the parental Huh7 cells with this virus generated some but few foci of infection. Infection was markedly enhanced in fDC-SIGN expressing Huh7 cells at all three time points (Fig.2A). In addition, analysis of the growth kinetics of FECV

5

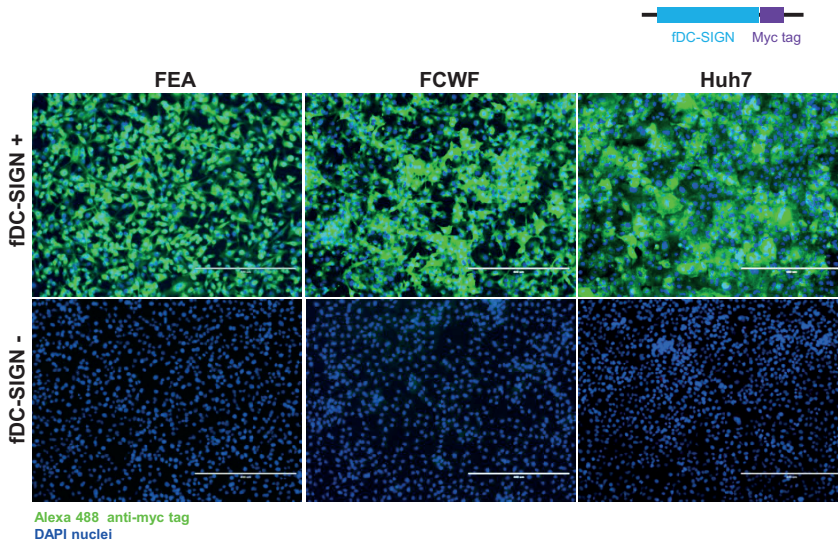


**Fig 1. Characterization of fDC-SIGN cell lines.** After selection using puromycin, the expression of fDC-SIGN on transduced cells (fDC-SIGN+) as compared to parental cells (fDC-SIGN-) was visualized by immunofluorescence staining against myc tag. Nuclei were stained with DAPI.

## Coronavirus spike-receptor interactions

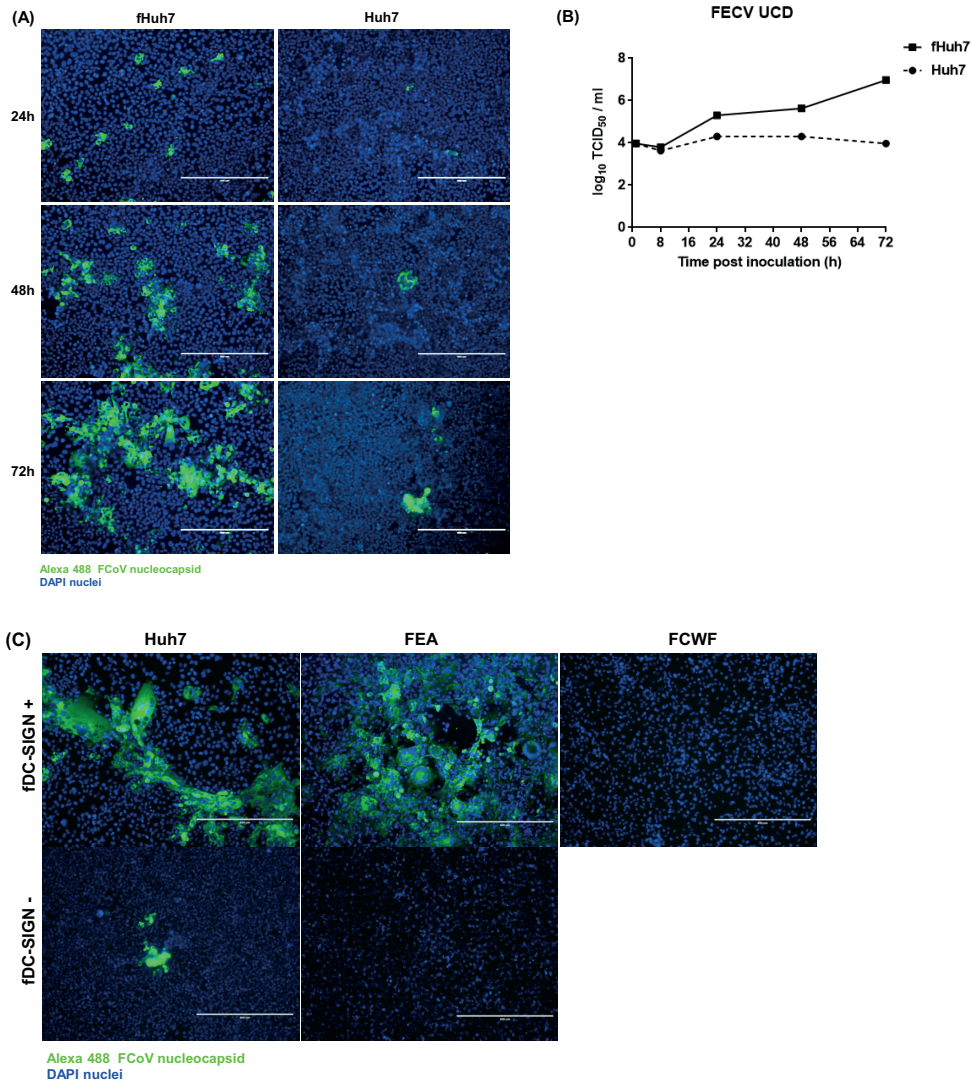


**Fig 2. Different fDC-SIGN cell lines show different susceptibility to FECV UCD.** (A) fHuh7 cells (fDC-SIGN+) and Huh7 cells (fDC-SIGN-) were infected with FECV UCD (MOI=1, titrated on IEC cells). At 24, 48 and 72 h p.i. infected cells were detected by immunofluorescence staining against nucleocapsid protein of FCoV (green). Nuclei were visualized by DAPI staining (blue). (B) fHuh7 and Huh7 cells were inoculated with FECV UCD (MOI=1, titrated on IEC cells). At 24, 48 and 72 h p.i. total virus was harvested and titrated on IEC cells. (C) fDC-SIGN cells (fDC-SIGN+) and corresponding parental cells (fDC-SIGN-) were infected with FECV UCD (MOI=1, titrated on IEC cells). At 72 h p.i. infected cells were immunostained using antibody against FCoV nucleocapsid protein (green). Nuclei were visualized by DAPI staining (blue).

UCD demonstrated fDC-SIGN expression in Huh7 cells to increase virus production by >2 logs, infectivity titers reaching a maximum of  $1 \times 10^7$  TCID<sub>50</sub>/ml at 72 hour post infection (p.i.) (Fig. 2B). Despite this clear increase, the kinetics of infection was rather slow and infection of all cells was never reached.

Next we comparatively analyzed the infection of FECV UCD on the three newly generated fDC-SIGN cell lines and their parental cells. The immunofluorescence analysis of infected cells confirmed the increased susceptibility of Huh7 cells due to the fDC-SIGN expression (Fig. 2C). Occasional foci of infection were observed in fDC-SIGN expressing FEA cells but not in the parental cells, whereas FCWF cells were resistant to UCD infection irrespective of fDC-SIGN expression.

**Passaging FECV UCD on fHuh7 cells improves virus infectivity on fDC-SIGN expressing cells.** Given the slow and limited replication of FECV UCD on fHuh7 cells, we allowed the virus to adapt to these cells by passaging. Already after one passage and sucrose purification, we noted that the passaged virus (FECV UCDp) possessed a higher infectivity on fHuh7 cells with formation of extensive syncytia and complete infection of the cell monolayer.

To compare the infectivities of FECV UCDp and UCD as well as their dependency on DC-SIGN, both the parental and fDC-SIGN expressing Huh7, FEA and FCWF cells were inoculated with each virus at equal MOI. Infected cells were visualized after 8 and 24 h p.i. by immunofluorescence staining. fDC-SIGN increased the entry and infection of both FECV UCD and FECV UCDp in Huh7 cells at 8 h p.i. and 24 h p.i., but the enhancement was more significant for the cell adapted virus UCDp. At 24 h p.i. with this virus, extensive syncytia formation and cell detachment was seen on fHuh7 cells. Intriguingly, the infectivity of FECV UCDp on the parental Huh7 cells was also higher than that of FECV UCD (Fig. 3A). Infection of fDC-SIGN expressing FEA and FCWF cells with FECV UCD was very limited or absent at 8 and 24 h p.i.. Similar to fHuh7 cells, expression of fDC-SIGN in fFEA and fFCWF cells greatly improved the infection of FECV UCDp (Fig. 3B and C).

Binding of mannose-rich carbohydrates to DC-SIGN can be blocked with the sugar-polymer mannan. To test the specificity of binding of FECV UCDp to fDC-SIGN, cells were preincubated with serial dilutions of mannan, followed by virus inoculation. Infection of FECV UCDp in all fDC-SIGN expressing cell lines was reduced by mannan in a dose dependent manner at both 8 h p.i. and 24 h p.i.. No significant inhibition was seen after galactose treatment, taken along as a control, not even at the highest concentration (Fig. 4). While the infection of fFEA and fFCWF cells with FECV UCDp could be fully blocked at 10 µg/ml of mannan, that of fHuh7 cells was also inhibited considerably by mannan, but inhibition was never complete, not even at the highest concentration used. This DC-SIGN-independent infection additionally confirms the presence of a type I FECV receptor orthologue on Huh7 cells that can be functionally recruited albeit with low efficiency.

## Coronavirus spike-receptor interactions

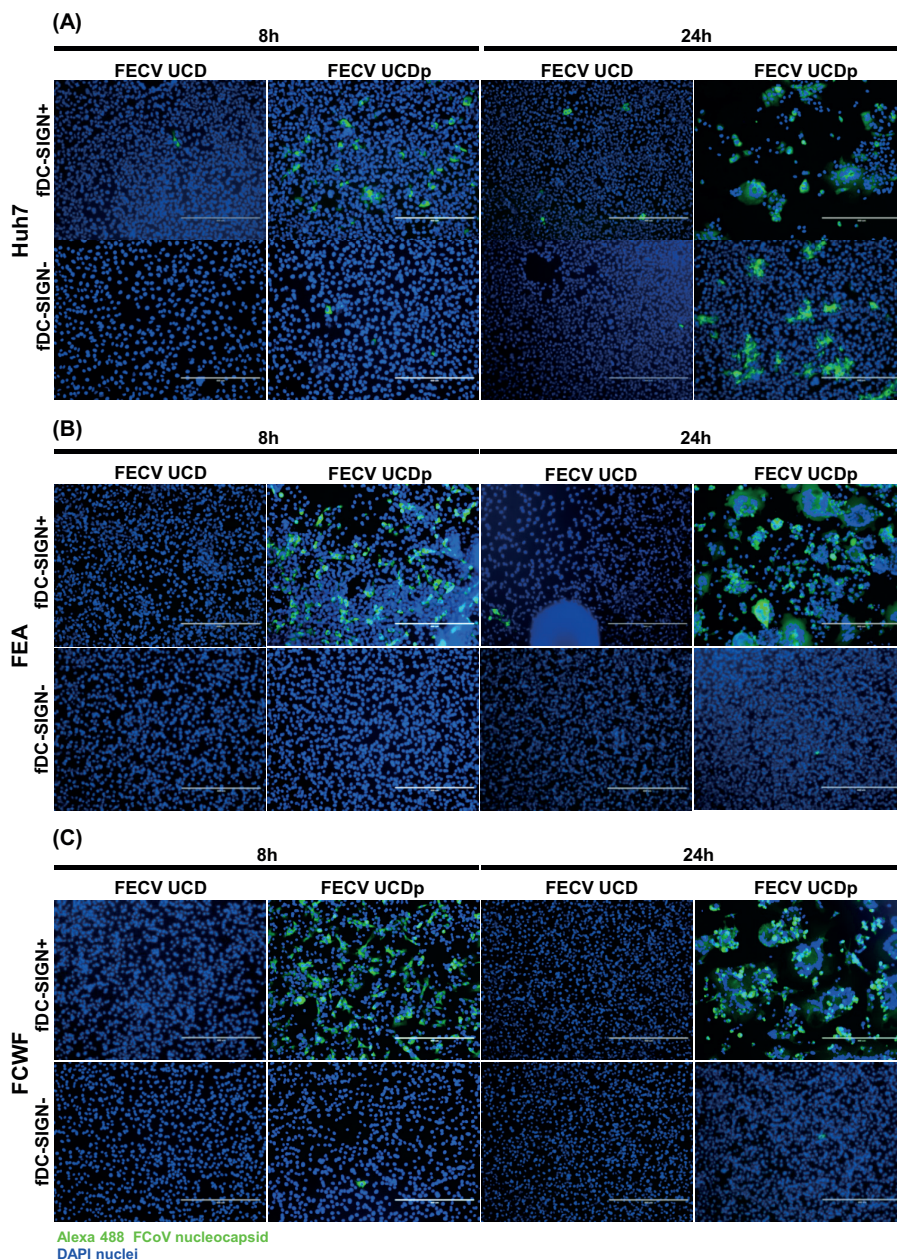
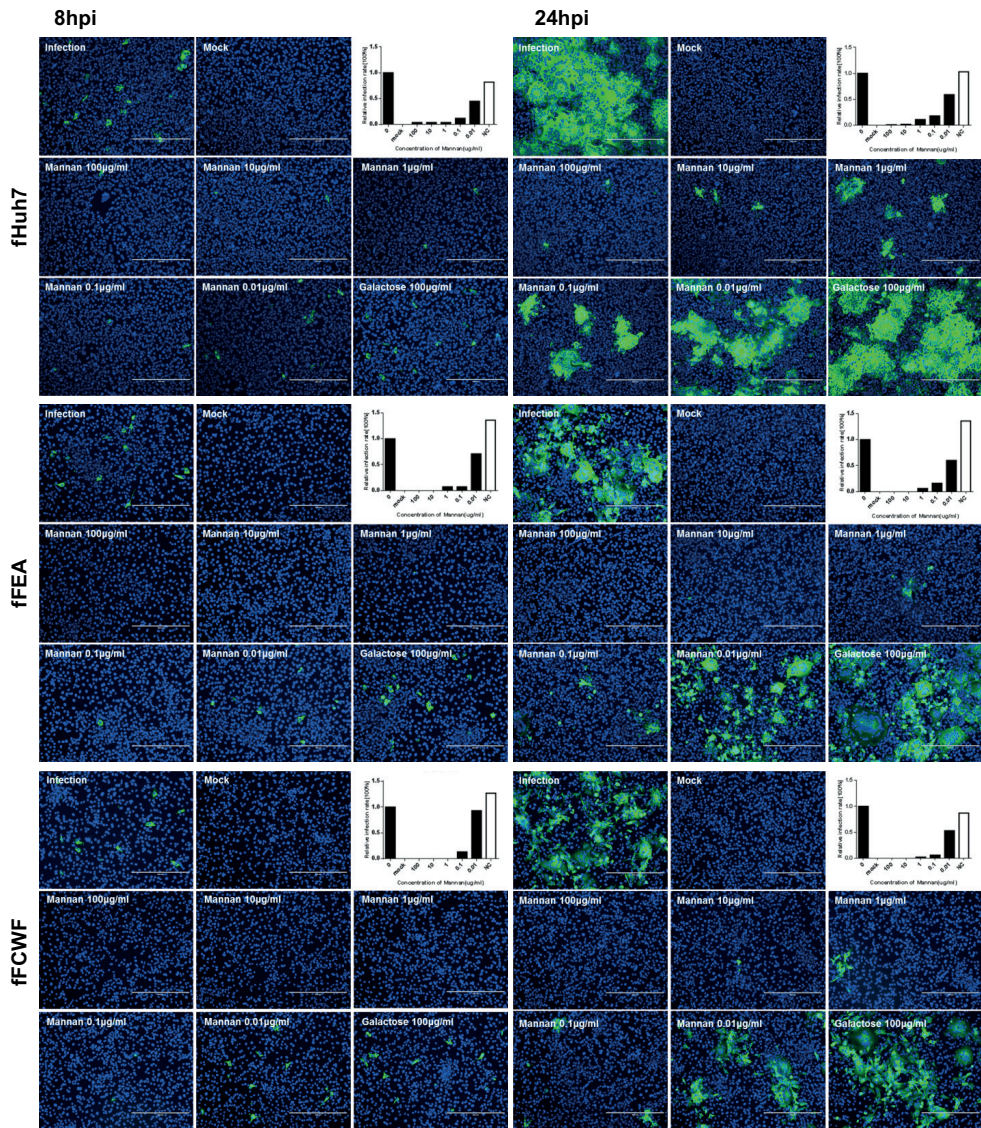


**Fig 3. fHuh7-adapted FCoV UCDp has increased infectivity towards fDC-SIGN expressing cell lines.** (A) fHuh7 cells (fDC-SIGN+) and Huh7 cells (fDC-SIGN-), (B) fFEA cells (fDC-SIGN+) and FEA cells (fDC-SIGN-) and (C) fFCWF cells (fDC-SIGN+) and FCWF cells (fDC-SIGN-) were infected with FCoV UCD or FCoV UCDp (MOI=1, titrated on IEC cells). At 24, 48 and 72 h p.i. infected cells were visualized by immunofluorescence staining against the FCoV nucleocapsid protein (green). Nuclei were visualized by DAPI staining (blue).





Alexa 488 FCoV nucleocapsid  
DAPI nuclei

**Fig 4. Mannan inhibits the infection of FECV UCDp in a dose-dependent manner.** fHuh7, fFEA and fFCWF cells were pretreated with serially diluted mannose starting at 100µg/ml at 37°C for 30 min, using galactose (100µg/ml) as negative control (NC), and then inoculated with FECV UCDp (MOI=0.5). At 8 and 24 h p.i. infected cells were visualized by immunofluorescence staining against FCoV nucleocapsid protein (green), and nuclei were visualized by DAPI staining (Blue). Infected cells were quantitated based on counting nuclei of fluorescent and non-fluorescent cells, and the extent of inhibition is expressed as the fraction of infected (positive) cells in the treated vs the non-treated cells. The black bars refer to mannose treatments, white bars to galactose treatment.

## Coronavirus spike-receptor interactions

We comparatively assessed the production of infectious FECV UCDp in fDC-SIGN positive Huh7 and FEA cells and the corresponding parental cells. At 8, 24 and 48 h p.i. the total virus infectivity as well as the intra- and extracellular infectivity were determined by titration on fHuh7 cells. The serotype II FIPV strain 79-1146, which utilizes fAPN as a functional receptor, was included as a control. Clearly, the expression of fDC-SIGN did not render Huh7 cells susceptible to FIPV 79-1146 nor did it change the infection of FEA cells by this virus (Fig.5D). In contrast, consistent with the immunofluorescence data, fDC-SIGN expression increased the production of FECV UCDp in Huh7 cells (Fig.5A). Also consistent with our previous observations, expression of fDC-SIGN rendered the FEA cells susceptible to FECV UCDp and allowed a productive infection (Fig. 5C). When comparing the intracellular and extracellular virus titers, infectious FECV UCDp virions seemed to remain more cell-bound than FIPV 79-1146, particularly at early time points after infection, which is suggestive of a slow release of the FECV particles produced.

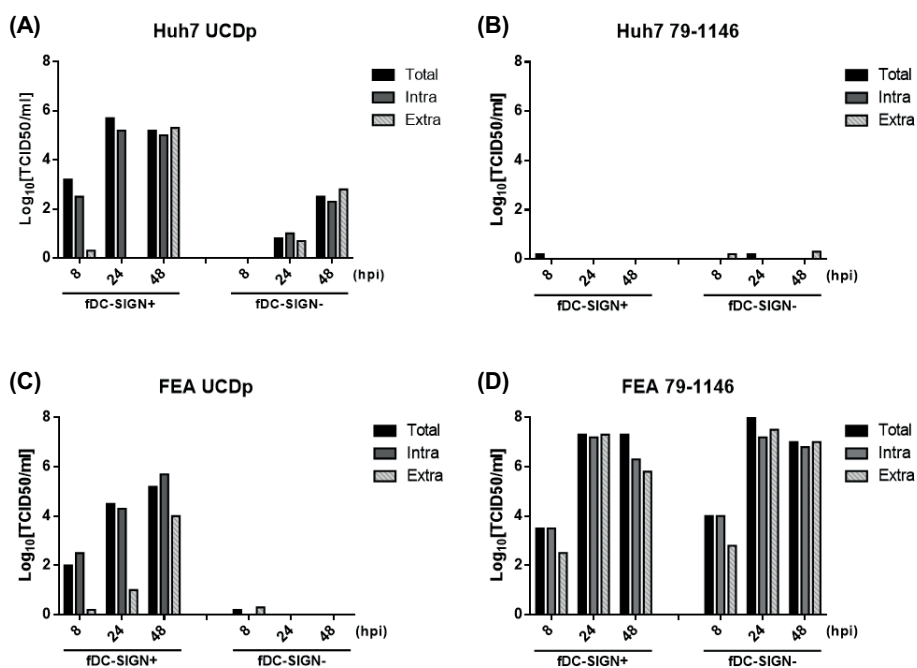


**Fig 5. Kinetics of FECV UCDp and FIPV 79-1146 infections.** fHuh7 and fFEA cells (fDC-SIGN+) as well as their parental cell lines (fDC-SIGN-) were inoculated with FECV UCDp (MOI=0.1) or FIPV 79-1146 (MOI=0.01) at 37°C for 1h after which unbound viral particles were removed by 3 washing steps. At 8, 24 and 48 h p.i. the total, intracellular and extracellular virus was harvested and titrated on fHuh7 cells (for FECV UCDp virus) or fFEA cells (for FIPV 79-1146). **(A)** Growth of FECV UCDp in Huh7 and fHuh7 cells. **(B)** Growth of FIPV 79-1146 in Huh7 fHuh7 cells. **(C)** Growth of FECV UCDp in FEA and fFEA cells. **(D)** Growth of FIPV 79-1146 in FEA and fFEA cells.

**A substitution in the FECV UCDp S prote in enhances entry into fDC-SIGN cell lines.** Passaging was required for FECV UCD to more efficiently infect DC-SIGN expressing cells, suggesting a role of adaptive mutations. Considering the key role of the S protein in initiation of coronavirus cell entry we sequenced the spike gene of FECVs UCD and UCDp. Two amino acid substitutions were identified, an aspartic acid to glycine mutation at amino acid position 142 (D142G) and an aspartic acid to histidine mutation at position 371 (D371H), both of which occur in the S1 subunit of the S protein (Fig. 6A). Neither of these mutations altered a predicted N-glycosylation site.

In order to assess the effect of the D142G and D371H substitutions in FECV UCD S protein mediated entry we employed a VSV pseudotyping system expressing a luciferase reporter gene. Concentrated preparations of VSV pseudotyped with wild-type S (VSV-S<sub>UCD</sub>) or mutant S proteins were used to inoculate our three fDC-SIGN expressing cells fHuh7, fFEA and fFCWF. The relative infection rates of the target cells, quantified by measuring luciferase activities, revealed that, while the D142G mutation did not affect the entry efficiency of VSV-S<sub>UCD</sub> in any of the cell lines, the

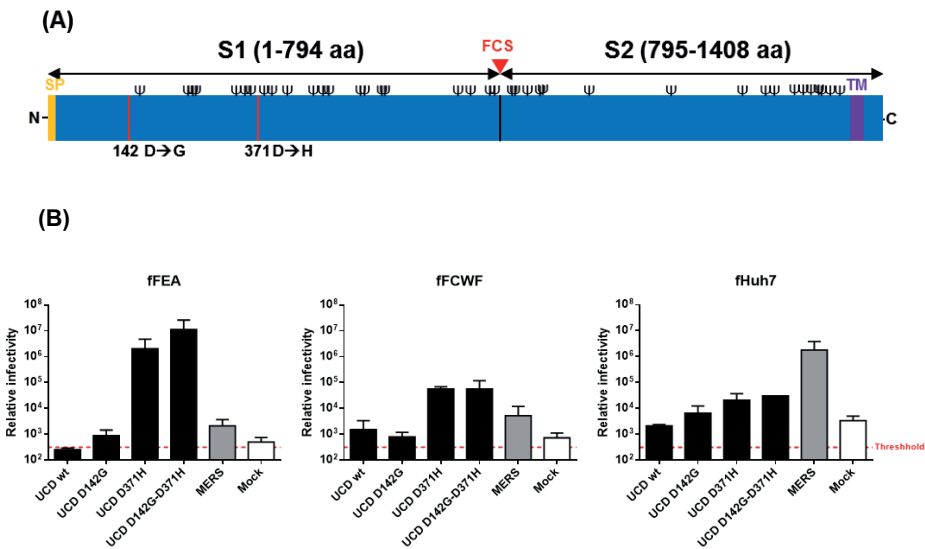


**Fig.6 Mutation D371H in the FECV UCDp S1 subunit is the main cause of entry enhancement in fDC-SIGN expressing cells.** (A) Schematic presentation of mutations identified in the S1 region of FECV UCDp spike protein. The positions of the transmembrane domain (purple bars; predicted by the TMHMM server) and of the predicted N-glycosylation sites (ψ; predicted by theNetNGlyc server) are indicated. The furin cleavage site between the S1 and S2 subunits are indicated by a red triangle. (B) The introduction of the mutation D371H significantly increased the entry efficiency the pseudotyped VSV virus bearing FECV UCD S protein (VSV-S<sub>UCD</sub>). Purified VSV-S<sub>UCD</sub> with and without mutations were inoculated on fHuh7, fFEA and fFCWF cells. The viral titers had been normalized by the incorporated spike proteins analyzed by western blot. After overnight incubation, the infection level was determined by measuring luciferase activity in the cell lysates. The red dashed lines show the threshold in this experiment.

## ***Coronavirus spike-receptor interactions***

---

D371H mutation - either alone or in combination with D142G - increased the entry efficiency of VSV-S<sub>UCD</sub> in all three DC-SIGN positive cell lines, the most obvious enhancement being observed in the fFEA cells.

***Introduction of mutation D371H affects cleavage of FECV UCD S protein.*** The FECV UCD S proteins incorporated into VSV-S<sub>UCD</sub> particles were analyzed by western blotting using a monoclonal antibody (MAb) against the Flag-tag C-terminally appended to the S protein and using a MAb targeting the S1 subunit. The FECV UCD S protein contains an optimal furin cleavage sequence (RRSRR) at the S1-S2 junction. The Flag-tag antibody detected different forms of the wild-type and mutant S proteins incorporated into the VSV-S<sub>UCD</sub> particles (Fig. 7A). Based on their migration pattern, these forms were interpreted as full-length S, S2, a truncated S2 (S2\*) and an SDS-resistant trimeric form of S2 (3XS2) migrating slower than the full length S protein with an apparent size of about 250kDa. Quantification by densitometry indicated the relative ratio of these bands to differ significantly for the S proteins containing the D371H mutation (Fig. 7A). While for the wild-type S and the S-D142G variant the S2 and S2\* bands comprised 86% and 83% of all S forms, respectively, these ratio's decreased to 33% and 25%, respectively, for the S proteins containing the D371H and D142G-D371H substitutions. In the latter two viruses the full-length S and trimeric 3XS2 were the dominant S forms. As revealed by the MAb against the S1 subunit, after the introduction of mutation D371H the cleavage of full-length S protein was reduced slightly (Fig.7B). Thus, the D371H substitution influences the S protein cleavage pattern and/or spike stability resulting in the appearance of an approximately 250 kDa large S form, which we hypothesize to be the trimeric S2\* form. Further analysis of transiently expressed FECV UCD S proteins by western blot also demonstrated reduced cleavage at the S1-S2 junction for S proteins containing the D371H mutation (Fig.7C). Inclusion of furin inhibitor in the cell culture medium during transient expression of S proteins in HEK293T cells reduced the levels of the S2 forms relative to full length S protein for the S-D371H mutant compared with wild-type S protein, confirming that furin is responsible for the observed cleavage (Fig. 7D).

***Increased infectivity of FECV UCDp on fDC-SIGN expressing cells is not heparan sulfate dependent.*** Some viruses utilize cell surface heparan sulfate proteoglycans as receptors, a trait which is often acquired by mutation upon passaging in cell culture (21-23). The cell passaged serotype I FIPV strain UCD1 has a mutation in the furin cleavage motif occurring at the S1/S2 junction that blocks furin cleavage but maintains a heparan sulfate proteoglycan binding site (BBxB; B = basic amino acid) that is functional in enabling the virus to use heparan sulfate as a receptor (23). Thus, in view of the altered furin cleavage pattern conferred by the D371H mutation, we examined the potential of heparan sulfate as a receptor for FECV UCDp by using heparin, a soluble glycosaminoglycan analogue, as a competitor of heparan sulfate binding. FECV UCDp, FIPV UCD1 and the heparan-sulfate dependent Enterovirus 71 were pretreated with heparin and subsequently

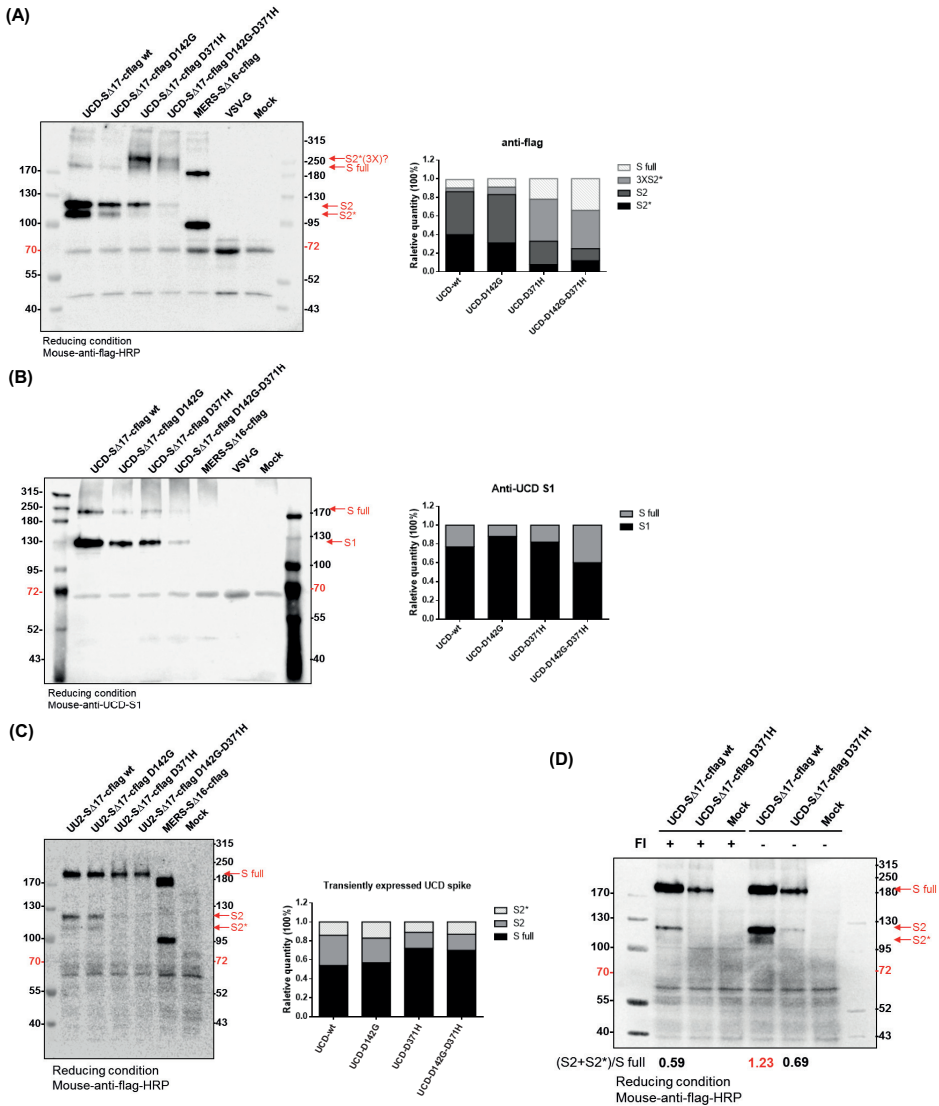


**Fig. 7 Mutation D371H inhibits S protein cleavage.** The VSV-S<sub>UCD</sub> wild-type and mutant viruses purified by pelleting through 20% sucrose were subjected to western blot analysis and S proteins were detected using (A) a mouse anti-flag Mab conjugated with horse-radish peroxidase or (B) a mouse anti-FECV UCD S1 Mab. The intensities of the different S1 bands were quantified using Quantity One® 1-D analysis software (Bio-Rad Laboratories, Inc.). (C) The HEK293T cells transiently expressing FECV UCD spike wild-type and mutant proteins were analyzed by western blotting and visualized by a mouse anti-flag Mab conjugated with horse-radish peroxidase. The intensities of the different S protein bands were quantified by Quantity One® 1-D analysis software. (D) Wild-type and D371H mutant spike proteins were transiently expressed in HEK293T cells in the absence or presence of furin inhibitor (FI). At 48h p.i. the cells were harvested for western blot analysis. Bands were visualized by the mouse anti-flag Mab conjugated with horse-radish peroxidase.

## Coronavirus spike-receptor interactions

added to FEA and fFEA cells after which the relative infection levels were measured by immunostaining. In parallel, as controls the same infections were performed after pretreatment of cells with mannan. Enterovirus 71 was neither influenced by the expression of fDC-SIGN nor by the pretreatment with mannan (Fig.8). In contrast, infection of FEA cells by both serotype I viruses, FECV UCDp and FIPV UCD1, was greatly enhanced by the expression of fDC-SIGN, while this enhancement was counteracted by the pretreatment of the cells with mannan. Preincubation of virus with soluble heparin greatly reduced infection of Enterovirus 71, but not that of FCoV UCD and UCD1. These observations indicate that the increased infectivity of FECV UCDp after passaging on DC-SIGN expressing cells cannot be attributed to the recruitment of heparan sulfate as a receptor.

### **Adaptive mutations in FECV UCDp do not confer macrophage tropism.**

The expression of DC-SIGN in combination with adaptive mutation(s) in FECV UCDp was sufficient for efficient infection of feline and human cells. To test whether FECV UCDp can infect DC-SIGN positive macrophages, we inoculated activated bone marrow macrophages with FECVs UCD and UCDp as well as with the macrophage-tropic type II FIPV 79-1146 control virus. In contrast to the successful infection by FIPV 79-1146, no infection was seen in macrophages inoculated with FECVs UCD or UCDp (Fig. 9). The result indicates that besides DC-SIGN additional determinants are involved in the acquisition of macrophage tropism.

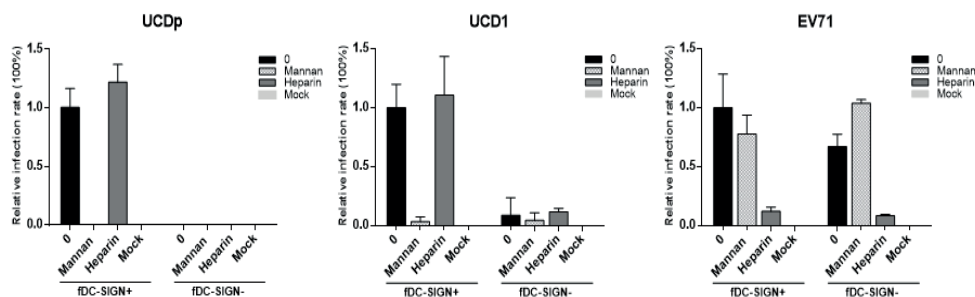
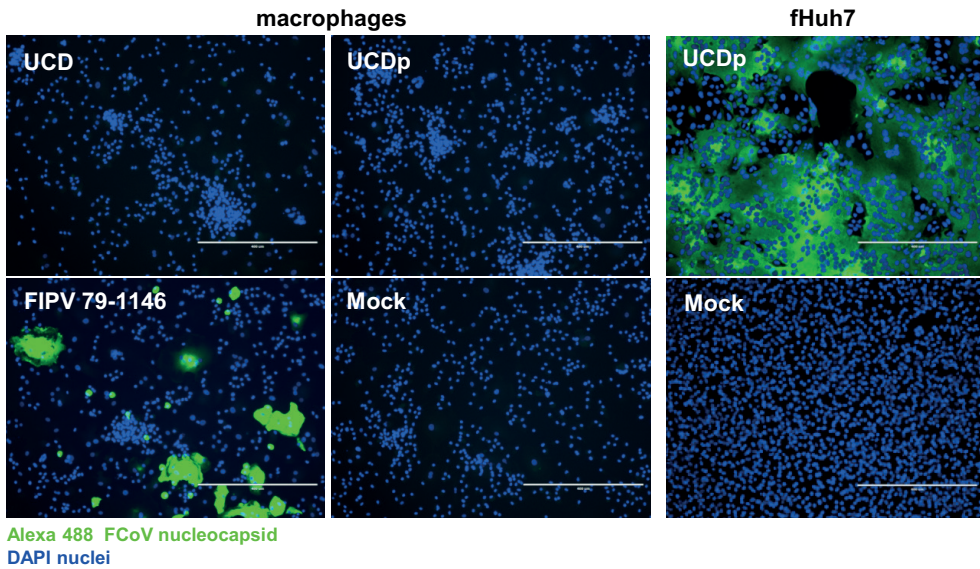


**Fig. 8 The cleavage inhibition of FECV UCD D371H mutant spike protein leads to fDC-SIGN usage not that of heparin sulfate.** fFEA (fDC-SIGN+) and FEA (fDC-SIGN-) cells were inoculated with FECV UCDp, FIPV UCD1 or EV71 in the presence of mannan (100 $\mu$ g/ml) or after pretreatment of the viruses with heparin (250 $\mu$ g/ml). Mock pretreatment and mock infection were included as controls. At 24h p.i. infected cells were detected using an antibody against FCoV nucleocapsid protein (for FIPV UCD1 and FECV UCDp) or an antibody against double strand RNA (for EV71) combined with goat anti-mouse IgG Alexa 488. Nuclei were visualized by DAPI staining. Infection levels were quantified by counting nuclei of fluorescent and non-fluorescent cells and expressing the relative rate of infection as the fraction of total cells fluorescing.



Alexa 488 FCoV nucleocapsid  
DAPI nuclei

**Fig. 9 Neither FECV UCD nor FECV UCDp can infect macrophages.** Feline bone marrow macrophages were cultured in medium supplemented with 100ng/ml fGM-CSF for 5 days. Parallel cultures were then inoculated with FECV UCD or FECV UCDp (MOI=1) taking type II FIPV 79-1146 as control (MOI=1, titrated on FCWF cells). The infection by FECV UCDp was also conducted in fHuh7 cells as positive control. At 24h p.i. cells were fixed and the infection was visualized by immunofluorescence staining of the FCoV nucleocapsid protein (green); cell nuclei were visualized by DAPI staining (Blue).

### **Discussion**

Efficient infection of macrophages is the main feature that functionally distinguishes the FIPV from FECV pathotype, yet the mechanism and genetic determinant(s) underlying this FIPV distinction are not understood (11). We hypothesized that adaptation of FECV to a macrophage receptor could be of critical importance for the pathotype transition. Type I FIPVs have been shown capable of infecting macrophages and monocytes using DC-SIGN as an entry receptor (19). Thus, we questioned whether type I FECV possesses the intrinsic ability to recruit DC-SIGN for entry or whether this trait is acquired during the virulence switch. Here we demonstrate that FECV could efficiently utilize feline DC-SIGN as a functional receptor on fDC-SIGN expressing cells, but only after cell culture adaptation. Efficient fDC-SIGN receptor utilization corresponded with the occurrence of two mutations in the S protein of the cell-adapted FECV, one of which (D371H) was shown to actually cause the infection enhancement. Yet, the efficient fDC-SIGN receptor recruitment was not sufficient to render the cell-adapted FECV capable of infecting macrophages.

A defined and high-titer stock of the serotype I FECV UCD virus was obtained using a recently established feline intestinal epithelial cell line that allows propagation of FECV field isolates (20). Using this stock we observed that human hepatoma cells have limited susceptibility to FECV I UCD. Also the serotype I FIPV Black strain had earlier been shown to replicate on these cells ((24) and own observations). The observations suggest that Huh7 cells express the orthologue receptor which - to some extent - can be recruited by serotype I FCoV.

Expression of fDC-SIGN alone was not sufficient for achieving efficient infection of serotype I FECV. It enhanced the infection of Huh7 cells and rendered FEA cells susceptible but FCWF cells remained refractory. However, already after one adaptive passage on fDC-SIGN expressing Huh7 cells the virus acquired the mutations that not only dramatically further enhanced the infection of Huh7 and FEA cells but also rendered FCWF cells largely susceptible. The responsible mutations (D142G and D371H) in the adapted S protein did not alter the number of predicted N-glycosylation sites, yet their strong effects were indeed due to the involvement of lectin as demonstrated by the inhibitory consequences of mannan treatment.

One of the two residue substitutions in the UCDp S protein (D371H) was shown to enhance  $S_{UCD}$  pseudotyped VSV entry into DC-SIGN expressing cells. Intriguingly, the D371H substitution reduced the cleavage of S proteins at S1/S2 junction, though the furin cleavage site itself was not altered. As shown earlier, reduced cleavage of coronavirus S proteins may generate a heparan sulfate binding site used for heparan sulfate-dependent entry (21, 23). Adaptation of UCDp to heparan sulfate as an attachment molecule appeared unlikely given the virus insensitivity for the heparan sulfate analogue heparin. The furin cleavage site within the serotype I S



## ***DC-SIGN usage and macrophage tropism***

---

protein (RRxRR) is highly conserved in FECV field strains (13). Mutations in the furin cleavage site strains are frequently observed in serotype I FIPV isolates and have hence been linked to the FECV-FIPV pathotype switch (13). Coincidentally, the five serotype I FIPV strains that can be propagated in cell culture all contained mutations in the furin cleavage site (Black (GenBank: BAC05493.1), KU-2 (GenBank: AAB47503.1), C3663 (GenBank: BAJ08255.1) and Yayoi (GenBank: BAM34500.1) (25)). How and whether reduced spike cleavage correlates with virus propagation in vitro and in vivo remains to be determined.

In summary, type I FECV UCD did not inherently possess the capacity to efficiently enter and replicate in DC-SIGN-expressing cells but obtained this ability by acquiring mutations during replication. However, DC-SIGN usage was not sufficient to render serotype I FECV infectious to macrophages. For serotype II FCoV, mutations in the S2 subunit of the spike protein correlated with macrophage infection (26). More efforts will be needed to identify the responsible mutations and clarify the mechanism facilitating the macrophage tropism switch in serotype I FCoV.

### **Methods and materials**

**Cells and viruses.** FCWF, FEA, Huh7 and 293T cells were maintained in Dulbecco's modified Eagle's medium supplemented with 10% fetal calf serum (FCS), 100U of penicillin/ml and 100µg of streptomycin/ml (all from Life Technologies, Ltd., UK). Feline intestinal epithelial cells (IECs) were cultured in Dulbecco's modified Eagle's medium/Ham's F12 Nutrient Mixture (1/1) supplemented with 100U of penicillin/ml, 100µg of streptomycin/ml, 100µg of gentamicin/ml, 5% FCS and 1% non-essential amino acids 100× (Gibco-BRL) (20). Macrophage culturing was done as described before (26). Briefly, the frozen bone marrow-derived mononuclear cells (BMMCs) were thawed, washed, and suspended in RPMI 1640 medium containing 10% FCS, 100U of penicillin/ml, 100µg of streptomycin/ml and recombinant feline GM-CSF (R&D) at a final concentration of 100ng/ml. Culture medium for macrophages was refreshed 5 days after seeding, and macrophages were ready for experimental infection at 7 days after seeding.

Serotype I FECV UCD was propagated in feline IECs in FCS-depleted medium and the third passage virus stock was used for all infection experiments. FECV UCD virus was blindly passaged once on fHuh7 cells at low MOI. Total virus was harvested 72h post infection (p.i.) by freeze-thawing cells and culture supernatant once, followed by removing cell debris by one round of low-speed centrifugation. The virus was then collected by pelleting through a 20% sucrose cushion at 30,000rpm at 4°C for 2.5h in a Beckman SW32 rotor. The pellet was dissolved in OPTI-MEM (Gibco-BRL) supplemented with 10mM HEPES (Gibco-BRL), and the virus was designated passaged FECV UCD (FECV UCDp).

VSV pseudotyped viruses were produced as described before (27). In general, the plasmids encoding FECV UCD and MERS-CoV S proteins were generated by cloning into the pCAGGS expression vector the S genes of these two viruses without the sequences encoding the ER and Golgi retention motif at the C-terminus (FECV UCD, 17 amino acids from C-terminal; MERS-CoV, 16 amino acids from C-terminal) but with a sequence encoding a C-terminal Flag tag for detection purposes. HEK293T cells were transfected with S protein expression vectors using polyethylenimine (PEI), and transfection medium was replaced with fresh culture medium after overnight incubation. At 24h post transfection, the transfected cells were infected with VSV-G pseudotyped VSVΔG/FLuc virus at a MOI=1. Coronavirus S-pseudotyped VSVΔG/FLuc virions produced were harvested 18h post infection, when about 90% of the cells were rounded up, and passed through a 0.45µm filter to get rid of cell debris. Harvested viruses were stored at -80°C after supplementation with HEPES to 10mM, or directly purified.

Purification of pseudotyped viruses was conducted by sedimenting the virus particles through a 20% sucrose cushion dissolved in PBS without Ca<sup>2+</sup> at 30,000rpm at 4°C for 2.5h in a Beckman SW32 rotor. After ultracentrifugation the supernatant was discarded and pellets were dissolved in OPTI-MEM supplemented with 10mM HEPES.

**Generation of fDC-SIGN expressing cell lines.** FCWF, FEA and Huh7 cell lines expressing fDC-SIGN were created by transduction with produced vesicular stomatitis virus (VSV) G protein-pseudotyped murine leukemia viruses (MLV) containing pQCXIP-fDC-SIGN-c-Myc as described before (28). Briefly, HEK293T cells were co-transfected with three plasmids, pMLV-gag-pol, pCAGGS-VSV-G and pQCXIP-pQCXIP-fDC-SIGN-c-Myc, and the medium was refreshed after overnight incubation of transfection mix. The supernatant with produced virus was harvested 48h post transfection and clarified by passing through 0.45µm filter. Three parental cell lines were transduced with generated MLV virus, and the fDC-SIGN-FCWF (fFCWF), fDC-SIGN-FEA (fFEA) and fDC-SIGN-Huh7 (fHuh7) cell lines were selected and maintained with medium containing puromycin (Sigma) (7.5µg/ml for FCWF and FEA cells; 2.5µg/ml for Huh7 cells). fDC-SIGN expression was confirmed by immunofluorescence staining using mouse monoclonal antibody against c-Myc antibody (Invitrogen) and Goat-anti-mouse Alexa 488 (Invitrogen).

**Virus infections.** To investigate the function of fDC-SIGN, Huh7 and fHuh7 cells were infected with FECV UCD (MOI=1, based on TCID<sub>50</sub> titration on IEC cells). Cells were fixed at 24, 48 and 72h p.i. with 3.7% paraformaldehyde (PFA) for immunofluorescence staining. Similarly, parallel cultures of fHuh7, fFEA and fFCWF cells were infected by FECV UCD at MOI=1 and cells were fixed at 72h p.i. with 3.7% PFA. Infection was visualized by immunofluorescence staining using a monoclonal antibody against the FCoV nucleocapsid protein (AbD Serotec).

To compare the infectivity of FECV UCDp with that of FECV UCD, fDC-SIGN expressing cells fHuh7, fFEA and fFCWF as well as their parental cell lines were inoculated with FECV UCD or FECV UCDp (MOI=1, according to the TCID<sub>50</sub> titrated on IEC cells). Infected cells were fixed with 3.7% PFA at 8h and 24hp.i. for immunofluorescence staining.

To examine the involvement of fDC-SIGN in FECV UCDp infection, fHuh7, fFEA and fFCWF cells were pretreated with serial dilutions of mannan, the natural ligand of DC-SIGN, at 37°C for 1h, and inoculated with FECV UCDp in medium containing the same concentration of mannan. Galactose was taken as negative control in this experiment. After inoculation, cells were further incubated at 37°C and 5% CO<sub>2</sub> and fixed at 8h and 24h p.i. with 3.7% PFA. Immunofluorescence staining was performed as above and infected cells were counted for further analysis.

In order to explore the use of heparan sulfate in FECV UCDp infection, fFEA cells were inoculated after a 30min preincubation of the virus at 37°C with 250µg/ml soluble heparin (Sigma). Enterovirus 71 which can enter cells via heparan sulfate was taken along as a positive control. Mannan inhibition was included to specify the involvement of fDC-SIGN. The inoculated cells were fixed at 24h p.i. with 3.7% PFA for immunofluorescence staining.

**Viral kinetics of FECV UCD and FECV UCDp.** In order to examine the function of fDC-SIGN in viral production of FECV UCD, Huh7 and fHuh7 cells were inoculated

## ***Coronavirus spike-receptor interactions***

---

with FECV UCD at a MOI=1 (based on titration on IEC cells) and incubated at 37°C for 1h. Subsequently, cells were washed three times to remove unbound virus particles and incubated further in fresh medium at 37°C and 5% CO<sub>2</sub>. Total virus was harvested at 1, 8, 24, 48 and 72h p.i., and then titrated on IEC cells.

Kinetics of FECV UCDp replication was studied by inoculation of Huh7, fHhu7, FEA and fFEA cells at a MOI=0.1 for 1h at 37°C. Cells were then washed three times to remove unbound virus particles and further incubated in fresh medium at 37°C, 5% CO<sub>2</sub>. FIPV 79-1146 (MOI=0.01) which uses pAPN as a functional receptor was taken as control for this experiment. Total, intracellular and extracellular viruses were harvested at 8h, 24h and 48h p.i., and titrated on fHuh7 (for FECV UCDp virus) or fFEA cells (for FIPV 79-1146).

**Sequencing.** The total RNA of the fHuh7 cell passaged FECV UCDp or FECV UCD from feces sample (29) was isolated using MACHEREY-NAGEL (MN) viral RNA extraction kit according to the manufacturer's protocol. cDNA was synthesized by SuperScript II Reverse Transcriptase (Invitrogen) with random primers (Thermo Scientific). Three partially overlapping PCR products covering the entire spike gene of both viruses were generated using three pairs of primers. The PCR products were purified with MN Gel recovery Kit, and sequenced by MacroGen (MacroGen Europe Inc.).

6976-2336	5'-ACTACTTAGGACCATACTGTGAC-3'
	5'-CGAATTCAAGTGTTGTTAGACCACGTTGGC-3'
3948-1873	5'-CAACCGCACCACGTATTATG-3'
	5'-CCCTCGAGCAAGACGTGCGCCAAGATTA-3'
6259-2973	5'-ACCTGTTGTTGTGGATTGTGC-3'
	5'-GTTCCGCGGCTCGTCAAGTACAGCGTC-3'

**Western blotting.** To analyze the incorporation of S proteins into pseudotyped VSV, purified viruses were heated at 95°C in reducing Laemmli sample buffer and subjected to sodium dodecyl sulfate polyacrylamide gel electrophoresis (SDS-PAGE) in a discontinuous gel with 8% acryl amide in the separating gel. The proteins were transferred to a polyvinylidene fluoride membrane (BioRad) which was then blocked with 5% FCS in PBS with 1% Tween 20. FECV UCD S protein was visualized by a mouse monoclonal anti-FLAG conjugated to horseradish peroxidase (Sigma) or by a mouse monoclonal antibody against serotype I S protein (5F8D8H9H9) diluted in PBS containing 5% FBS and 1% Tween 20, the latter subsequently being visualized with Rabbit anti-mouse immunoglobulin G conjugated horseradish peroxidase. Bands on the blots was detected using the Odyssey imaging system (LI-COR Ltd.) and the intensities of the bands were quantified by Quantity One (BioRad).

***Entry assay.*** Entry efficiency of VSV pseudotyped viruses carrying the FECV UCD S proteins with and without mutations was measured by titrating the purified viruses on three fDC-SIGN expressing cell lines starting from 1:100 dilution. At 16h post infection, infected cells were washed once with PBS+Ca<sup>2+</sup> and lysed with 100µl lysis buffer (1% Triton X-100, 50mM Tricine pH8, 100µM EDTA, 2.5mM MgSO<sub>4</sub>, 10mM DTT). 40µl lysate was used to determine firefly luciferase activity in a luminescence plate reader (Berthold Centro LB 960).

***Immunofluorescence staining.*** Cells were fixed with 3.7% PFA diluted in PBS containing Ca<sup>2+</sup> for 15min at room temperature (RT), and then permeabilized by 0.1% TritonX-100 for 10min at RT. The infection of FECV UCD or UCDp was visualized by immunostaining using a mouse monoclonal antibody anti-FIPV-nucleocapsid protein (AbD Serotec, UK) followed by Goat-anti-mouse Alexa 488 (Invitrogen). The infection of EV71 was visualized with a mouse monoclonal antibody against viral double strand RNA followed by Goat-anti-mouse Alexa 488 (Invitrogen). Cell nuclei were stained with DAPI.

***Computational analysis.*** The position of the transmembrane domain and N-glycosylation sites were predicted by the TMHMM server and the NetNGlyc server, respectively. The furin cleavage site between S1 and S2 subunits of the spike protein was predicted by ProP 1.0 server. Western blot signals were quantified by Quantity One® 1-D analysis software. Statistical analysis was performed with GraphPad Prism version 6.0. Cell counting was done using ImageJ.

### **References**

1. Kipar A, Meli ML. Feline Infectious Peritonitis Still an Enigma? *Veterinary Pathology*. 2014;51(2):505-26.
2. Ksiazek TG, Erdman D, Goldsmith CS, Zaki SR, Peret T, Emery S, et al. A novel coronavirus associated with severe acute respiratory syndrome. *N Engl J Med*. 2003;348(20):1953-66.
3. Drechsler Y, Alcaraz A, Bossong FJ, Collisson EW, Diniz PP. Feline coronavirus in multicat environments. *Vet Clin North Am Small Anim Pract*. 2011;41(6):1133-69.
4. Shiba N, Maeda K, Kato H, Mochizuki M, Iwata H. Differentiation of feline coronavirus type I and II infections by virus neutralization test. *Vet Microbiol*. 2007;124(3-4):348-52.
5. Herrewegh AA, Smeenk I, Horzinek MC, Rottier PJ, de Groot RJ. Feline coronavirus type II strains 79-1683 and 79-1146 originate from a double recombination between feline coronavirus type I and canine coronavirus. *J Virol*. 1998;72(5):4508-14.
6. Pedersen NC. A review of feline infectious peritonitis virus infection: 1963-2008. *J Feline Med Surg*. 2009;11(4):225-58.
7. Benbacher L, Kut E, Besnardeau L, Laude H, Delmas B. Interspecies aminopeptidase-N chimeras reveal species-specific receptor recognition by canine coronavirus, feline infectious peritonitis virus, and transmissible gastroenteritis virus. *Journal of Virology*. 1997;71(1):734-7.
8. Porter E, Tasker S, Day MJ, Harley R, Kipar A, Siddell SG, et al. Amino acid changes in the spike protein of feline coronavirus correlate with systemic spread of virus from the intestine and not with feline infectious peritonitis. *Vet Res*. 2014;45:49.
9. Vennema H, Poland A, Foley J, Pedersen NC. Feline infectious peritonitis viruses arise by mutation from endemic feline enteric coronaviruses. *Virology*. 1998;243(1):150-7.
10. Poland AM, Vennema H, Foley JE, Pedersen NC. Two related strains of feline infectious peritonitis virus isolated from immunocompromised cats infected with a feline enteric coronavirus. *J Clin Microbiol*. 1996;34(12):3180-4.
11. Pedersen NC, Boyle JF, Floyd K, Fudge A, Barker J. An enteric coronavirus infection of cats and its relationship to feline infectious peritonitis. *Am J Vet Res*. 1981;42(3):368-77.
12. Chang HW, Egberink HF, Halpin R, Spiro DJ, Rottier PJ. Spike protein fusion peptide and feline coronavirus virulence. *Emerg Infect Dis*. 2012;18(7):1089-95. Epub 2012/06/20.
13. Licitra BN, Millet JK, Regan AD, Hamilton BS, Rinaldi VD, Duhamel GE, et al. Mutation in Spike Protein Cleavage Site and Pathogenesis of Feline Coronavirus. *Emerging Infectious Diseases*. 2013;19(7):1066-73.
14. Geijtenbeek TB, Torensma R, van Vliet SJ, van Duijnhoven GC, Adema GJ, van Kooyk Y, et al. Identification of DC-SIGN, a novel dendritic cell-specific ICAM-3 receptor that supports primary immune responses. *Cell*. 2000;100(5):575-85.
15. Geijtenbeek TB, Kwon DS, Torensma R, van Vliet SJ, van Duijnhoven GC, Middel J, et al. DC-SIGN, a dendritic cell-specific HIV-1-binding protein that enhances trans-infection of T cells. *Cell*. 2000;100(5):587-97.
16. Alvarez CP, Lasala F, Carrillo J, Muniz O, Corbi AL, Delgado R. C-type lectins DC-SIGN and L-SIGN mediate cellular entry by Ebola virus in cis and in trans. *J Virol*. 2002;76(13):6841-4.
17. Lozach PY, Lortat-Jacob H, de Lacroix de Lavalette A, Staropoli I, Foung S, Amara A, et al. DC-SIGN and L-SIGN are high affinity binding receptors for hepatitis C virus glycoprotein E2. *J Biol Chem*.

- 2003;278(22):20358-66.
18. Regan AD, Ousterout DG, Whittaker GR. Feline Lectin Activity Is Critical for the Cellular Entry of Feline Infectious Peritonitis Virus. *Journal of Virology*. 2010;84(15):7917-21.
  19. Van Hamme E, Desmarets L, Dewerschin HL, Nauwynck HJ. Intriguing interplay between feline infectious peritonitis virus and its receptors during entry in primary feline monocytes. *Virus Research*. 2011;160(1-2):32-9.
  20. Desmarets LM, Theuns S, Olyslaegers DA, Dedeurwaerder A, Vermeulen BL, Roukaerts ID, et al. Establishment of feline intestinal epithelial cell cultures for the propagation and study of feline enteric coronaviruses. *Vet Res*. 2013;44:71.
  21. de Haan CA, Li Z, te Lintelo E, Bosch BJ, Haijema BJ, Rottier PJ. Murine coronavirus with an extended host range uses heparan sulfate as an entry receptor. *J Virol*. 2005;79(22):14451-6.
  22. Madu IG, Chu VC, Lee H, Regan AD, Bauman BE, Whittaker GR. Heparan sulfate is a selective attachment factor for the avian coronavirus infectious bronchitis virus Beaudette. *Avian Dis*. 2007;51(1):45-51.
  23. de Haan CA, Haijema BJ, Schellen P, Wichgers Schreur P, te Lintelo E, Vennema H, et al. Cleavage of group 1 coronavirus spike proteins: how furin cleavage is traded off against heparan sulfate binding upon cell culture adaptation. *J Virol*. 2008;82(12):6078-83.
  24. Tekes G, Hofmann-Lehmann R, Bank-Wolf B, Maier R, Thiel HJ, Thiel V. Chimeric feline coronaviruses that encode type II spike protein on type I genetic background display accelerated viral growth and altered receptor usage. *J Virol*. 2009;84(3):1326-33.
  25. Terada Y, Shiozaki Y, Shimoda H, Mahmoud HY, Noguchi K, Nagao Y, et al. Feline infectious peritonitis virus with a large deletion in the 5'-terminal region of the spike gene retains its virulence for cats. *J Gen Virol*. 2012;93(Pt 9):1930-4.
  26. Rottier PJM, Nakamura K, Schellen P, Volders H, Haijema BJ. Acquisition of macrophage tropism during the pathogenesis of feline infectious peritonitis is determined by mutations in the feline coronavirus spike protein. *Journal of Virology*. 2005;79(22):14122-30.
  27. Tani H, Komoda Y, Matsuo E, Suzuki K, Hamamoto I, Yamashita T, et al. Replication-competent recombinant vesicular stomatitis virus encoding hepatitis C virus envelope proteins. *J Virol*. 2007;81(16):8601-12.
  28. Wicht O, Burkard C, de Haan CA, van Kuppeveld FJ, Rottier PJ, Bosch BJ. Identification and characterization of a proteolytically primed form of the murine coronavirus spike proteins after fusion with the target cell. *J Virol*. 2014;88(9):4943-52.
  29. Vogel L, Van der Lubben M, te Lintelo EG, Bekker CP, Geerts T, Schuijff LS, et al. Pathogenic characteristics of persistent feline enteric coronavirus infection in cats. *Vet Res*. 2010;41(5):71.





# CHAPTER 6

## Summarizing discussion



## ***Coronavirus spike-receptor interactions***

---

Coronaviruses are widely distributed among mammals and birds and are notorious for their ability to change or expand their tropism, presumably due to their ability to adapt to or recruit new host receptors. All four human coronaviruses (HCoV-229E, HCoV-NL63, HCoV-OC43) and HCoV-HKU1 have been predicted to originate from an animal reservoir (1-8). Apart from these more ancient cross-species transmission events, the recent emergence of the zoonotic SARS and MERS coronaviruses further indicates the capacity of coronaviruses to cross the species barrier. In addition to host tropism switches, coronaviruses also can alter their cell tropism within an infected animal, as exemplified by the feline coronavirus. Feline coronaviruses come in two pathotypes, the low-pathogenic FECV and the highly virulent feline infectious peritonitis virus (FIPV) (9). FECV can infect enterocytes and causes a clinically mild or unapparent enteritis in cats (10). FIPV targets macrophages and causes a highly lethal systemic infection in cats, called feline infectious peritonitis (FIP) (11). It has been hypothesized that FIPV originates from FECV by (the accumulation of) mutations that accommodate the observed cell-tropism switch (12).

The presence of an appropriate receptor on the cell surface is a prerequisite for virus infection. Receptors are hence key determinants for virus cell, tissue and host tropism. Hence studying coronavirus-receptor interaction is important to understand the tropism switches as well as the pathogenesis and epidemiology of coronaviruses. In this thesis, we investigated the receptor interaction of two coronavirus species: the recently identified, zoonotic MERS-CoV and the serotype I feline coronavirus (FCoV). In chapter 2 and 3, we identified dipeptidyl peptidase 4 (DPP4) as the functional receptor for MERS-CoV and mapped the receptor binding domain (RBD) in its S protein. In chapter 4, we described a serological microarray assay using the S1 receptor binding subunit of the coronavirus S protein as an antigen which appeared efficient in the study of the MERS-CoV epidemiology. In chapter 5, we investigated the genetic determinants of FECV for adaptation to the FIPV-macrophage receptor, the dendritic cell-specific intercellular adhesion molecule-3-grabbing non-integrin (DC-SIGN) receptor usage, which may be a critical step in the FECV-FIPV transition. In this chapter, I will concisely summarize and discuss our main observations chapter by chapter.

## DPP4: a novel peptidase receptor identified for coronaviruses ( Chapter 2)

### DPP4 usage and entry of coronaviruses

Soon after the identification of MERS-CoV, researchers investigated whether this virus was able to utilize ACE2, the receptor for SARS-CoV, given the similar clinical manifestations of infectious diseases caused by these two viruses. Müller et al concluded that MERS-CoV does not use ACE2 as a functional receptor but a novel receptor which is conserved among bats, pigs and humans (13). In chapter 2, we identified DPP4 (also known as CD26) as the functional receptor for MERS-CoV (14).

Coronaviruses seem to prefer exopeptidases as receptors for entry. After the discovery of APN and ACE2, DPP4 is the third exopeptidase identified as a functional protein receptor for coronaviruses (Fig.6.2). Most alphacoronaviruses utilize APN as a receptor; however, the alphacoronavirus HCoV-NL63 utilizes ACE2, which also serves as the receptor of the betacoronavirus SARS-CoV. This strongly suggests that during evolution an APN-dependent ancestral HCoV-NL63 has switched receptors by selecting another peptidase (ACE2) as its new receptor. So the convergent

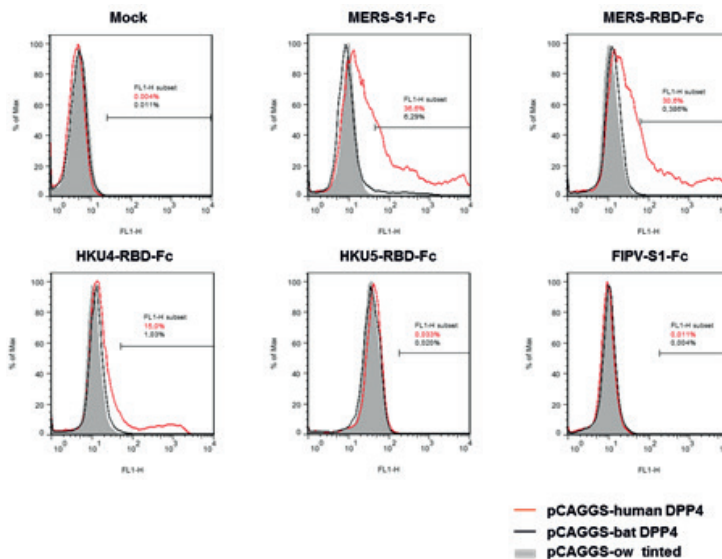


**Fig 6.1** Flow cytometry analysis of binding of MERS-S1-Fc, MERS-RBD-Fc, HKU4-RBD-Fc, HKU5-RBD-Fc recombinant proteins to DPP4 expressing cells. HEK293T cells transfected with pCAGGS-human DPP4 (Red line) or pCAGGS-bat DPP4 (black line) expression plasmids with pCAGGS (filled grey) as control were incubated with 15µg/ml of the indicated Fc recombinant proteins followed by incubation with Alexa 488 labeled goat-anti-human IgG antibody and analysis by flow cytometry. Fc-chimera containing the S1 of FIPV 79-1146 (FIPV-S1-Fc) was taken along as a negative control.

## **Coronavirus spike-receptor interactions**

---

evolution of alpha- and betacoronaviruses for ACE2 receptor usage underlines the strong preference of coronaviruses for cell-surface peptidases as receptors. Since the catalytic function of these proteases is not relevant for virus entry, the reason for this phenomenon remains unclear (14-18). Further investigation into this subject may provide a theoretical basis for prediction of next potential receptor candidates.

The ACE2 and APN receptor are utilized by different coronaviruses (Fig.6.2). It is hence conceivable that DPP4 is also used as a receptor by more coronaviruses than MERS-CoV alone. Phylogenetic analysis demonstrated that MERS-CoV is genetically closely related to two bat coronaviruses, HKU4 and HKU5, whose genomic RNAs were isolated from lesser bamboo bats (*Tylonycteris pachypus*) and Japanese pipistrelles (*Pipistrellus abramus*), respectively (19-20). To assess DPP4 receptor usage of the HKU4 and HKU5 bat coronaviruses, we expressed and purified the regions of the HKU4 and HKU5 S proteins homologous to MERS-CoV S-RBD. The putative HKU4-RBD but not the putative HKU5-RBD showed binding activity to human DPP4 (Fig.6.1). No obvious binding of the HKU4-RBD to the DPP4 of the *Pipistrellus* bat was detected, presumably explained by the divergence in DPP4 sequences of *Pipistrellus* and the HKU4 host, *Tylonycteris pachypus*. We have shown that MERS-CoV can bind and functionally use *Pipistrellus* DPP4 as a receptor (Chapter 2 and Fig.6.1). Recent results from Yang et al confirmed that the S protein of HKU4 - but not of HKU5 - was able to functionally recruit human and bat DPP4 as receptors for cell entry (21). Thus, bats harbor coronaviruses that can utilize human DPP4 as a receptor, at least in vitro, and hence are a possible reservoir for MERS-CoV and other, potentially zoonotic coronaviruses.

Recent data from the study of Yang et al indicated that efficient entry of HKU4 via DPP4 into human cells was dependent on the activation by exogenously added proteases such as trypsin (21). In contrast, HKU4 mediated entry into bat cells was not dependent on trypsin activation, presumably due to the presence of activating proteases on bat cells. Trypsin-dependent entry has also been observed for PEDV (22-23). There is mounting evidence that entry of coronaviruses - and consequently virus tropism - is determined by two aspects: the binding to cognate receptors as well as the presence of activating proteases.

### **The zoonotic SARS and MERS coronaviruses: the spike protein is a key determinant of host tropism**

The SARS-CoV and MERS-CoV are recent examples of zoonotic coronaviruses that both cause severe lower respiratory tract infections in humans (1, 24-25). Yet their mechanism for cross-species transmission seems quite distinct.

Zoonotic transmission of SARS-CoV has been related to adaptation to the human ACE2 receptor ortholog. SARS-like viruses have been identified in horseshoe bats and civet cats (1, 26). Civet cats, traded at wild-game markets for consumption, were

postulated as an intermediate reservoir from which the SARS-CoV made its way to humans after adapting its spike protein to the human ACE2 receptor ortholog (27). However, recent studies showed that SARS-like viruses from horseshoe bats were able to use human ACE2 indicating that direct transmission of bat SARS-like viruses to humans is possible (8). Furthermore, investigation of the binding affinity of SARS-CoV isolated during the SARS epidemic showed that human-adapted SARS-CoV acquired a much higher receptor affinity to human ACE2 receptor than civet isolates. Increased receptor interaction affinity was considered to be the central contributor to the acquisition of the epidemic potential of SARS-CoV (28-30). During this adaptation event, the virus switched sides and lost its old host gaining the capacity to invade a new host (such as human). Altogether these data indicated that a successful host switch of bat SARS-like viruses to human SARS-CoV, either directly or via the civet-reservoir, is determined by acquisition of higher binding affinity to human ACE2. Though direct transmission of SARS-like viruses from bats to humans cannot be excluded, transmission via an intermediate host with an increased animal contact time and consequent chances for a spill-over event, is more likely.

In contrast to SARS-CoV, MERS-CoV appears a classical zoonotic virus that repeatedly crosses over to humans from the dromedary camel reservoir (7, 31-33). This suggests that adaptation of the dromedary MERS-CoV towards the human DPP4 receptor ortholog is not required for cross-species transmission. Indeed, the binding affinity of MERS-CoV S1 to DPP4 of camels was comparable to that of human DPP4 (34). Likewise, the binding affinity of MERS-CoV S1 to DPP4 of horses and goats was similar to that of human DPP4. Indeed, structural analysis of the DPP4-MERS-RBD interface indicates a high conservation of the virus contacting residues in the DPP4 sequences of these species (35-36). Moreover, sequences of MERS-CoV isolated from camels in Saudi Arabia and Qatar were closely related to human MERS-CoV isolates (7, 37). In particular, no mutations have been found in the receptor binding domains of the spike proteins of dromedary and human MERS-CoV isolates, suggesting that cross-species transmission from camels to humans does not require adaptation towards the human DPP4 ortholog (38).

The evolutionary conservation of DPP4, particularly at the MERS-RBD binding interface, may be associated with its function as a receptor for a natural ligand, the adenosine deaminase (ADA) (39). Binding of ADA to DPP4 is involved in T-cell activation and regulation of epithelia and lymphocyte cell adhesion (40-41). The elucidated structures of MERS-RBD-DPP4 and ADA-DPP4 complexes showed a remarkable overlap in the footprint of ADA and MERS-RBD on DPP4 (35-36, 42-44). The overlap in DPP4-binding sites is also demonstrated by the ability of ADA to interfere with the binding of MERS-CoV S1 to DPP4 and the ability to inhibit MERS-CoV infection in cell culture (35). Furthermore, the DPP4-interacting residues of ADA - which are shared by MERS-CoV - display a high level of conservation. The use of evolutionarily conserved host molecules as functional receptors by viruses including MERS-CoV facilitates their cross-species transmission.

## ***Coronavirus spike-receptor interactions***

---

---

### ***Techniques used for receptor identification***

The conventional process to identify a functional protein receptor of a coronavirus is mainly divided into two steps: isolation of the molecule that can provide coronaviruses entry into cells, and identification of the isolated molecule.

Multiple techniques have been applied to isolate receptor molecules. To sequester the MERS-CoV receptor, we applied a straightforward co-purification technique based on the specific interaction of the receptor binding subunit with its receptor. To isolate the MERS-CoV receptor, we expressed recombinant S1 proteins tagged with the Fc part of human IgG. This chimeric molecule was used to fish out the receptor from a lysate of susceptible cells using protein-A chromatography (14). This approach was successfully used earlier to identify the ACE2 receptor of SARS-CoV (17). The S1-based receptor-isolation method is time-efficient, relatively cheap and independent of using infectious viruses. In addition, this method is relatively simple and specific since it relies on the interaction between S1 and the receptor. However, a direct, durable and strong binding affinity of the S1 subunit with the receptor is required to maintain the interaction during the co-purification procedure.

An alternative method independent of high virus-receptor affinity had been utilized in the identification of APN as the receptor for TGEV. This technique was based on monoclonal antibodies raised against solubilized membrane proteins of a susceptible cell line. Monoclonal antibodies that neutralized virus infection were subsequently used to precipitate the receptor APN (15). This approach is also direct and straightforward, yet rather time-consuming and costly because of the generation of numerous hybridoma cell lines and subsequent testing of antibodies for neutralizing activity.

Alternative to the methods described above, the receptor can also be identified by the virus overlay protein binding assay (VOPBA). This method has been successfully used for the identification of CEACAM1 and APN as receptors for MHV and PEDV, respectively (45-46). The VOPBA approach relies on the direct interaction between virus particles and solubilized membrane proteins of susceptible cells that have been subjected to Western blotting. The advantage of the VOPBA method is the high avidity of intact viruses due to the ability to bind to multiple receptors blotted on the membrane support. However, the native structure of solubilized membrane proteins may be lost due to the SDS-detergent used in SDS-PAGE, which may be detrimental for receptor interaction.

Recently novel, sophisticated techniques have been developed to identify ligand-receptors interactions. One promising technique that may be used for identification of coronavirus receptors is called avidity-based extracellular interaction screen (AVEXIS). This technique has been used to screen receptor–ligand pairs in the zebrafish immunoglobulin superfamily and to identify novel ligands for the receptor

(47). The AVEXIS technique was also used to identify the Ok blood group antigen, basigin, as the receptor for erythrocyte invasion in all tested *P. falciparum* strains (48). Typically, the ligand and receptor are expressed as two different forms: a monomeric biotinylated “bait” which can be captured on streptavidin-coated microtiter plates, and a pentamerized “prey” tagged with  $\beta$ -lactamase for detection purposes. Pentamerization of the ‘prey’ protein provides a higher binding avidity to the bait. For coronavirus receptor identification, the S1 receptor binding subunit can be expressed as bait while ectodomains of cell surface receptor candidates can be expressed as preys. After binding of the prey protein, the colorimetric enzymatic turnover of nitrocefin by the  $\beta$ -lactamase subunit will indicate the interaction. AVEXIS can be applied as a high-throughput assay due to its high protein-protein avidity and the ability to detect transient protein interactions with a low false-positive rate. However, this technique relies on the generation of a large prey library containing pentameric versions of all cell surface protein ectodomains as receptor candidates.

Another promising technique for isolation of coronavirus receptors is called ligand-based receptor capture (LRC) which can be achieved using a trifunctional reagent called TRICEPS (49). TRICEPS is a three-armed molecule containing i) an NHS ester enabling cross-linking to ligands via primary amines, ii) a trifluoroacetyl-protected hydrazine for the subsequent capture of glycoprotein receptors on gently oxidized living cells and iii) a biotin tag for the affinity purification of captured glycopeptides. To identify the receptors for coronaviruses, TRICEPS can be coupled to a purified S1 subunit or to intact viruses via the NHS ester. After binding to the receptors on the target cell, the S1- or virus-bound TRICEPS molecules can be coupled to the carbohydrates of glycoprotein-type receptors via the aldehyde-reactive hydrazine group. The biotin group of the TRICEPS molecule can subsequently be used for affinity isolation of the captured glycopeptides for mass spectrometry analysis. LRC is designed to detect ligand-receptor interactions under natural, biological conditions. In addition, this technique is also suitable for identification of cell surface proteins with weak or transient interactions by using multivalent ligands. Furthermore, this method seems highly specific and efficient. However, this LRC-TRICEPS methodology, which is marketed by Dualsystems Biotech company (<http://www.dualsystems.com/services/>), is rather expensive.

After isolation of the receptor molecule, the isolated receptor can be identified either by N-terminal protein sequencing or by mass spectrometry. Prior to the late 1970s, N-terminal sequence analysis using Edman degradation was the main assay to identify proteins (50-51). Starting from the mid-1990s, the application of N-terminal sequencing was gradually replaced by mass spectrometry given its higher sensitivity and efficiency with no need for purifying the affinity-isolated proteins to homogeneity (52-55). However, N-terminal sequencing is more applicable if the host proteome, a requirement for MS detection, is not known. The current N-terminal sequencing technology can detect at least 20 to 25 residues of the N-terminus of proteins and large peptides in the low picomolar range (56).

## Coronavirus spike-receptor interactions

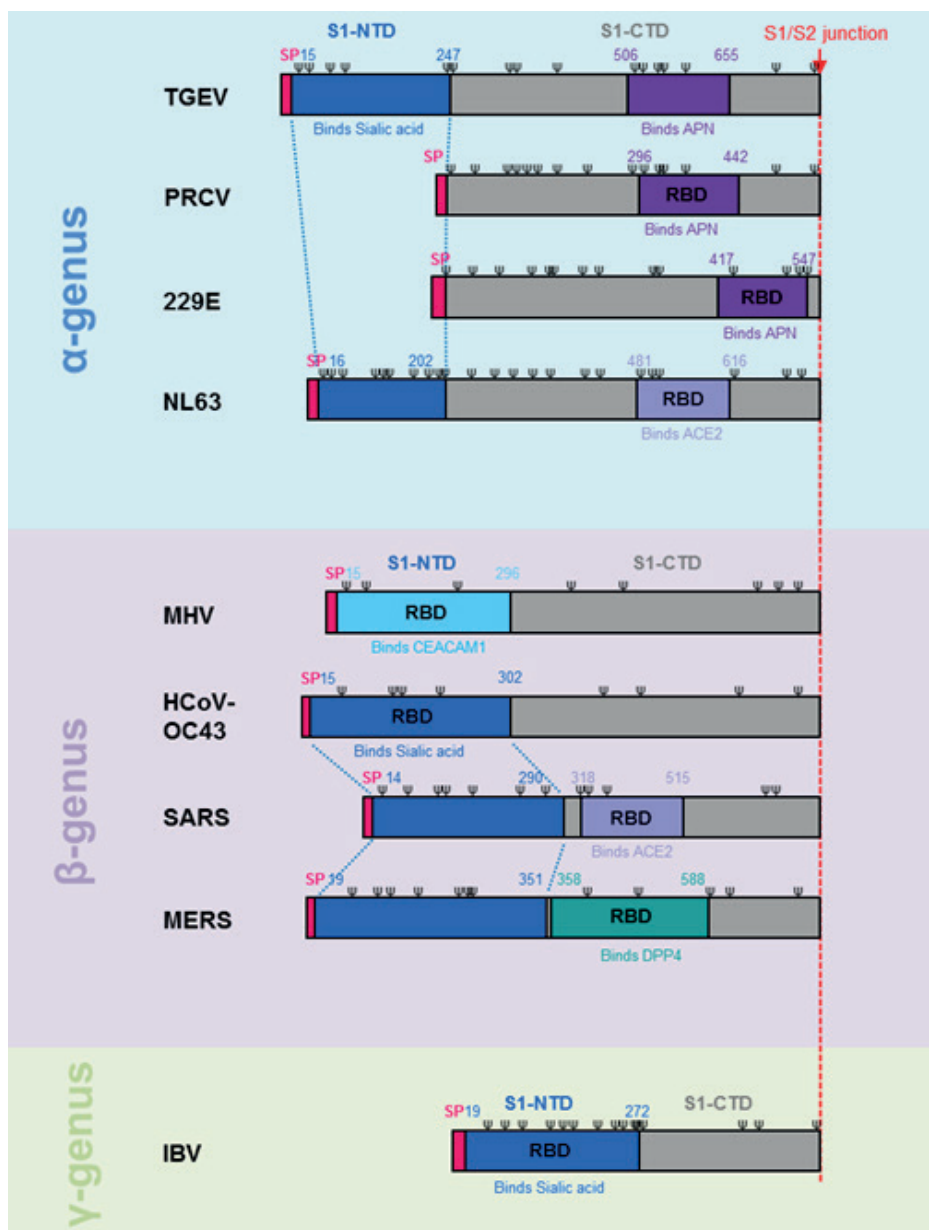


**Fig.6.2** Location of the N-terminal (NTD; indicated in blue) and C-terminal (CTD, indicated in grey) domains in S1 receptor binding subunit of representative coronavirus species from different genera. We define NTDs of  $\alpha$ -CoV species based on homology with PRCV S1 compared with TGEV while NTDs of  $\beta$ -CoV species are based on homology with MHV NTD. The RBD of  $\gamma$ -CoV is defined based on the identified sialic acids binding domain. The receptor and the location of the receptor binding domain are indicated for each virus. N-Glycosylation sites of different spikes were predicted by NetNGlyc 1.0 (Technical University of Denmark) and are indicated by  $\Psi$ .



## **Receptor binding domain (RBD): the main player in receptor binding (Chapter 3)**

The coronavirus S glycoprotein has a multidomain structure. It is generally divided into two functionally distinct subunits, S1 and S2, responsible for receptor binding and membrane fusion, respectively. The S1 subunit is further divided into two subdomains, the N-terminal domain (NTD) and C-terminal domain (CTD). One - or in some occasions both - of these two domains may comprise a receptor binding domain (RBD), and mediate the entry of coronaviruses. For some coronaviruses the S1-NTD has been shown to display sialic acid binding activity. The receptor binding domain for protein receptors has been mapped to the S1-CTD with the exception for MHV which binds its protein receptor CEACAM1 via the S1 N-terminal domain (Fig.6.2).

In chapter 3, we mapped the receptor binding domain of MERS-CoV to a 231-aa long fragment within the CTD of S1. We used in silico prediction of potential receptor binding domains in the MERS-S1 based on the available functional and structural data for the receptor binding domains of related betacoronaviruses. Subsequently this information was used to construct truncated MERS-CoV S1 proteins, which we assessed for their DPP4 binding capacity using different biochemical assays. Our data were confirmed by the elucidation of the crystal structure of the MERS-RBD in complex with DPP4 (43-44). Identification of the coronavirus RBD and visualizing the RBD-receptor interaction paves the way for the development of prevention and therapeutic strategies.

### **Receptor binding domain of coronavirus, a promising target for development of intervention strategies**

The S-RBD is the main target for neutralizing antibodies that makes it a promising candidate for vaccine development and generation of therapeutic neutralizing antibodies (57-58). Our immunization studies with different S1 variants indicated that the RBD was most efficient in eliciting neutralizing antibodies (59). SARS-RBD-Fc was demonstrated to be able to induce highly potent neutralizing antibodies with high titer, and this antibody could neutralize the infectivity of pseudotyped viruses carrying SARS-CoV spikes of both homologous and heterologous isolates (60-61). Murine and human monoclonal antibodies (mAbs) targeting RBD of SARS-CoV were produced, but mouse mAbs against SARS-CoV can just be administered to patients in the early disease stage or for urgent treatment because of the human anti-mouse immune response induced that will lead to the clearance of the antibody and a potential allergic reaction (62). Recently, two neutralizing human mAbs targeting MERS-RBD were isolated and characterized which were able to inhibit the infection of both pseudotyped and live MERS-CoV at nanomolar concentrations. These monoclonal

## **Coronavirus spike-receptor interactions**

---

antibodies targeted different regions and neutralized pseudotyped MERS-CoV synergistically (63). Thus, human neutralizing antibodies were considered to be more suitable for development of therapeutic strategies.

The RBD of the coronavirus spike protein is also a promising vaccine candidate. An earlier study on SARS-CoV demonstrated that vaccination with recombinant SARS-RBD was able to induce long-term protection against a homologous challenge in an animal model (64). In addition, the RBD is also the main domain to induce T-cell immune responses against viral infection by harboring multiple conformation-dependent epitopes. Two epitopes in the SARS-CoV spike protein responsible for inducing CD8<sup>+</sup> T-cell responses were mapped to aa436-433 and aa366-374, respectively (65). Immunization of mice with a vaccine based on SARS-CoV spike fragment (aa318-510) elicited not only neutralizing antibodies but also cellular immune responses to against SARS-CoV infection collaboratively (66).

Apart from the generation of neutralizing antibodies, the development of drug compounds may be explored to prevent the binding of the virus with its cognate receptor. Receptor binding cannot be effectively competed with conventional small-drug molecules. Larger compounds are needed instead that interact with a high affinity with a larger surface on the receptor binding domain. One intriguing possibility is the use of oligo-nucleotide aptamers that can be selected to e.g. antagonize receptor binding. Using a protein (e.g. the receptor binding domain) as a bait, interacting aptamers can be affinity-selected from a library of randomized -20nt long oligonucleotides through a high-flux screening technique called Systematic Evolution of Ligands by Exponential Enrichment (SELEX) (67-68). These stable and low-immunogenicity aptamers can target small organic molecules to complex proteins or even intact cells with high affinity and specificity (69-71). Aptamers targeting viral glycoproteins have been developed as promising anti-viral agents for both HIV and influenza virus (72-73). Thus, synthesized and selected aptamers might represent another prospective prevention and therapeutic strategy against coronavirus infection targeting the RBD of coronaviruses.

## **Function of the N-terminal domain of the coronavirus S protein**

The function of the NTD in the S1 subunit of coronaviruses has not been scrutinized since more attention was given to the C-terminal domain (CTD), which contains the RBD for most coronaviruses. The S1-NTDs of viruses belonging to the alpha, beta and gammacoronavirus genera can act as lectins allowing binding to carbohydrate receptors. Unlike MHV that evolved to bind to the CEACAM1 protein for entry, the spike proteins of the betacoronaviruses HCoV-OC43 and Bovine coronavirus (BCoV) recognize N-acetyl-9-O-acetylneuraminic acid (Neu5,9Ac2) carbohydrates with a binding preference for  $\alpha$ -2,6 linked Neu5,9Ac2 and  $\alpha$ -2,3 linked Neu5,9Ac2,

respectively (74-75). In addition, the NTD of the gammacoronavirus IBV was identified as a lectin required for binding to chicken respiratory tract tissues in an  $\alpha$ -2,3-sialic acid-dependent way (76). For the alphacoronavirus TGEV, it was postulated that the sialic acid binding activity located in the S1-NTD was related to its enteropathogenicity (77). TGEV initiates its infection by binding to its species-specific protein receptor APN, but its S1-NTD recognizes N-glycolylneuraminic acid (Neu5Gc) and N-acetylneuraminic acid (Neu5Ac) (78-79). The virus PRCV, a spike mutant of TGEV containing a deletion of the NTD, fails to bind sugars and has an altered tissue tropism only infecting respiratory tissues (80). A similar situation is seen for the two pathotypes of FECV and FIPV with enteric and macrophage tropism, respectively. Type I FECV UCD strain showed sialic acids binding activity (81) while some FIPV strains (e.g. UCD4, UCD5 and UCD8) have a deletion of the S1-NTD with tropism switch from intestine epithelial cells to macrophages. It has been suggested that the sialic binding capacity of the S1-NTD is required for virus replication in the gut but can be missed once the virus changes its tropism to outside the gut environment (12).

Structural studies on the S1-NTD may facilitate the understanding of coronavirus evolution. Such studies have demonstrated that the coronavirus S1-NTD shares the same fold with host galectins, but divergent evolution lead to the different binding ability of this domain to different sugar receptors or even a protein receptor (for example CEACAM1 receptor for MHV) (82-83). Differences in binding capacity may indicate the selection process during coevolution in different hosts. In addition, compared with the human host galectins, viral lectins displayed hidden sugar binding sites that are not easily accessible to host antibodies and immune cells, which may be an evolutionary advantage for coronaviruses (84).

### **S1 protein microarray assay, a reliable and fast way for diagnosis (Chapter 4)**

Crucial to the containment of a new, emerging virus epidemic is the rapid development of diagnostic assays to identify the infected individuals or the virus reservoir. Within two weeks after identifying the sequence of MERS-CoV, the Drosten lab developed and published a protocol for the detection of viral RNA by real-time reverse transcription polymerase chain reaction (RT-PCR) for which materials were made available to many labs in the world (85). Moreover, they also developed a protocol for detection of virus-specific antibodies based on whole cell immunofluorescence assay (IFA) (86). The reliability of these diagnostic assays depends on their sensitivity and specificity. Cross-reactivity with related viruses can lead to false-positive results whereas positive cases may be missed if the assay is not sensitivity enough.

In Chapter 4, we developed a serological assay based on expressed and purified recombinant S1 receptor binding subunits (87). The spike protein, particularly the S1 subunit, is the major antigenic determinant for coronaviruses which contains the majority of neutralizing epitopes and is highly immunogenic upon infection or after immunization. Therefore, the S1 subunit is a potentially ideal antigen to develop a serological diagnostic method (88-91). Furthermore, compared to other immunogenic viral proteins, the S1 subunit displays the highest sequence diversity across different coronavirus species (92-93). These antigen characteristics are crucial to develop a sensitive and specific serological assay. In an earlier immunological study, the fragment consisting of amino acids 441-700 of SARS-CoV S protein has been identified as a major immune antigen, which could serve as a useful tool to monitor the antibody response from suspected SARS patients (92). In a recent study on the antigenic relationship of PEDV and TGEV, cross-reactivity was not observed for antibodies against the S protein but the N-protein contained at least one cross-reactive epitope. (94). Indeed, in our S1-based serological assay, no cross-reactivity was seen for the related betacoronaviruses MERS-CoV and SARS-CoV in the detection of virus-specific IgM and IgG antibodies (87).

The glycan-array set-up of the serological assay used in our study is feasible for high-throughput applications allowing the analysis of large numbers of sera simultaneously. Moreover, only tiny amount of antigens and sera are required which is of importance when analyzing sera of animals. The coronavirus S1-based microarray has been successfully exploited by Reusken et al in the search for the MERS-CoV animal host by analyzing sera from livestock in the Middle-East region leading to the identification of the dromedary camel as the zoonotic reservoir of MERS-CoV (7, 31, 95).

## **DC-SIGN usage, not sufficient to switch cell tropism of FECV to FIPV (Chapter 5)**

The origin of FIPVs has been debated for years, but evidence accumulates that FIPVs emerge as virulent variants of FECVs (10, 12, 96). The most accepted hypothesis named the internal mutation theory postulates that FIPVs arise from FECVs by the acquisition of mutation(s) during virus replication, which confers to the virus the ability to efficiently infect macrophages (12). This hypothesis is supported by several observations. One is that FECV and FIPV strains isolated from the same cat shelter were genetically very closely related, while significant genetic variation existed between FECVs and FIPVs that were from different geographic areas (12). In addition, there is no evidence for horizontal transmission of FIPV from cat to cat (97).

Acquisition of macrophage tropism is a hallmark that functionally distinguishes FIPV from FECV strains (98). FECVs preferentially replicate in intestinal epithelial cells while FIPVs exhibit a preference to infect macrophages and monocytes (10-11, 99-103). Type I FIPV was shown to infect macrophages by recruiting DC-SIGN as a receptor (104). Whether type I FECV has an inherent capacity to utilize DC-SIGN for entry or acquires this capacity during the FECV to FIPV transition was still unknown. In Chapter 5, our study demonstrated that adaptation of type I FECV to DC-SIGN-expressing cells could be attributed to the acquisition of the mutation D371H into the S1 binding subunit, but this adaptation was not sufficient to enable replication capacity in macrophages, suggesting that more mutations may be needed for the successful transition from FECV to FIPV pathotype.

Whitaker et al demonstrated that the loss of an intact furin cleavage site at the S1-S2 junction of the S protein is correlated with the observed cell tropism change of FECV to FIPV. Sequence analyses of a number of FECV and FIPV strains indicated that all FECVs contain an intact furin cleavage site at the S1-S2 junction of their S protein whereas 64% of FIPVs have lost this furin cleavage site (105). Our study on the FECV serotype I strain, described in chapter 5, also implied that impaired furin cleavage of the S protein correlates with more efficient entry of DC-SIGN expressing cells. The proteolytic requirements of S protein fusion activation of FCoV may hence also somehow determine cell tropism and pathogenicity.

Transition to the lethal pathotype FIPV may also require mutations in the S2 subunit. Research based on the serotype II FECV strain 79-1683 and FIPV strain 79-1146, indicated that mutations in the S2 subunit of the S protein were vital for gaining macrophage tropism (98). Sequence comparison of the spike genes of feline coronaviruses from serotype I FECV and FIPV infected cats revealed the occurrence of two mutations (M1058L and S1060A) in the S2 subunit of the S protein that together make a distinction between FECV from FIPV in >95% of the cases.

## ***Coronavirus spike-receptor interactions***

---

---

Chang et al hypothesized that these two mutations, perhaps in combination with other mutations, may be responsible for the cell tropism switch (106). Since the S2 subunit mediates membrane fusion, the crucial step for cell tropism switch might be the fusion function of viral membrane with macrophage membrane (106).

The transition from FECV to FIPV was postulated to be influenced by the immune status of FECV-infected cats. Immunosuppression induced by feline immunodeficiency virus (FIV) infection in cats co-infected with FECV increased the chances for these cats to develop FIP (107). In FIV positive cats, FCoV titers in faeces were 10 to 100-fold higher while virus shedding lasted longer and induction of antibodies was delayed and reaching lower titers as compared to control cats (96). The immunosuppression status likely supports the replication of FECV which may increase the emergence of mutations. To exclude a direct role of FIV, it would be interesting to study the effects of immune suppression induced by alternative methods such as by using immune suppressive agents.

To further clarify the molecular mechanism of the observed cell tropism change of feline coronaviruses, the phenotype of these mutations in the virus context should be investigated using a reverse-genetics system.

## **Concluding remarks**

Knowledge on the receptor usage of coronaviruses will shed light on the biology of coronaviruses and provide a theoretical basis for the development of prevention and therapeutic strategies. In this thesis, we investigated the receptor interactions of two coronavirus species, MERS-CoV and FCoV.

In the study of MERS-CoV, we identified DPP4 as a functional receptor and mapped the receptor binding domain within the S1 subunit of the S protein. Because of its high immunogenicity and sequence diversity, the S1 subunit of the S protein was used to setup a serological microarray. This tool was instrumental in the identification of the zoonotic reservoir for MERS-CoV, which appeared to be the dromedary camel. The high level of sequence homology between the human and camel DPP4 domains interacting with the MERS-CoV spike at least partially explains the successful transmission of MERS-CoV from dromedary camel to humans. However, human-to-human transmission appears inefficient indicating that other factors (e.g. DPP4 receptor expression along the respiratory tract) may determine the efficiency of virus transmission. The receptors for several coronaviruses have not been identified yet. Intriguingly, of the four protein receptors thus far identified for coronaviruses, three are proteases; yet the reason for this preference is still a mystery. Identification of novel receptors and further study of known receptors of coronaviruses may help to answer these questions.

For FCoVs, we demonstrated that the capacity of an enteric feline coronavirus to use DC-SIGN for cell entry could be achieved by the acquisition of mutations in the S1 subunit, but the mechanisms involved are not understood. In addition, the key determinants for the FECV to FIPV transition are still under debate. More research is needed to uncover the underlying mechanism for this virus pathotype change.

### **References**

1. Guan Y, Zheng BJ, He YQ, Liu XL, Zhuang ZX, Cheung CL, et al. Isolation and characterization of viruses related to the SARS coronavirus from animals in southern China. *Science*. 2003;302(5643):276-8.
2. Li W, Shi Z, Yu M, Ren W, Smith C, Epstein JH, et al. Bats are natural reservoirs of SARS-like coronaviruses. *Science*. 2005;310(5748):676-9.
3. Vijgen L, Keyaerts E, Moes E, Thoelen I, Wollants E, Lemey P, et al. Complete genomic sequence of human coronavirus OC43: molecular clock analysis suggests a relatively recent zoonotic coronavirus transmission event. *J Virol*. 2005;79(3):1595-604.
4. Pfefferle S, Oppong S, Drexler JF, Gloza-Rausch F, Ipsen A, Seebens A, et al. Distant relatives of severe acute respiratory syndrome coronavirus and close relatives of human coronavirus 229E in bats, Ghana. *Emerg Infect Dis*. 2009;15(9):1377-84.
5. Huynh J, Li S, Yount B, Smith A, Sturges L, Olsen JC, et al. Evidence supporting a zoonotic origin of human coronavirus strain NL63. *J Virol*. 2012;86(23):12816-25.
6. Ithete NL, Stoffberg S, Corman VM, Cottontail VM, Richards LR, Schoeman MC, et al. Close relative of human Middle East respiratory syndrome coronavirus in bat, South Africa. *Emerg Infect Dis*. 2013;19(10):1697-9.
7. Haagmans BL, Al Dhahiry SH, Reusken CB, Raj VS, Galiano M, Myers R, et al. Middle East respiratory syndrome coronavirus in dromedary camels: an outbreak investigation. *Lancet Infect Dis*. 2013;14(2):140-5.
8. Ge XY, Li JL, Yang XL, Chmura AA, Zhu G, Epstein JH, et al. Isolation and characterization of a bat SARS-like coronavirus that uses the ACE2 receptor. *Nature*. 2013;503(7477):535-8.
9. Pedersen NC. A review of feline infectious peritonitis virus infection: 1963-2008. *J Feline Med Surg*. 2009;11(4):225-58.
10. Pedersen NC, Boyle JF, Floyd K, Fudge A, Barker J. An enteric coronavirus infection of cats and its relationship to feline infectious peritonitis. *Am J Vet Res*. 1981;42(3):368-77.
11. Ward JM. Morphogenesis of a virus in cats with experimental feline infectious peritonitis. *Virology*. 1970;41(1):191-4.
12. Vennema H, Poland A, Foley J, Pedersen NC. Feline infectious peritonitis viruses arise by mutation from endemic feline enteric coronaviruses. *Virology*. 1998;243(1):150-7.
13. Muller MA, Raj VS, Muth D, Meyer B, Kallies S, Smits SL, et al. Human coronavirus EMC does not require the SARS-coronavirus receptor and maintains broad replicative capability in mammalian cell lines. *MBio*. 2012;3(6).
14. Raj VS, Mou H, Smits SL, Dekkers DH, Muller MA, Dijkman R, et al. Dipeptidyl peptidase 4 is a functional receptor for the emerging human coronavirus-EMC. *Nature*. 2013;495(7440):251-4.
15. Delmas B, Gelfi J, L'Haridon R, Vogel LK, Sjoström H, Noren O, et al. Aminopeptidase N is a major receptor for the entero-pathogenic coronavirus TGEV. *Nature*. 1992;357(6377):417-20.
16. Yeager CL, Ashmun RA, Williams RK, Cardellicchio CB, Shapiro LH, Look AT, et al. Human aminopeptidase N is a receptor for human coronavirus 229E. *Nature*. 1992;357(6377):420-2.
17. Li W, Moore MJ, Vasilieva N, Sui J, Wong SK, Berne MA, et al. Angiotensin-converting enzyme 2 is a functional receptor for the SARS coronavirus. *Nature*. 2003;426(6965):450-4.
18. Li F, Li W, Farzan M, Harrison SC. Structure of SARS coronavirus spike receptor-binding domain complexed with receptor. *Science*. 2005;309(5742):1864-8.



19. Lau SK, Li KS, Tsang AK, Lam CS, Ahmed S, Chen H, et al. Genetic characterization of Betacoronavirus lineage C viruses in bats reveals marked sequence divergence in the spike protein of pipistrellus bat coronavirus HKU5 in Japanese pipistrelle: implications for the origin of the novel Middle East respiratory syndrome coronavirus. *J Virol.* 2013;87(15):8638-50.
20. Woo PC, Lau SK, Li KS, Poon RW, Wong BH, Tsoi HW, et al. Molecular diversity of coronaviruses in bats. *Virology.* 2006;351(1):180-7.
21. Yang Y, Du L, Liu C, Wang L, Ma C, Tang J, et al. Receptor usage and cell entry of bat coronavirus HKU4 provide insight into bat-to-human transmission of MERS coronavirus. *Proc Natl Acad Sci U S A.* 2014;111(34):12516-21.
22. Wicht O, Li W, Willems L, Meuleman TJ, Wubbolts RW, van Kuppeveld FJ, et al. Proteolytic activation of the porcine epidemic diarrhea coronavirus spike fusion protein by trypsin in cell culture. *J Virol.* 2014;88(14):7952-61.
23. Belouzard S, Millet JK, Licitra BN, Whittaker GR. Mechanisms of coronavirus cell entry mediated by the viral spike protein. *Viruses.* 2012;4(6):1011-33.
24. van Boheemen S, de Graaf M, Lauber C, Bestebroer TM, Raj VS, Zaki AM, et al. Genomic characterization of a newly discovered coronavirus associated with acute respiratory distress syndrome in humans. *MBio.* 2012;3(6).
25. Zaki AM, van Boheemen S, Bestebroer TM, Osterhaus AD, Fouchier RA. Isolation of a novel coronavirus from a man with pneumonia in Saudi Arabia. *N Engl J Med.* 2012;367(19):1814-20.
26. Lau SK, Woo PC, Li KS, Huang Y, Tsoi HW, Wong BH, et al. Severe acute respiratory syndrome coronavirus-like virus in Chinese horseshoe bats. *Proc Natl Acad Sci U S A.* 2005;102(39):14040-5.
27. Song HD, Tu CC, Zhang GW, Wang SY, Zheng K, Lei LC, et al. Cross-host evolution of severe acute respiratory syndrome coronavirus in palm civet and human. *Proc Natl Acad Sci U S A.* 2005;102(7):2430-5.
28. Li W, Zhang C, Sui J, Kuhn JH, Moore MJ, Luo S, et al. Receptor and viral determinants of SARS-coronavirus adaptation to human ACE2. *EMBO J.* 2005;24(8):1634-43.
29. Li W, Wong SK, Li F, Kuhn JH, Huang IC, Choe H, et al. Animal origins of the severe acute respiratory syndrome coronavirus: insight from ACE2-S-protein interactions. *J Virol.* 2006;80(9):4211-9.
30. Wu K, Peng G, Wilken M, Geraghty RJ, Li F. Mechanisms of host receptor adaptation by severe acute respiratory syndrome coronavirus. *J Biol Chem.* 2012;287(12):8904-11.
31. Reusken CB, Haagmans BL, Muller MA, Gutierrez C, Godeke GJ, Meyer B, et al. Middle East respiratory syndrome coronavirus neutralising serum antibodies in dromedary camels: a comparative serological study. *Lancet Infect Dis.* 2013;13(10):859-66.
32. Memish ZA, Cotten M, Meyer B, Watson SJ, Alsaahafi AJ, Al Rabeeah AA, et al. Human infection with MERS coronavirus after exposure to infected camels, Saudi Arabia, 2013. *Emerg Infect Dis.* 2014;20(6):1012-5.
33. Muller MA, Corman VM, Jores J, Meyer B, Younan M, Lijander A, et al. MERS coronavirus neutralizing antibodies in camels, Eastern Africa, 1983-1997. *Emerg Infect Dis.* 2014;20(12):2093-5.
34. Barlan A, Zhao J, Sarkar MK, Li K, McCray PB, Jr., Perlman S, et al. Receptor variation and susceptibility to Middle East respiratory syndrome coronavirus infection. *J Virol.* 2014;88(9):4953-61.
35. Raj VS, Smits SL, Provacia LB, van den Brand JM, Wiersma L, Ouwendijk WJ, et al. Adenosine deaminase acts as a natural antagonist for dipeptidyl peptidase 4-mediated entry of the Middle East respiratory syndrome coronavirus. *J Virol.* 2013;88(3):1834-8.
36. Bosch BJ, Smits SL, Haagmans BL. Membrane ectopeptidases targeted by human coronaviruses.

## ***Coronavirus spike-receptor interactions***

---

- Curr Opin Virol. 2014;6:55-60.
37. Chu DK, Poon LL, Gomaa MM, Shehata MM, Perera RA, Abu Zeid D, et al. MERS coronaviruses in dromedary camels, Egypt. *Emerg Infect Dis*. 2014;20(6):1049-53. Epub 2014/05/27. doi: 10.3201/eid2006.140299.
  38. Briese T, Mishra N, Jain K, Zalmout IS, Jabado OJ, Karesh WB, et al. Middle East respiratory syndrome coronavirus quasispecies that include homologues of human isolates revealed through whole-genome analysis and virus cultured from dromedary camels in Saudi Arabia. *MBio*. 2014;5(3):e01146-14.
  39. Kameoka J, Tanaka T, Nojima Y, Schlossman SF, Morimoto C. Direct association of adenosine deaminase with a T cell activation antigen, CD26. *Science*. 1993;261(5120):466-9.
  40. Franco R, Valenzuela A, Lluís C, Blanco J. Enzymatic and extraenzymatic role of ecto-adenosine deaminase in lymphocytes. *Immunol Rev*. 1998;161:27-42.
  41. Gines S, Marino M, Mallol J, Canela EI, Morimoto C, Callebaut C, et al. Regulation of epithelial and lymphocyte cell adhesion by adenosine deaminase-CD26 interaction. *Biochem J*. 2002;361(Pt 2):203-9.
  42. Weihofen WA, Liu J, Reutter W, Saenger W, Fan H. Crystal structure of CD26/dipeptidyl-peptidase IV in complex with adenosine deaminase reveals a highly amphiphilic interface. *J Biol Chem*. 2004;279(41):43330-5.
  43. Lu G, Hu Y, Wang Q, Qi J, Gao F, Li Y, et al. Molecular basis of binding between novel human coronavirus MERS-CoV and its receptor CD26. *Nature*. 2013;500(7461):227-31.
  44. Wang N, Shi X, Jiang L, Zhang S, Wang D, Tong P, et al. Structure of MERS-CoV spike receptor-binding domain complexed with human receptor DPP4. *Cell Res*. 2013;23(8):986-93.
  45. Boyle JF, Weismiller DG, Holmes KV. Genetic resistance to mouse hepatitis virus correlates with absence of virus-binding activity on target tissues. *J Virol*. 1987;61(1):185-9.
  46. Oh JS, Song DS, Park BK. Identification of a putative cellular receptor 150 kDa polypeptide for porcine epidemic diarrhea virus in porcine enterocytes. *J Vet Sci*. 2003;4(3):269-75.
  47. Bushnell KM, Sollner C, Schuster-Boeckler B, Bateman A, Wright GJ. Large-scale screening for novel low-affinity extracellular protein interactions. *Genome Res*. 2008;18(4):622-30.
  48. Crosnier C, Bustamante LY, Bartholdson SJ, Bei AK, Theron M, Uchikawa M, et al. Basigin is a receptor essential for erythrocyte invasion by *Plasmodium falciparum*. *Nature*. 2011;480(7378):534-7.
  49. Frei AP, Moest H, Novy K, Wollscheid B. Ligand-based receptor identification on living cells and tissues using TRICEPS. *Nat Protoc*. 2013;8(7):1321-36.
  50. Edman P. A method for the determination of amino acid sequence in peptides. *Arch Biochem*. 1949;22(3):475.
  51. Edman P, Begg G. A protein sequenator. *Eur J Biochem*. 1967;1(1):80-91.
  52. Yates JR, 3rd, Eng JK, McCormack AL. Mining genomes: correlating tandem mass spectra of modified and unmodified peptides to sequences in nucleotide databases. *Anal Chem*. 1995;67(18):3202-10.
  53. Perkins DN, Pappin DJ, Creasy DM, Cottrell JS. Probability-based protein identification by searching sequence databases using mass spectrometry data. *Electrophoresis*. 1999;20(18):3551-67.
  54. Aebersold R, Mann M. Mass spectrometry-based proteomics. *Nature*. 2003;422(6928):198-207.
  55. Tanner S, Shu H, Frank A, Wang LC, Zandi E, Mumby M, et al. InsPecT: identification of posttranslationally modified peptides from tandem mass spectra. *Anal Chem*. 2005;77(14):4626-39.
  56. Speicher KD, Gorman N, Speicher DW. N-terminal sequence analysis of proteins and peptides. *Curr Protoc Protein Sci*. 2009;Chapter 11:Unit11 0.
  57. Kubo H, Yamada YK, Taguchi F. Localization of neutralizing epitopes and the receptor-binding

- site within the amino-terminal 330 amino acids of the murine coronavirus spike protein. *J Virol.* 1994;68(9):5403-10.
58. Bonavia A, Zelus BD, Wentworth DE, Talbot PJ, Holmes KV. Identification of a receptor-binding domain of the spike glycoprotein of human coronavirus HCoV-229E. *J Virol.* 2003;77(4):2530-8.
59. Mou H, Raj VS, van Kuppeveld FJ, Rottier PJ, Haagmans BL, Bosch BJ. The receptor binding domain of the new Middle East respiratory syndrome coronavirus maps to a 231-residue region in the spike protein that efficiently elicits neutralizing antibodies. *J Virol.* 2013;87(16):9379-83.
60. He Y, Zhou Y, Liu S, Kou Z, Li W, Farzan M, et al. Receptor-binding domain of SARS-CoV spike protein induces highly potent neutralizing antibodies: implication for developing subunit vaccine. *Biochem Biophys Res Commun.* 2004;324(2):773-81.
61. He Y, Li J, Li W, Lustigman S, Farzan M, Jiang S. Cross-neutralization of human and palm civet severe acute respiratory syndrome coronaviruses by antibodies targeting the receptor-binding domain of spike protein. *J Immunol.* 2006;176(10):6085-92.
62. Skowronski DM, Astell C, Brunham RC, Low DE, Petric M, Roper RL, et al. Severe acute respiratory syndrome (SARS): a year in review. *Annu Rev Med.* 2005;56:357-81.
63. Jiang L, Wang N, Zuo T, Shi X, Poon KM, Wu Y, et al. Potent neutralization of MERS-CoV by human neutralizing monoclonal antibodies to the viral spike glycoprotein. *Sci Transl Med.* 2014;6(234):234ra59.
64. Du L, Zhao G, He Y, Guo Y, Zheng BJ, Jiang S, et al. Receptor-binding domain of SARS-CoV spike protein induces long-term protective immunity in an animal model. *Vaccine.* 2007;25(15):2832-8.
65. Zhi Y, Kobinger GP, Jordan H, Suchma K, Weiss SR, Shen H, et al. Identification of murine CD8 T cell epitopes in codon-optimized SARS-associated coronavirus spike protein. *Virology.* 2005;335(1):34-45.
66. Zakhartchouk AN, Sharon C, Satkunarajah M, Auperin T, Viswanathan S, Mutwiri G, et al. Immunogenicity of a receptor-binding domain of SARS coronavirus spike protein in mice: implications for a subunit vaccine. *Vaccine.* 2007;25(1):136-43.
67. Ellington AD, Szostak JW. In vitro selection of RNA molecules that bind specific ligands. *Nature.* 1990;346(6287):818-22.
68. Tuerk C, Gold L. Systematic evolution of ligands by exponential enrichment: RNA ligands to bacteriophage T4 DNA polymerase. *Science.* 1990;249(4968):505-10.
69. Shangguan D, Li Y, Tang Z, Cao ZC, Chen HW, Mallikaratchy P, et al. Aptamers evolved from live cells as effective molecular probes for cancer study. *Proc Natl Acad Sci U S A.* 2006;103(32):11838-43.
70. Gopinath SC, Misono TS, Kawasaki K, Mizuno T, Imai M, Odagiri T, et al. An RNA aptamer that distinguishes between closely related human influenza viruses and inhibits haemagglutinin-mediated membrane fusion. *J Gen Virol.* 2006;87(Pt 3):479-87.
71. Cao X, Li S, Chen L, Ding H, Xu H, Huang Y, et al. Combining use of a panel of ssDNA aptamers in the detection of *Staphylococcus aureus*. *Nucleic Acids Res.* 2009;37(14):4621-8.
72. Khati M, Schuman M, Ibrahim J, Sattentau Q, Gordon S, James W. Neutralization of infectivity of diverse R5 clinical isolates of human immunodeficiency virus type 1 by gp120-binding 2'F-RNA aptamers. *J Virol.* 2003;77(23):12692-8.
73. Jeon SH, Kayhan B, Ben-Yedidia T, Arnon R. A DNA aptamer prevents influenza infection by blocking the receptor binding region of the viral hemagglutinin. *J Biol Chem.* 2004;279(46):48410-9.
74. Kunkel F, Herrler G. Structural and functional analysis of the surface protein of human coronavirus OC43. *Virology.* 1993;195(1):195-202.
75. Schultze B, Gross HJ, Brossmer R, Herrler G. The S protein of bovine coronavirus is a hemagglutinin

## ***Coronavirus spike-receptor interactions***

---

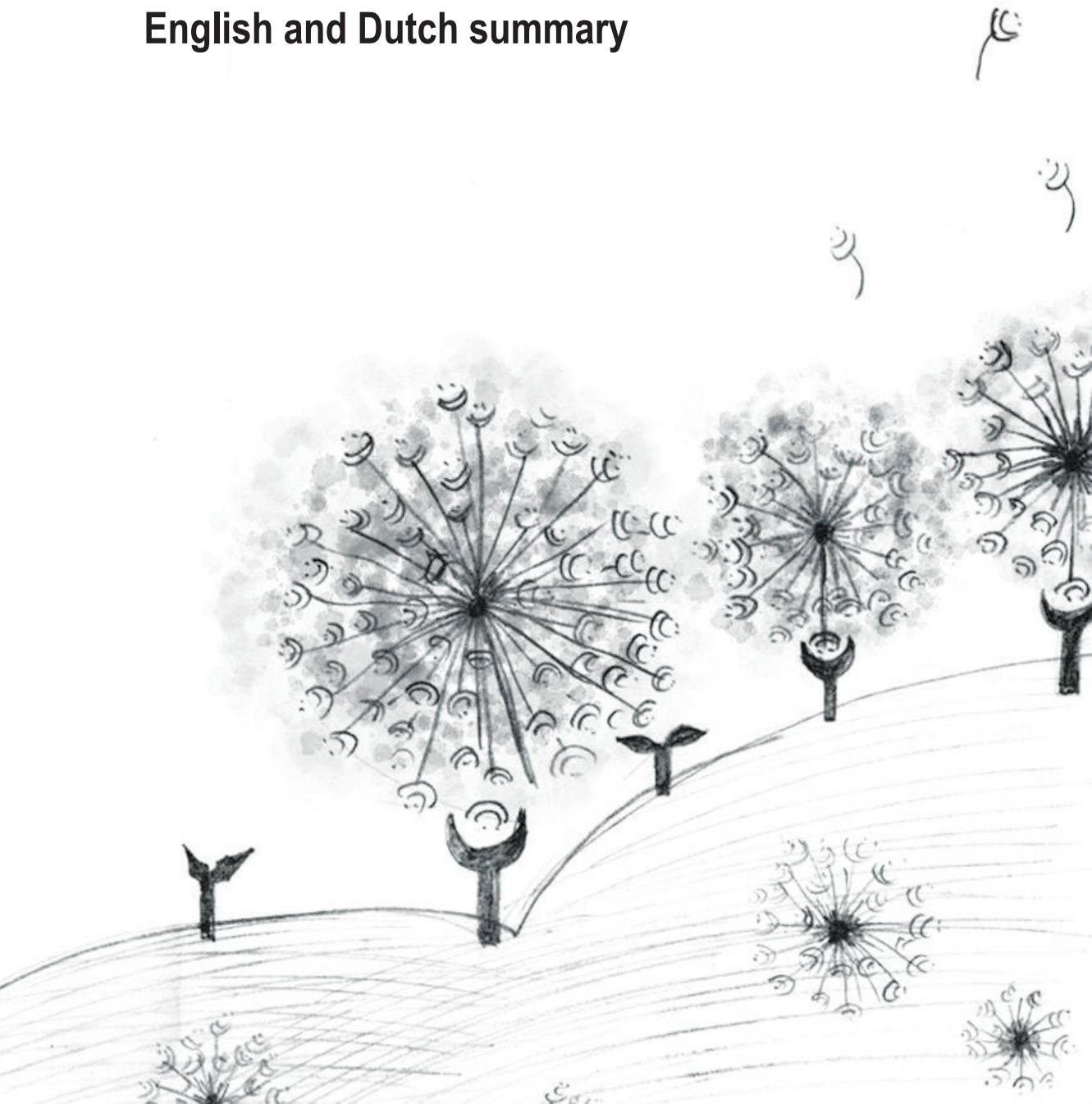
- recognizing 9-O-acetylated sialic acid as a receptor determinant. *J Virol.* 1991;65(11):6232-7.
- 76.Promkuntod N, van Eijndhoven RE, de Vrieze G, Grone A, Verheije MH. Mapping of the receptor-binding domain and amino acids critical for attachment in the spike protein of avian coronavirus infectious bronchitis virus. *Virology.* 2013;448:26-32.
- 77.Reynolds DJ, Debney TG, Hall GA, Thomas LH, Parsons KR. Studies on the relationship between coronaviruses from the intestinal and respiratory tracts of calves. *Arch Virol.* 1985;85(1-2):71-83.
- 78.Kreml C, Schultze B, Laude H, Herrler G. Point mutations in the S protein connect the sialic acid binding activity with the enteropathogenicity of transmissible gastroenteritis coronavirus. *J Virol.* 1997;71(4):3285-7.
- 79.Delmas B, Gelfi J, Sjostrom H, Noren O, Laude H. Further characterization of aminopeptidase-N as a receptor for coronaviruses. *Adv Exp Med Biol.* 1993;342:293-8.
- 80.Schultze B, Kreml C, Ballesteros ML, Shaw L, Schauer R, Enjuanes L, et al. Transmissible gastroenteritis coronavirus, but not the related porcine respiratory coronavirus, has a sialic acid (N-glycolylneuraminic acid) binding activity. *J Virol.* 1996;70(8):5634-7.
- 81.Desmarets LM, Theuns S, Roukaerts ID, Acar DD, Nauwynck HJ. Role of sialic acids in feline enteric coronavirus infections. *J Gen Virol.* 2014;95(Pt 9):1911-8.
- 82.Peng G, Xu L, Lin YL, Chen L, Pasquarella JR, Holmes KV, et al. Crystal structure of bovine coronavirus spike protein lectin domain. *J Biol Chem.* 2012;287(50):41931-8.
- 83.Peng G, Sun D, Rajashankar KR, Qian Z, Holmes KV, Li F. Crystal structure of mouse coronavirus receptor-binding domain complexed with its murine receptor. *Proc Natl Acad Sci U S A.* 2011;108(26):10696-701.
- 84.Li F. Receptor Recognition Mechanisms of Coronaviruses: a Decade of Structural Studies. *J Virol.* 2014;89(4):1954-64.
- 85.Corman VM, Eckerle I, Bleicker T, Zaki A, Landt O, Eschbach-Bludau M, et al. Detection of a novel human coronavirus by real-time reverse-transcription polymerase chain reaction. *Euro Surveill.* 2012;17(39).
- 86.Corman VM, Muller MA, Costabel U, Timm J, Binger T, Meyer B, et al. Assays for laboratory confirmation of novel human coronavirus (hCoV-EMC) infections. *Euro Surveill.* 2012;17(49).
- 87.Reusken C, Mou H, Godeke GJ, van der Hoek L, Meyer B, Muller MA, et al. Specific serology for emerging human coronaviruses by protein microarray. *Euro Surveill.* 2013;18(14):20441.
- 88.Moore KM, Jackwood MW, Hilt DA. Identification of amino acids involved in a serotype and neutralization specific epitope within the s1 subunit of avian infectious bronchitis virus. *Arch Virol.* 1997;142(11):2249-56.
- 89.Koo M, Bendahmane M, Lettieri GA, Paoletti AD, Lane TE, Fitchen JH, et al. Protective immunity against murine hepatitis virus (MHV) induced by intranasal or subcutaneous administration of hybrids of tobacco mosaic virus that carries an MHV epitope. *Proc Natl Acad Sci U S A.* 1999;96(14):7774-9.
- 90.Song CS, Lee YJ, Lee CW, Sung HW, Kim JH, Mo IP, et al. Induction of protective immunity in chickens vaccinated with infectious bronchitis virus S1 glycoprotein expressed by a recombinant baculovirus. *J Gen Virol.* 1998;79 ( Pt 4):719-23.
- 91.Du L, He Y, Zhou Y, Liu S, Zheng BJ, Jiang S. The spike protein of SARS-CoV--a target for vaccine and therapeutic development. *Nat Rev Microbiol.* 2009;7(3):226-36.
- 92.Lu L, Manopo I, Leung BP, Chng HH, Ling AE, Chee LL, et al. Immunological characterization of the spike protein of the severe acute respiratory syndrome coronavirus. *J Clin Microbiol.* 2004;42(4):1570-6.

93. Li F. Evidence for a common evolutionary origin of coronavirus spike protein receptor-binding subunits. *J Virol.* 2012;86(5):2856-8.
94. Lin CM, Gao X, Oka T, Vlasova AN, Esseili MA, Wang Q, et al. Antigenic Relationships among Porcine Epidemic Diarrhea Virus and Transmissible Gastroenteritis Virus Strains. *J Virol.* 2015.
95. Meyer B, Muller MA, Corman VM, Reusken CB, Ritz D, Godeke GJ, et al. Antibodies against MERS coronavirus in dromedary camels, United Arab Emirates, 2003 and 2013. *Emerg Infect Dis.* 2014;20(4):552-9.
96. Poland AM, Vennema H, Foley JE, Pedersen NC. Two related strains of feline infectious peritonitis virus isolated from immunocompromised cats infected with a feline enteric coronavirus. *J Clin Microbiol.* 1996;34(12):3180-4.
97. Barker EN, Tasker S, Gruffydd-Jones TJ, Tuplin CK, Burton K, Porter E, et al. Phylogenetic analysis of feline coronavirus strains in an epizootic outbreak of feline infectious peritonitis. *J Vet Intern Med.* 2013;27(3):445-50.
98. Rottier PJ, Nakamura K, Schellen P, Volders H, Haijema BJ. Acquisition of macrophage tropism during the pathogenesis of feline infectious peritonitis is determined by mutations in the feline coronavirus spike protein. *J Virol.* 2005;79(22):14122-30.
99. Pedersen NC, Black JW, Boyle JF, Evermann JF, McKeirnan AJ, Ott RL. Pathogenic differences between various feline coronavirus isolates. *Adv Exp Med Biol.* 1984;173:365-80.
100. Pedersen NC. Morphologic and physical characteristics of feline infectious peritonitis virus and its growth in autochthonous peritoneal cell cultures. *Am J Vet Res.* 1976;37(5):567-72.
101. Petersen NC, Boyle JF. Immunologic phenomena in the effusive form of feline infectious peritonitis. *Am J Vet Res.* 1980;41(6):868-76.
102. Weiss RC, Scott FW. Pathogenesis of feline infectious peritonitis: pathologic changes and immunofluorescence. *Am J Vet Res.* 1981;42(12):2036-48.
103. Dean GA, Olivry T, Stanton C, Pedersen NC. In vivo cytokine response to experimental feline infectious peritonitis virus infection. *Vet Microbiol.* 2003;97(1-2):1-12.
104. Van Hamme E, Desmarets L, Dewerchin HL, Nauwynck HJ. Intriguing interplay between feline infectious peritonitis virus and its receptors during entry in primary feline monocytes. *Virus Research.* 2011;160(1-2):32-9.
105. Licitra BN, Millet JK, Regan AD, Hamilton BS, Rinaldi VD, Duhamel GE, et al. Mutation in Spike Protein Cleavage Site and Pathogenesis of Feline Coronavirus. *Emerging Infectious Diseases.* 2013;19(7):1066-73.
106. Chang HW, Egberink HF, Halpin R, Spiro DJ, Rottier PJ. Spike protein fusion peptide and feline coronavirus virulence. *Emerg Infect Dis.* 2012;18(7):1089-95.
107. Vennema H. Genetic drift and genetic shift during feline coronavirus evolution. *Vet Microbiol.* 1999;69(1-2):139-41.



# CHAPTER 7

English and Dutch summary



### **English summary**

Infectious diseases caused by virus infections account for a significant part of public health problems, with consequent economic losses. Viruses are ubiquitous in nature causing disease in animals and humans. Coronaviruses, the viruses of study in this dissertation, are pathogens that can infect birds and mammals. The first identified coronavirus was the infectious bronchitis virus (IBV), the etiologic agent of infectious bronchitis in poultry flocks. Since then coronaviruses have been detected in numerous avian and mammalian species generally causing respiratory and gastrointestinal infections. In humans coronaviruses have been identified as causative agents of the common cold. However, coronavirus infection may also lead to severe disease in humans, exemplified by the zoonotic, severe acute respiratory syndrome coronavirus (SARS-CoV) that caused a world-wide epidemic in 2002-2003.

Coronaviruses are enveloped viruses and their corona-like morphology originates from the protrusion of trimers of the large envelope protein Spike (S) from the virion surface. The S protein, a type I membrane protein, can be divided into two subunits - S1 and S2 - that display distinct functions. Coronavirus infection starts with the virus contacting the receptor molecules present on the host cell surface through their S1 subunit which is followed by fusion of the viral membrane with the cell membrane mediated by the membrane-anchored S2 subunit. The receptor molecules that are exploited by coronaviruses can be proteins such as the angiotensin-converting enzyme 2 (ACE2) for SARS-CoV, or sugar moieties such as sialic acids for HCoV-OC43.

The entry of coronaviruses depends on the specific binding of the spike proteins with their cognate receptors on the host cell, which can be viewed as a key (spike) and lock (receptor). The specific interaction of spikes with the receptors determines the virus' cell, tissue and host tropism, and further influences the pathogenesis of viral infections. Changes in the receptor binding region of the spike protein that occur during replication of viral RNA genomes may result in the recruitment of new receptors and adaptation to a new host or a different cell type. These changes in host and cell tropism may lead to infection with different, potentially lethal outcome.

The zoonotic SARS coronavirus likely evolved to infect humans by a number of changes in the spike protein that allowed the efficient interaction with the human ACE2 receptor. Ten years after the SARS outbreak, a new zoonotic coronavirus emerged in Saudi Arabia, named Middle East respiratory syndrome coronavirus (MERS-CoV). MERS-CoV causes a severe and often lethal respiratory infection in humans, reminiscent of that of SARS. However, MERS-CoV does not enter cells via ACE2, the receptor for SARS-CoV. In a collaborative effort with scientists of the Erasmus Medical Centre in Rotterdam we identified the cell surface protein DPP4 as



the receptor for the MERS coronavirus (Chapter 2). Based on the specific interaction between the receptor binding subunit S1 of the S protein and the receptor, we precipitated dipeptidyl peptidase 4 (DPP4) from the cell lysate of susceptible cells. Further studies demonstrated that DPP4 is indeed a functional receptor for MERS-CoV since overexpression of DPP4 in non-susceptible cells endowed binding of the S1 subunit and susceptibility to virus infection. Furthermore, by tissue staining, MERS-CoV infection was localized to the non-ciliated cells of human bronchiolar epithelia that express DPP4, consistent with the clinical symptoms. The identification of a functional receptor for MERS-CoV turned out to be a key finding to understand how this coronavirus can cross species borders.

In the receptor recognition process, coronaviruses bind to receptors via their independently folded receptor binding domain (RBD) localized within S1 subunit. Previous studies with other coronaviruses demonstrated that the RBD comprises the main B-cell epitopes that induce potent neutralizing antibodies. Thus, identification of the RBD of MERS-CoV could facilitate the development of prevention and therapeutic strategies for MERS-CoV. In Chapter 3, we mapped the putative RBD regions to the N- and C-terminal domains of S1, based on the location of the RBD of two other coronaviruses of the betacoronavirus genus, MHV and SARS-CoV. We expressed variant recombinant S1-Fc chimera's with N and C-terminal truncations encompassing the S1 N- and/or C-domain and used these proteins in a receptor pull-down assay and FACS cell binding analysis. The RBD of MERS-CoV was mapped to the C-domain (residues 358 to 588) of the MERS-CoV S protein. In contrast to the N-terminal domain (residues 1-357), antibodies raised against the RBD were highly efficient in neutralizing MERS-CoV infection.

The S1 subunit of the coronavirus S protein is highly immunogenic and displays a high sequence diversity across different coronavirus species. As such the S1 antigen was considered as a potentially ideal antigen candidate for the development of a robust and specific serological diagnostic method for coronaviruses. In Chapter 4, a serological assay was developed in collaboration with scientist from the RIVM using recombinantly expressed and purified S1 subunits of SARS-CoV and MERS-CoV as antigens. These S1-based serological assay showed high specificity in the detection of antibodies against these human coronaviruses and was later found to be of great value in the identification of the dromedary camels as the zoonotic reservoir of MERS-CoV as well as for the study of the MERS-CoV epidemiology in humans and animals.

Feline coronaviruses are hypothesized to undergo a pathotype switch by mutation, changing from a clinically mild or asymptomatic, enteric infection to a fatal, systemic infection. Recruitment of novel receptors might be one of the underlying mechanisms for this phenomenon. The receptors for type I enteric FCoVs have not been identified yet. The DC-SIGN molecule has been demonstrated to function as a receptor for the systemically replicating, macrophage-tropic FIPV strains. These cell surface

## ***Coronavirus spike-receptor interactions***

---

---

molecules are present on immune cells including macrophages, but not on enterocytes, the primary target cell of the enteric form (FECV) of type I FCoV. In Chapter 5 we probed the question whether FECV has already the inherent ability to recruit DC-SIGN as a functional receptor or whether the virus requires adaptation towards this FIPV-receptor during the pathotype switch (Chapter 5). Our results showed that type I FECV UCD strain can recruit DC-SIGN to some extent for virus entry in a cell type dependent manner. Passaging of the virus in DC-SIGN expressing cells conferred increased infection capacity in DC-SIGN expressing cells, which correlated with a mutation in the receptor binding subunit of the virus' S protein. However, the ability of the cell-adapted virus to recruit DC-SIGN as a receptor appeared not sufficient for acquiring macrophage tropism. Thus, the cell tropism switch of type I FCoVs from enterocytes to macrophages is not determined by DC-SIGN usage alone but also by other factors that need to be determined in the future.

Coronavirus infection of the host cell is largely determined by the specific interactions between the spike protein and the receptor. Receptor interaction is hence considered as the main determinant for the tropism of the virus. Our studies on the functional receptors of coronaviruses will help to clarify the coronavirus entry mechanism and may aid in understanding the cell, tissue and host tropism switches of coronaviruses that can lead to new (zoonotic) severe diseases. Moreover, the acquired knowledge on the function of the coronavirus S protein can be translated into prevention and therapeutic strategies against coronavirus infection.

## Nederlands samenvatting

Infectieziekten veroorzaakt door virussen zijn verantwoordelijk voor een belangrijk deel van de volksgezondheidsproblematiek. Virussen die ziekte veroorzaken zijn wijdverspreid onder mensen en dieren. Coronavirussen - de virussen die in dit proefschrift bestudeerd worden - kunnen ziekte veroorzaken bij vogels en zoogdieren, inclusief de mens. Het eerst geïdentificeerde coronavirus was het infectieuze bronchitis virus (IBV), het etiologisch agens van infectieuze bronchitis in pluimvee. Sindsdien zijn er vele coronavirussen gevonden in vogels en zoogdieren; ze veroorzaken veelal respiratoire en gastro-enterale infecties. Coronavirusinfecties leiden bij mensen doorgaans tot een gewone verkoudheid. Coronavirussen kunnen echter ook ernstige ziekte veroorzaken bij mensen. Het 'severe acute respiratory syndrome' coronavirus (SARS-CoV) dat in 2002-2003 een wereldwijde epidemie veroorzaakte is daarvan een indringend voorbeeld.

Coronavirussen zijn membraan-omhulde virussen. Hun corona-achtige morfologie wordt veroorzaakt door grote, trimere complexen van het Spike (S) glycoproteïne op het virion oppervlak. Het S eiwit is een type I membraan eiwit en is onderverdeeld in twee subunits – S1 en S2 – met onderscheiden functies. Coronavirusinfectie begint met binding aan het receptor molecuul op het oppervlak van de gastheercel via het S1 subunit gevolgd door fusie van het virale membraan met het celmembraan, een proces dat wordt gemedieerd door het membraan-verankerde S2 subunit. De receptoren gebruikt door coronavirussen kunnen bestaan uit eiwitten (b.v. het angiotensin-converting enzym 2 [ACE2] voor SARS-CoV) ofwel suikers (b.v. sialzuren voor het humane coronavirus OC43 [HCoV-OC43]).

Het binnendringen ("entry") van coronavirussen in cellen is afhankelijk van de binding van de spike eiwitten aan hun specifieke receptoren op de gastheercel. De 'sleutel-slot' interactie tussen de gastheer-receptor en het virale receptor bindende eiwit is cruciaal voor het vermogen c.q. de specificiteit van virussen om cellen, weefsels en gastheren te infecteren. Veranderingen in het receptor-bindende domein van het spike eiwit die optreden tijdens de genoom-replicatie van RNA-virussen kunnen leiden tot het rekruteren van nieuwe receptoren met als gevolg de aanpassing van het virus aan een ander celtype of zelfs een nieuwe gastheer. Deze veranderingen in cel- en gastheertropisme van het virus kunnen leiden tot een heel ander type infectie c.q. ziektebeeld met soms dodelijke afloop.

Het van oorsprong animale SARS coronavirus heeft zich waarschijnlijk aan mensen aangepast na een aantal wijzigingen in het spike eiwit die een meer efficiënte interactie met de humane receptor ACE2 receptor mogelijk maakten. Tien jaar na de SARS-uitbraak dook er in 2012 een nieuw, zoönotische coronavirus op in Saoedi-Arabië, het Middle East respiratory syndrome coronavirus (MERS-CoV). MERS-CoV veroorzaakt bij de mens een ernstige en vaak dodelijke infectie van de luchtwegen,

## ***Coronavirus spike-receptor interactions***

---

vergelijkbaar met SARS. Echter, MERS-CoV maakt geen gebruik van ACE2, de receptor voor SARS-CoV. In samenwerking met wetenschappers van het Erasmus Medisch Centrum in Rotterdam hebben wij het cel oppervlakte-eiwit dipeptidyl peptidase 4 (DPP4) als de receptor voor het MERS-CoV geïdentificeerd (hoofdstuk 2). Gebruikmakend van de specifieke interactie tussen het receptor-bindende S1 subunit van het S eiwit en de receptor, konden wij het DPP4 eiwit precipiteren uit een cel-lysaat van MERS-CoV ontvankelijke cellen. Kunstmatige expressie van DPP4 in niet-ontvankelijke cellen maakte binding van het S1 subunit aan deze cellen mogelijk en zorgde er voor dat deze cellen nu ontvankelijk werden voor MERS-CoV. Hiermee was aangetoond dat het DPP4 een functionele receptor is voor MERS-CoV. MERS-CoV infectie van menselijke bronchiolaire epitheel cellen co-localiseerde met de DPP4-positieve, niet-gecilleerde epitheel cellen. De identificatie van een functionele receptor voor MERS-CoV is belangrijk gebleken om te begrijpen hoe dit coronavirus van dier naar mens kan overspringen.

Coronavirussen binden hun receptoren via een receptor bindings domein (RBD) in het S1 subunit van het spike eiwit. Eerdere studies aan andere coronavirussen lieten zien dat het RBD de belangrijkste B-cel epitopen bevat van neutraliserende antilichamen. De identificatie van het RBD in het MERS-CoV S eiwit is daarom van belang voor de ontwikkeling van preventie- en therapeutische strategieën voor MERS-CoV. In hoofdstuk 3, hebben we de mogelijke RBD regio's in de N- en C-terminale domeinen van het S1 subunit gelokaliseerd, gebaseerd op de locatie van de RBD van twee andere coronavirussen in het betacoronavirus genus, n.l. muizenhepatitisvirus (MHV) en SARS-CoV. We hebben S1 varianten met deleties van het N- of C-terminale domein geproduceerd en de interactie met de receptor getest in een receptor precipitatie assay en een FACS-gebaseerde cel binding assay. De RBD van MERS-CoV bleek gelokaliseerd in het C-terminale domein (aminozuur 358-588) van het MERS-CoV S eiwit. In tegenstelling tot het N-terminale domein (aminozuur 1-357) bleken antilichamen opgewekt tegen het RBD zeer efficiënt in neutralisatie van de MERS-CoV infectie.

Het S1 subunit van het coronavirus S eiwit is zeer immunogeen en laat tussen de verschillende coronavirus species een grote sequentiediversiteit zien. Door deze twee eigenschappen is het S1 deel van het S eiwit een goed kandidaat antigeen voor een robuuste en specifieke serologische test voor coronavirussen. In hoofdstuk 4 is een dergelijke serologische test in samenwerking met wetenschappers van het RIVM ontwikkeld. De test is gebaseerd op het gezuiverde S1 subunit van de S eiwitten van SARS- en MERS-CoV. Deze test liet een hoge gevoeligheid en specificiteit zien in de detectie van antilichamen tegen deze humane coronavirussen en is later gebruikt bij de identificatie van de dromedarissen als het zoönotisch reservoir van MERS-CoV en bij het bestuderen van de epidemiologie van het MERS-CoV bij mens en dier.

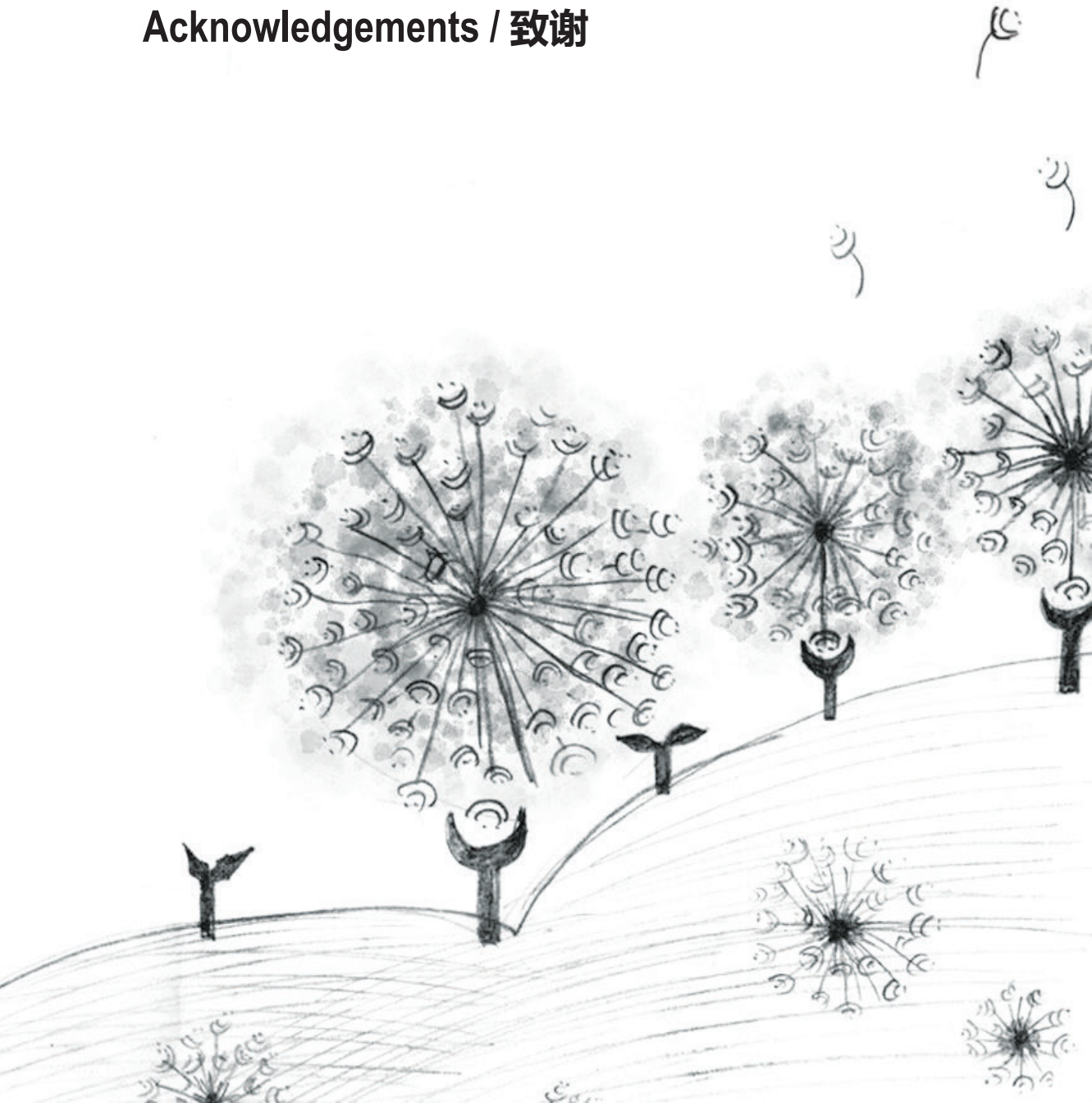
Kattencoronavirussen kunnen van pathotype veranderen, mogelijk als gevolg van mutatie. Daarbij verandert de doorgaans milde of asymptomatische darminfectie in

een fatale, systemische infectieuze peritonitis (FIP). Het onderliggend mechanisme hiervan is onbekend, maar de acquisitie van nieuwe receptoren speelt hierbij mogelijk een rol. De receptoren van de enteraal replicerende feliene coronavirussen (FECV) zijn nog niet geïdentificeerd. Voor de systemisch replicerende virussen (FIPV) die macrofagen infecteren is het zgn. DC-SIGN molecuul aangetoond als een functionele receptor. Deze cel oppervlakte moleculen zijn aanwezig op bepaalde immuuncellen - zoals macrofagen - maar niet op enterocyten, wat de doelcellen van FECV zijn. In hoofdstuk 5 hebben we onderzocht of FECV de capaciteit heeft om DC-SIGN te gebruiken als een functionele receptor of dat er in de FECV-naar-FIPV switch aanpassingen nodig zijn om deze FIPV receptor te kunnen rekruteren (hoofdstuk 5). Onze resultaten toonden aan dat – afhankelijk van het celtype – FECV (i.c. de serotype I UCD stam) DC-SIGN-positieve cellen kan infecteren. Het passeren van het virus in DC-SIGN-positieve cellen leidde tot een geadapteerde variant met een sterk toegenomen infectiviteit op DC-SIGN-positieve cellen, wat correleerde met een mutatie in het S1 subunit van het S eiwit. Echter, het vermogen van het aangepaste virus om DC-SIGN te rekruteren als functionele receptor bleek niet voldoende voor het verkrijgen van een macrofaagtropisme. Hieruit blijkt dat de cel tropisme verschillen tussen FECV naar FIPV niet (alleen) door aanpassing aan DC-SIGN verklaard kunnen worden en dat verder onderzoek nodig is om hiervoor een verklaring te vinden.

Coronavirusinfectie van de gastheercel wordt grotendeels bepaald door de specifieke interacties tussen het spike eiwit en de receptor. Receptor interactie wordt derhalve beschouwd als de belangrijkste determinant van het tropisme van het virus. Studies naar de receptor interactie van coronavirussen kunnen inzicht geven in het mechanisme van de cel, weefsel en gastheer tropisme veranderingen die coronavirussen kunnen ondergaan. Bovendien is kennis over de receptor interactie van het coronavirus S eiwit belangrijk bij de ontwikkeling van strategieën voor de preventie en de therapie van coronavirusinfecties.



**Acknowledgements / 致谢**



## ***Coronavirus spike-receptor interactions***

---

---

Life is like a soap series in which every episode has a different topic and tells a different story, but about the same theme. The episode describing my PhD study has certainly been one of the most fantastic parts in my story since I learned a lot, experienced a lot and grew a lot. Yet, without you all, I could not have made it successfully. Here, I would like to express my most sincere appreciation to all the actors who completed this episode together with me.

First of all, I would like to thank my supervisors, promotor Peter Rottier and co-promotor Berend Jan Bosch. I really appreciate that you gave me the chance to join your group. I learned a lot from both of you during this period. Before my study here, I could not even design primers for PCR, but now learned to design and plan experiments and (dis)prove our hypotheses independently. **Peter**, I always could get valuable suggestions from you to figure out the problems I encountered. I guess I would have had more problems without your supervision. Although you have retired, you still work and supervise us in the lab. Your passion for science and research inspired me. Wish you a happy and healthy life in the future. **Berend**, you are always patient to me and explain the details to me very carefully. During the exciting period we were working on the MERS project, you also guided me and worked together with me at the bench. In addition, you always reminded me to read more and try to learn more from the literature. By your continuous support I can work more efficiently and independently in the lab. Thanks for the supervision and all the help from you. Best wishes to you and your family.

In addition, I would like to acknowledge all our main collaborators who contributed to my progress most. **Bart** and **Stalin** from the Erasmus University, I am really lucky I had the chance to work with you on the MERS project. Without your hard and excellent work, we would not have succeeded. Best wishes for you! I also want to thank Hans and Lowiese of the Ghent University for the collaboration on the FCoV project. **Lowiese**, you are smart and also work hard. I really enjoyed the time working together with you in the lab. Wish you a good future with both your new job and life. Furthermore, I would like to thank Helene and Iresha for their contribution as well. We did not get good progress in our work, but I also learned by our collaboration. **Helene**, your enthusiasm and attitude about research were very stimulating and I am grateful we could collaborate. **Iresha**, I must say that you are a really tough girl but now also a tough mum. We started our PhD work at almost the same time, and we will also finish at the same time. I really appreciate your patient training in immunohistochemistry staining as well as your support and help during my study. Wish you a pleasant and happy life with your family.

I also want to thank **Frank** for all your suggestions and support whenever I asked. **Herman**, I always got answers from you if I asked you some details concerning my FCoV study. **Erik**, you must be a walking encyclopedia. You always had valuable information and suggestions when I asked. Thanks for all your help and input.



Furthermore, I would like to thank several colleagues in our group. Qiushi and Oliver, who helped me a lot at the beginning of my PhD project. **Qiushi**, thanks for all your help during this period; you always guided me and showed me how to work in the lab. I learned protein expression from you, and you were always around if I encountered some problems. I think I could not have gone through the tough beginning so smoothly without your support. I also enjoyed the time we spent together after work. Wish you a prosperous and happy life in the future. **Oliver**, I really appreciate your instructions in doing the FACS analyses. I also enjoyed the times when we had dinner and made cakes together. It is good to know you and Anna. Wish both of you a happy life together. In addition, I would like to thank Qian. **Qian**, I always feel that you are much more mature and independent than me even though we are about the same age. It is good to know you, and thanks for all your help in job searching and grant application. Wish you a happy life in Switzerland. Furthermore, I would like to say thank you to **Nancy** and **Arno**. Without your quick and kind responses to my ordering and technical support requests, my work in the lab would have been much less efficient. It was always good to have you around.

I also would like to thank all my office mates, Kazuya, Floor, Jojanneke and Wouter for all the happy and funny times we had together. **Kazuya**, although we were working together for just one year, you impressed me by your enthusiasm for science. It was nice to see you again and communicate with you in Salamanca. **Floor**, you always shared good news and funny things with me. Wish you a happy life in the future.

It is because of all these and other wonderful colleagues that I had a really great time in the Virology Division. Wish all of you a happy life in the future.

My life abroad would not have been so joyful without all the additional new friends that came into my world. The first friend I had in Utrecht is **Xueqing**. Already before my arrival I received an e-mail from you and afterwards you were not able to get rid of me until you left Utrecht after finishing your PhD here. You picked me up at the central station when I arrived in Utrecht, and took me in on the first day. Every time I needed some help, you were always available. I really like the cover you designed for my thesis. Wish you and Xin have a happy life in Atlanta. Two best friends, also roommate or officemate to me, **Jiefei and Hongbo** are the people I spent the most unforgettable time together with. We made trips together, went shopping together, cooked together and even were stupid together. During my most stressful and frustrating period, you tried to encourage me and cheer me up. **Jiefei**, you certainly must be the best roommate in the world. You are a funny and also a tough girl, so I always feel better after talking with you. Without you my PhD life would not have been so colorful. Wish you can finish your PhD successfully. **Hongbo**, thanks for all the help and support from you. Wish you and Wenshi a happy life in the Netherlands and I hope you finish your PhD successfully.

## ***Coronavirus spike-receptor interactions***

---

---

I also want to thank some of my friends in the Netherlands, **Bin Chen, Can Cui, Fang Wang, Haoran, Yipu** as well as **Koen** and **Brian** in Geoscience. Thanks for all the grateful time we spent together. 谢谢使馆教育处的**夏磊**老师，感谢你给予的帮助，祝你在南农生活工作一切顺意。另外还要感谢使馆的**张明明、张振亮**夫妇，很幸运能认识你们，也很开心能有机会和你们一起出游，祝你们在今后的日子里事事顺心，幸福美满。

此外，我还要感谢同在欧洲求学的大学同学，柏林的**翟雪珍**，埃森的李**李草**，格罗林根的**李明**。很开心和你们一起去柏林，一起去希腊，我想以后这些都会是很美好的回忆。我还要谢谢国内一直支持我的朋友们。谢谢**谌平**师兄，每次我给你发的奇奇怪怪的问题，你总是在百忙中回答，谢谢你在工作中给予的支持。**张晨宇**，从大学到现在这么多年，我们还是能无话不说。还有**洪亮**和**江滢**，谢谢你们的支持和帮助，不管是生活上还是工作上的，你们总能给我很好的建议。祝愿所有的朋友们幸福快乐。

Mr. Fang Yan，这么多年，除了本科毕业的致谢里，我似乎没有认真地跟你说声谢谢。但是在快走完博士这个重要阶段的时候，我真心地想要对你表示感谢，感谢你带给我的成长，还有所有一切美好的回忆。就像我曾经说的，我们就像是相遇的两条直线，遇见之后注定了越走越远。但是我还是感谢你的出现，亦或是离开，让我学会依赖更学会独立，学会坚持也学会放弃。不管今后各自际遇如何，我真诚祝你幸福快乐。也祝你爸爸妈妈身体健康，一切顺利。

最后也是最重要的，我想感谢我的爸爸妈妈，感谢这么多年你们对我的教导还有溺爱。从牙牙学语蹒跚学步，到我能独自求学在外，我看到了自己的成长，相信你们也很高兴看到我的蜕变。这些年，不管我经历过什么，也即将要去经历什么，那都是我成长所必需经历的部分。这一路走来，你们总是相信我支持我的选择。此时任何语言都不能表达我对你们的感谢，藉此祝你们幸福安康。

牟卉卉

Utrecht, 20150702





# Curriculum vitae



### **Education background**

09. 2011 -present	PhD candidate	Virology Division, Department of Infectious Diseases and Immunology, Faculty of Veterinary Medicine, <b>Utrecht University</b> , Utrecht, The Netherlands.
09. 2008 -06. 2011	Master of Science	State Key Laboratory of Virology, Wuhan Institute of Virology, <b>Chinese Academy of Sciences</b> , P.R.China
09. 2004 -06.2008	Bachelor of Science	Tongji Medical college, <b>Huazhong University of Science and Technology</b> , Wuhan, P.R.China

### **Presentations**

**Dipeptidyl peptidase-4 is a functional receptor for the emerging human coronavirus-EMC.** The scientific spring meeting organized by the Dutch Society of Medical Microbiology (NVMM) and the Royal Dutch Society of Microbiology (KNVM), April 2013, Papendel, The Netherlands. Oral presentation.

**Dipeptidyl peptidase 4: Entry Portal for the Emerging MERS coronavirus.** Veterinary Science Day, November 2013, Utrecht, The Netherlands. Oral presentation.

**MERS-CoV spike interaction with a novel receptor.** XIII<sup>th</sup> International Nidovirus Symposium, June 2014, Salamanca, Spain. Poster presentation.

### **Rewards**

**FEMS Young Scientist Meeting Grant** for XIII<sup>th</sup> International Nidovirus Symposium, Salamanca, Spain. April 2014.

**Best Oral Presentation Awards**, Veterinary Science Day, Utrecht, the Netherlands. November 2013.

## List of publications

Raj VS\*, **Mou H\***, Smits SL, Dekkers DH, Müller MA, Dijkman R, Muth D, Demmers JA, Zaki A, Fouchier RA, Thiel V, Drosten C, Rottier PJ, Osterhaus AD, Bosch BJ, Haagmans BL. Dipeptidyl peptidase 4 is a functional receptor for the emerging human coronavirus-EMC. *Nature*. 2013 Mar 14; 495(7440):251-4.

Reusken C\*, **Mou H\***, Godeke GJ\*, van der Hoek L, Meyer B, Müller MA, Haagmans B, de Sousa R, Schuurman N, Dittmer U, Rottier P, Osterhaus A, Drosten C, Bosch BJ, Koopmans M. Specific serology for emerging human coronaviruses by protein microarray. *Euro Surveill*. 2013 Apr 4; 18(14):20441.

**Mou H**, Raj VS, van Kuppeveld FJ, Rottier PJ, Haagmans BL, Bosch BJ. The receptor binding domain of the new MERS coronavirus maps to a 231-residue region in the spike protein that efficiently elicits neutralizing antibodies. *J Virol*. 2013 Aug; 87(16):9379-83.

Ohnuma, K., Haagmans, B.L., Hatano, R., Stalin Raj, V., **Mou, H.**, Iwata, S., Dang, N.H., Bosch, B.J. & Morimoto, C. (2013). Inhibition of Middle East Respiratory Syndrome Coronavirus Infection by Anti-CD26 Monoclonal Antibody. *J Virol*. 87(24), 13892-13899.

Raj VS, Lamers MM, Smits SL, Demmers JA, **Mou H**, Bosch BJ, Haagmans BL. Identification of protein receptors for coronaviruses by mass spectrometry. *Methods Mol Biol*. 2015; 1282:165-82.

**Huihui Mou**, Lowiese M.B. Desmarets, Frank J. M. van Kuppeveld, Herman F. Egberink, Hans J. Nauwynck, Peter J. M. Rottier, Berend-Jan Bosch. An S protein mutation adapting feline enteric coronavirus to using DC-SIGN for cell entry does not confer macrophage tropism. To be submitted.

\* These authors contributed equally to this work.

